A Model of the Assembly of Compliant Parts

by

Narendra Amalendu Soman

B. Tech., Mechanical Engineering
Indian Institute of Technology-Bombay, 1990

M. S., Mechanical Engineering
Arizona State University, 1992

Submitted to the Department of Mechanical Engineering
in Partial Fulfillment of the Requirements for the Degree of

Doctor of Philosophy in Mechanical Engineering

at the

MASSACHUSETTS INSTITUTE OF TECHNOLOGY

August 1996
[September 1996]

Signature of Author .....
Department of Mechanical Engineering
August 12, 1996

Certified by .....
David C. Gossard
Professor of Mechanical Engineering
Thesis Supervisor

Accepted by .....
Professor Ain A Sonin
Chairman, Department Committee

A MODEL OF THE ASSEMBLY OF COMPLIANT PARTS

by

Narendra Amalendu Soman

Submitted to the Department of Mechanical Engineering
on August 12, 1996 in partial fulfillment of the
requirements for the Degree of Doctor of Philosophy in
Mechanical Engineering

ABSTRACT

Assemblies of compliant parts are widely used in industries such as automobile, aerospace, textile and furniture-making. Unlike rigid parts, compliant parts can deform, changing their geometry during the assembly process. When parts and tools are manufactured, there is unavoidable variation from their nominal shape. Such non-nominal geometry results in fit-up problems during the assembly process. To compensate for such manufacturing variations, designers often provide intentional gaps between adjacent parts. When parts are fastened, they deform and this intentional gap is closed. Thus, although parts with nominal geometry but intentional gaps are assembled, the resulting assembly has non-nominal geometry. In the presence of manufacturing variations, there is further deformation. Most current computer-aided design (CAD) systems are based on rigid body geometry, and hence, cannot be used to predict the geometry of compliant parts as they propagate through the assembly line.

The objective of this thesis is to model the assembly of compliant parts as they propagate through the assembly process.

The geometry of parts and tools is represented as a set of finite elements and nodes. The relationships between parts, tools and assembly configuration are depicted as a connectivity graph. Sources of error are identified and quantified. Every operation in the assembly process is examined in detail to study the propagation of non-nominal geometry from one operation to the next. This model can be used to automate the process of predicting the geometry of the assembled product, in the presence of intentional gaps and non-nominal geometry. It can also be used as a design tool to evaluate the sensitivity of product or process design on the final geometry of the product.

Thesis Supervisor: David C. Gossard
Title: Professor of Mechanical Engineering

ACKNOWLEDGMENTS

I want to express my deep appreciation to the many people who made my Ph. D. very enjoyable.

Prof. Gossard: Thank you for your constant guidance and advice. I have learnt a lot from you.

Prof. Boyce and Prof. Fine: Thanks for your encouragement and help in formulating my research problem.

Applicon and the U. S. Airforce: Thanks for your financial support.

Rama and Ganti: Thanks for the numerous late-night coffees, the camping trips, and also proof-reading my thesis. I owe you.

Srihari and Kots: Thanks for laughing even though you knew my jokes weren't funny.

Ajee, Aiee, Baba, Kaku, Kaka: Thanks for teaching me not to follow the dotted line without asking why.

Leena, Amit, and Vidyut: Thanks for the wonderful days when we could fly if we just stretched our arms and ran.

Table of Contents

List of Figures

List of Tables

1.

Introduction

Assemblies of compliant parts are widely used in automobile, aerospace, textile and furniture-making industries. Unlike rigid parts, compliant parts can deform, changing their geometry during the assembly process. The objective of this thesis is to model the assembly[1] of compliant parts. This thesis focuses on the automobile assembly.

1.1 Automobile Body Assembly

A generic automobile body is made up of 300-350 stamped sheet metal parts, which propagate through an assembly line having 60-80 assembly stations. The automobile body undergoes 3500-4000 weld spots. The assembly line has 1700-2500 locators that position the parts in the assembly stations. The rate of production is around 20,000 automobiles per month and the cycle time is 45 sec (from Naitoh et al). In every assembly station, parts are loaded on assembly fixtures and fastened together to form a sub-assembly. The most common mode of fastening is spot welding. After parts are fastened together, the resulting sub-assembly goes to the next assembly station where more parts are added to it. The sub-assembly propagates through the assembly line till the entire automobile body is assembled. The body is then painted and fastened on to the automobile chassis.

[1] We use the word "assembly" both, as a noun (when we refer to the physical product) and as a verb (when we to refer to the process of assembling the product).

1.1.1 Assembly dimensions of interest

The dimensions of interest on an automobile body are characterized as margins and flushness values (see Figure 1-1). Margins are the gaps between adjacent parts, and flushness values are a measure of how level adjacent parts are with each other. Margins and flushness values quantify the "fit" between two parts. Margins and flushness values affect the function of the automobile body. For example, consider the flushness between the door and the door-frame. If the flushness it too low, the door closing effort is high and this adversely affects the operation of the door. If the flushness it too high, the weather strip between the door and the door-frame gets loose and causes water to leak inside the car. Also, well-maintained margins and flushness give the automobile body a pleasing and aesthetic look. So for functional and aesthetic reasons, the geometry of the automobile body is monitored closely during its assembly process to ensure good margins and flushness values after the assembly is complete.

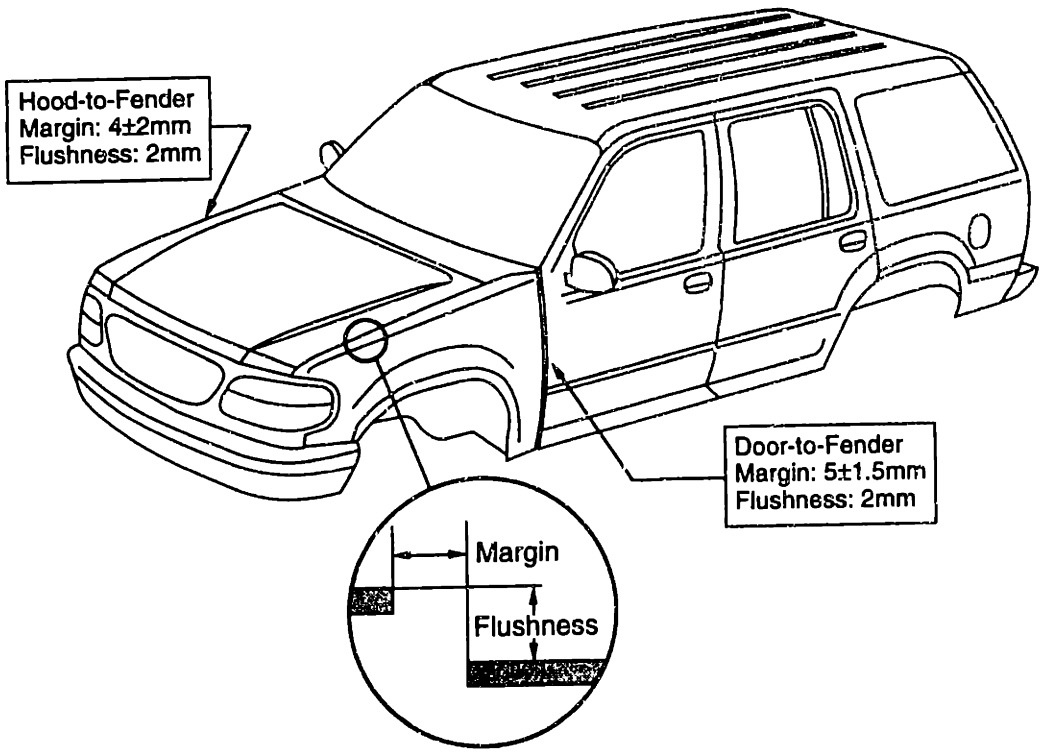

Figure 1-1. An automobile body showing margins and flushness values

Typical values for margins lie between 4-5 mm with a tolerance value of 2-3 mm. The nominal values of flushness are typically 0 mm with a tolerance value of ± 2 mm. Table 1-1 shows margins and flushness values for the Ford Windstar (from Sweder94). Parts are stamped out of sheet metal having a thickness of 1-2 mm.

Table 1-1. Body margins and flushness for the Ford Windstar (Sweder94)

Assembly dimension	Margin	Flushness
Hood to Fender	4.0 ± 2.0 mm	0.0 ± 2.0 mm
Front Door to Fender	4.1 ± 1.5 mm	0.0 ± 2.0 mm

1.1.2 Manufacturing variations and non-nominal geometry

When parts and tools are manufactured, there is an unavoidable variation from their nominal shape. This results in non-nominal part geometry. The stamping operation has inherent limitations and produces parts which have a variation of 2-3mm in their geometry. This variation refers to both, part-to-part and shift-to-shift variation. The fixtures and weld guns can also have non-nominal geometry due to manufacturing capabilities. In addition to manufacturing variation, there is additional variation introduced by the wear and tear of the equipment during normal operation. Such non-nominal geometry results in fit-up problems during the assembly process.

Fixtures and weld guns are relatively rigid as compared to the sheet metal parts. Non-nominal geometry of parts, fixtures and weld guns cause unintentional deformation of the parts during assembly. These deformed parts form non-nominal sub-assemblies. The effect of non-nominal geometry propagates through the assembly line. This finally affects the margin and flushness values of the automobile body after the assembly process is complete.

1.1.3 Intentional gaps

If the assembly is designed for nominal geometry, serious problems arise in the presence of non-nominal geometry. To compensate for such non-nominal geometry, designers often provide intentional gaps between adjacent parts. When parts are fastened, they deform and this intentional gap is closed.

Figure 1-2 shows the front end assembly. It shows the top view of the assembly station where the inner fender and radiator support are welded to the body. First, the inner fender, the radiator support and the body are first loaded into their respective fixtures. The fixture for the inner fender and radiator support is then moved towards the body. This is done to facilitate the loading of the parts into their fixtures. If the radiator is shorter than its nominal value (see Figure 1-3), then the inner fenders crumble when the fixture approaches the body. This is avoided by providing an intentional gap between the inner fender and the body (see Figure 1-4).

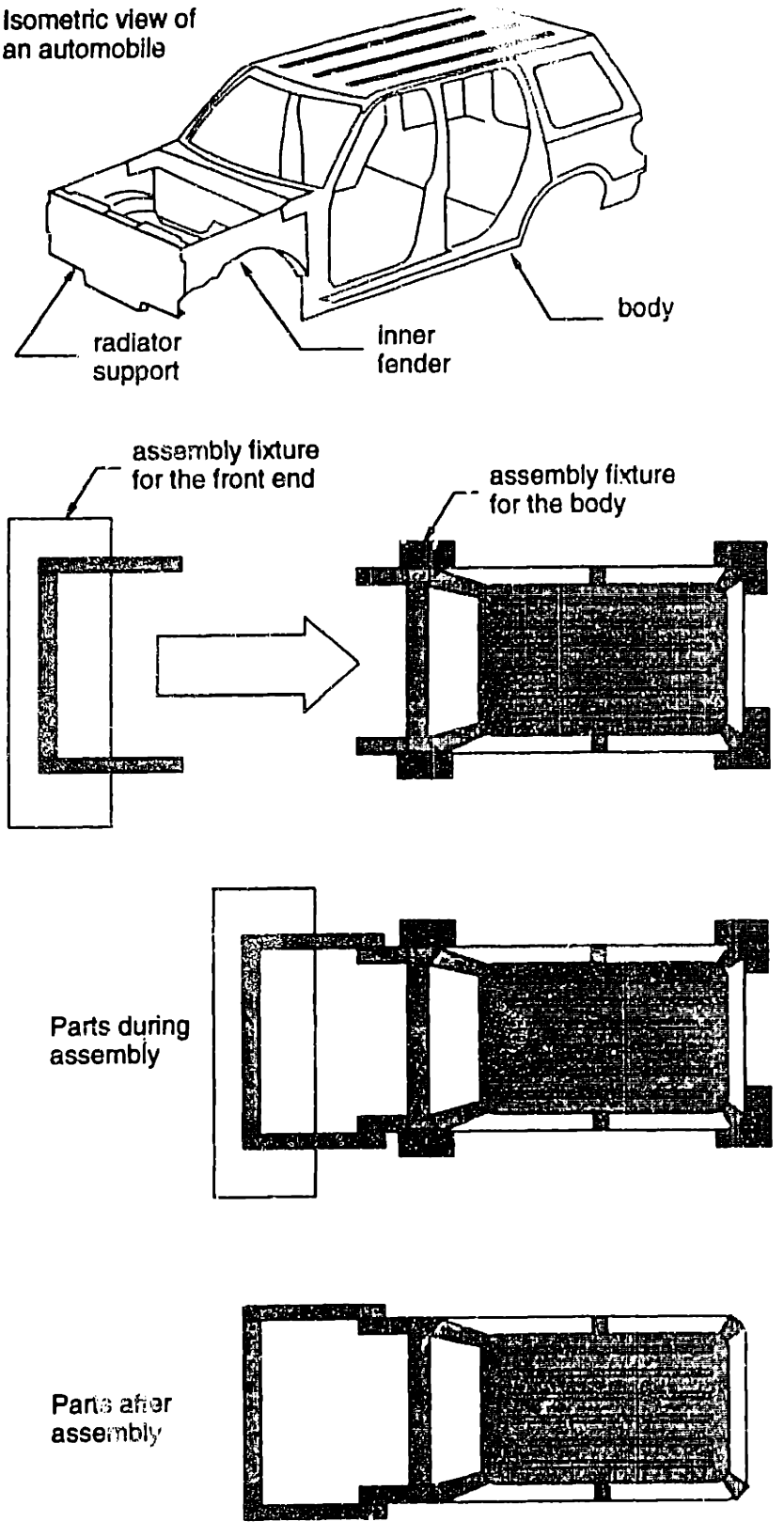

Figure 1-2. The front end assembly

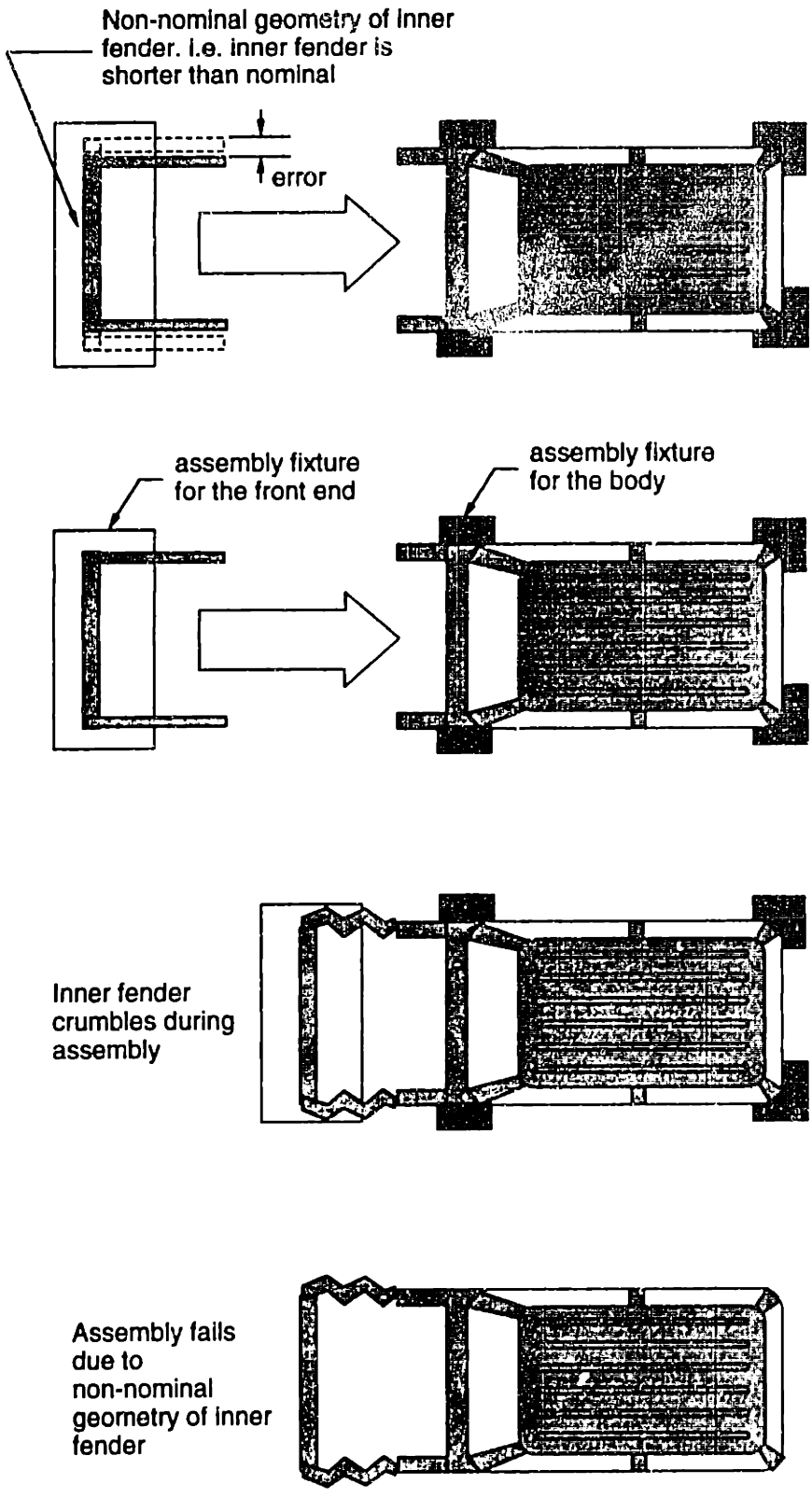

Figure 1-3. The front end assembly with non-nominal geometry of inner fender

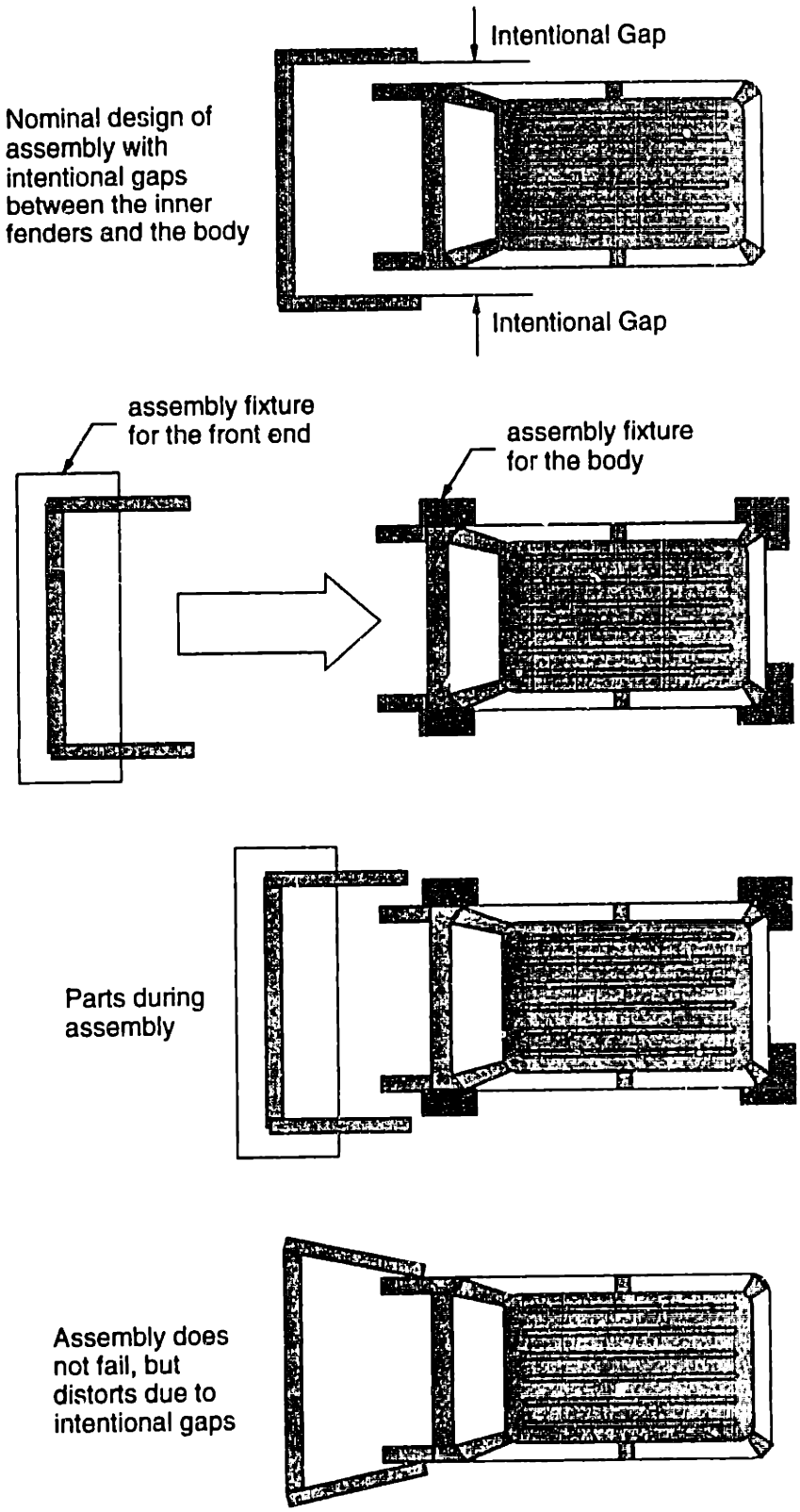

Figure 1-4. The front end assembly with intentional gaps

In this scenario with intentional gaps[2], the assembly operation can be performed even in the presence of non-nominal geometry. This is done at the expense of deforming the inner fender under assembly forces that close the gap between the inner fender and the body. Thus, intentional gaps act as "buffers" to adjust for non-nominal geometry. The deformed sub-assembly now propagates through the assembly line subsequently affecting the margins and flushness of the automobile body. These intentional gaps have a non-ignorable effect on the assembly.

1.2 Need for Model

In order to prevent interference of parts during loading into the assembly fixture, gaps are designed into the product. Although these gaps are closed by assembly forces during the assembly process, parts are designed and shown on engineering drawings (and/or in their CAD models) with gaps between them. Thus, in spite of having parts that are nominal according to the design, the assembled product exhibits deviation from its nominal design. There exists no model to predict the resulting non-nominal geometry of assembled product.

Most current computer-aided design (CAD) systems are based on rigid body geometry. Rigid parts cannot be assembled if there is any error in the geometry of parts, fixtures or weld guns. Only when parts are compliant that they deform to "absorb" these variations and make the assembly feasible. Sheet metal assemblies cannot be assumed to be rigid since compliance of the parts has such a profound influence on the assembly. Hence, current CAD systems which can represent only rigid bodies, cannot be used to predict the geometry of an assembly of compliant parts.

Hence, there is a need for a model to predict geometry of compliant parts as they propagate through the assembly process.

1.3 Problem Statement

The objective of this thesis is to model the assembly of compliant parts as they propagate through the assembly line.

This involves several aspects:

- Representation of the different aspects of the assembly
  - Nominal geometry of the parts/sub-assemblies, fixtures and weld guns

---

[2] Intentional gaps should not be confused with margins. Intentional gaps are gaps between mating surfaces of parts *before* they are assembled and margins are gaps between parts *after* they are assembled.

    - Assembly sequence
    - Connectivity information
    - Non-nominal geometry of the parts/sub-assemblies, fixtures and weld guns
- Detailed analysis of an assembly station
    - An assembly station is a unit of the assembly process. A detailed analysis of one assembly station is essential to understand the behavior of parts within that assembly station. Operations that occur in every assembly station need to be identified and examined for a better understanding of the assembly process.
- Prediction of part geometry
    - Parts go through an assembly line, which has a number of assembly stations. Usually, parts and sub-assemblies are inspected after every few assembly stations as a part of statistical process control to ensure the dimensional integrity of the assembly. The model should be able to predict the geometry of the assembly after any assembly operation..
- Assembly with intentional gaps and nominal geometry
    - Nominal parts can lead to non-nominal assemblies in the presence of intentional gaps. i.e. the effect of intentional gaps cannot be ignored. The assembly model should be able to predict the resulting geometry when nominal parts with intentional gaps are assembled.
- Assembly with intentional gaps and non-nominal geometry
    - In real life situations, parts, fixtures and weld guns have non-nominal geometry. The model should be able to represent is non-nominal geometry and be able to quantify its effects on the assembly.

1.4 Organization of Thesis

Chapter 2 discusses past research efforts in the area of this thesis. It discusses existing ways to model the assembly rigid and compliant bodies. It provides an overview of research work specific to assemblies of sheet metal parts.

Chapter 3 describes the assembly model presented in this thesis. It presents the representations used for the different aspects of the assembly process, such as, nominal and non-nominal geometry of parts and sub-assembly, the assembly sequence, and connectivity information. It examines one assembly station in detail and identifies the assembly operations that influence the geometry of parts. It then provides a step-by-step procedure to predict the geometry of parts after any operation of the assembly process. It provides an example of application of this method.

Chapter 4 presents application of the model to the assembly of the front end of an automobile. This assembly has five parts: inner fender, reinforcement, radiator support, body, and outer fender. The geometry of this assembly after as it propagates through three assembly stations and one inspection station is predicted.

Chapter 5 discusses the application of this model to the design of locator schemes for parts. A locator scheme is the number, type and position of locators used to position a part on its fixture. Fixtures play a central role in the assembly of compliant parts. Chapter 5 provides metrics that can be used to compare candidate locator schemes for a part. It then describes a two-dimensional and a three-dimensional scenario of selecting locator schemes for the inner fender.

Chapter 6 summarizes the thesis and presents the conclusions. It provides direction for future work that can be pursued in this area. It discusses opportunities for improvement on this model.

2.

Related Work

This chapter discusses related work in the current literature. Assemblies have been modeled in various ways by a number of researchers including Lee and Gossard (Lee85), Turner (Turner90) and Wang and Ozsoy (Wang90). Here we consider two areas of interest: assembly of rigid parts and assembly of compliant parts.

2.1 Assembly of Rigid Parts

The study of the assembly of rigid parts deals with influence of part tolerances on assembly dimensions. This research area examines multiple rigid parts in multiple assembly stations to determine the final assembly dimensions.

Tolerance is defined as the permissible variation of a dimension in engineering drawings or designs (ANSI 1983). Guilford and Turner suggested classifying various representation methods into parameter space, solid offset and feasibility space approaches (Guilford93). The parameter space approach is described by Hillyard and Braid (Hillyard78), Light and Gossard (Light82) and Martino and Gabriele (Martino89). The offset solid approach is described by Requicha (Requicha83) and the feasibility space approach is described by Turner and Wozny (Turner90).

When part geometry is not ideal, the spatial relations between adjacent parts are not always satisfied. Fleming proposed a method to find the range of part positions in an assembly of rigid parts with known ranges of error (Fleming88). He modeled spatial relations between parts as inequality constraint equations for non-interference of parts. Turner formulated the part positioning problem as a constrained optimization problem (Turner90). He used the sum of the gaps between mating parts as the objective function.

Part positions are used as variables and non-interference requirements are formulated as constraints for the optimization problem.

Study of assemblies of rigid parts also involves tolerance analysis of these assemblies. Bjorke provided a comprehensive approach to statistical tolerance analysis for open dimensional stackups (Bjorke89). The worst case method evaluates an assembly by assuming that the dimensions of all components occur at their extreme permissible values at the same time (Spotts78; Chase87). While the worst case method is simple, it overestimates the result. In the statistical method, the dimensions are assumed to have known probabilistic distributions. This method is more effective, but is computationally intensive. Early and Thompson presented a report on the commercial software VSA, to perform variation analysis of the assembly of rigid parts using Monte Carlo simulation.

Whitney proposed a methodology to represent ANSI Y 14.5M tolerances using homogeneous matrix transforms (Whitney93). He calculated a statistical estimate of the location of the n th part in an assembly starting from the first part.

2.2 Assembly of Compliant Parts

The research work pertaining to assembly of compliant parts can be classified into two broad areas: assembly of prismatic parts and assembly of sheet metal parts.

2.2.1 Assembly of prismatic parts

Most of the research literature in assembly of prismatic parts studied the fixturing of a part and focused primarily on the design of fixtures.

Lee and Haynes performed a finite element analysis of a prismatic workpiece under clamping force, friction force and the machining force (Lee86). They called the deformation of the workpiece under clamping force as "tightness." They plotted the deformation at certain other nodes, total work done, maximum stress values as a function of tightness. Based on this graph, they chose an appropriate value of tightness.

Menassa and DeVries developed a method for selecting an optimal position of the fixture supports (Menassa88). The optimization is done is two parts. In the first part, they determined optimal position of the supports using the BFGS optimization algorithm (Broyden-Fletcher-Goldfarb-Shanno). In the second part, they used a finite element model to evaluate their objective function. Their objective function was a measure of workpiece deflection at selected points. They remeshed the workpiece and iterated till they got the optimal solution.

Pham and Lazaro developed an expert system AUTOFIX for fixture design (Pham90). It interfaced with the interactive CAD package I-DEAS, for defining part geometry and for finite element analysis. The workpiece was drawn in I-DEAS in terms of primitives and was meshed manually. I-DEAS calculated the min/max deflections and AUTOFIX automatically repositioned the supports.

2.2.2 Assembly of sheet metal parts

This section focuses on current literature on the analysis of sheet metal assemblies. It discusses statistical analysis for root cause detection, tolerancing, and modeling of the assembly process.

Takezawa claimed that dimensional variation of sheet metal assemblies was different from that of a rigid body (Takezawa80). He showed that the addition theorem of variance is invalid for the assembly of sheet metal parts.

Plonka provided an algorithm for tolerancing sheet metal parts and sub-assemblies by formulating a least-cost tolerancing problem (Plonka74). He estimated the components of variance for the major process factors and conducted experiments to correlate predicted and actual process transformations.

Youcef-Toumi, Liu and Asada used finite element analysis to find normal stresses in a workpiece under machining forces (Youcef-Toumi88). They used a fixturing layout which was characterized by a parameter. They performed the analysis a number of times to find the parameter value that minimized the stresses and strains in the workpiece.

Du and Chan proposed a beam model to calculate the torsional and bending stiffness of an automobile body (Du83). Chan proposed a method based on Castigliano's theorem to perform design sensitivity analysis for large-scale structures such as the automobile body (Chan83). Chon et al developed a stick-model for measuring the bending and torsional stiffness of vehicle structures (Chon86). Kang presented a beam based skeleton-model of the body structure to optimize it for overall static stiffness (Kang91). Fenyes examined the structure of a front-wheel drive compact car for selective replacement of strength constrained members with alternate materials (Fenyes81).

Hu proposed principal component analysis as a statistical tool to identify sources of dimensional variation in automobile body assembly (Hu92). In his technique, the eigenvectors and eigenvalues of the correlation matrix represent the principal components and their variances respectively. Ceglarek proposed a knowledge-based diagnostic approach for the auto-body assembly process launch (Ceglarek94). He used

statistical techniques on in-line dimensional measurements to identify a candidate station and a candidate component to localize the fault in the assembly process.

Liu et al evaluated the effects of deformation on component tolerances using linear mechanics (Liu96). They studied two basic configurations, assembly in series and assembly in parallel, of one-dimensional parts at being assembled at one assembly station. They used finite element analysis to examine the effects of assembly sequencing and the effects of multiple joints on the assembly tolerance.

Chang proposed a two-step process to simulate the propagation of variations in the assembly process (Chang96). He first calculates the deviation of weld spots and then finds the variations in assembly from constitutive relations, geometric compatibility and force continuity.

2.3 Discussion

This chapter presented research literature relevant to this thesis. The research work in assembly of rigid parts considers multiple rigid parts. The current literature in assembly of compliant parts focuses primarily on one part in one assembly station. The focus of this thesis is the assemblies of multiple compliant parts that propagate through multiple assembly stations. There exists little research literature on this area.

3.

Assembly Modeling

This chapter describes the assembly process of a generic automobile body. It then discusses in detail the assembly model and the representations used. It describes the method to predict the geometry of the final product as it goes through this assembly process.

3.1 Automobile Body Assembly Process

Major stages of the manufacturing process are stamping and assembly. The assembly process can be further classified into (1) sub-assembly (2) body framing, and (3) panel hanging. Let us discuss these processes in detail.

3.1.1 Stamping

The stamping of a sheet metal part involves five operations (see Figure 3-1),

1. Blank: Rectangular sheets (also called, blanks) are cut from the roll of sheet metal.
2. Draw: Gross geometry is made at this stage. Locator surfaces are established. Locator holes and slots cannot be established at this stage, since they would get distorted in subsequent operations.
3. Pierce: The panel is pierced using punches. Cavities are made in the panel in this process. All locator holes are established in this first pierce operation. Since draw-and-pierce operations are performed by one die, distortion of the locator holes is minimized. These holes are used in subsequent operations to locate the part in the stamping die, assembly fixture, or inspection gage.

4. Trim: Extra material is trimmed from the panel.
5. Flange: Flanges are made by bending the sheet metal at an angle with respect to the punching direction.
6. Restrike: Final geometry is made.

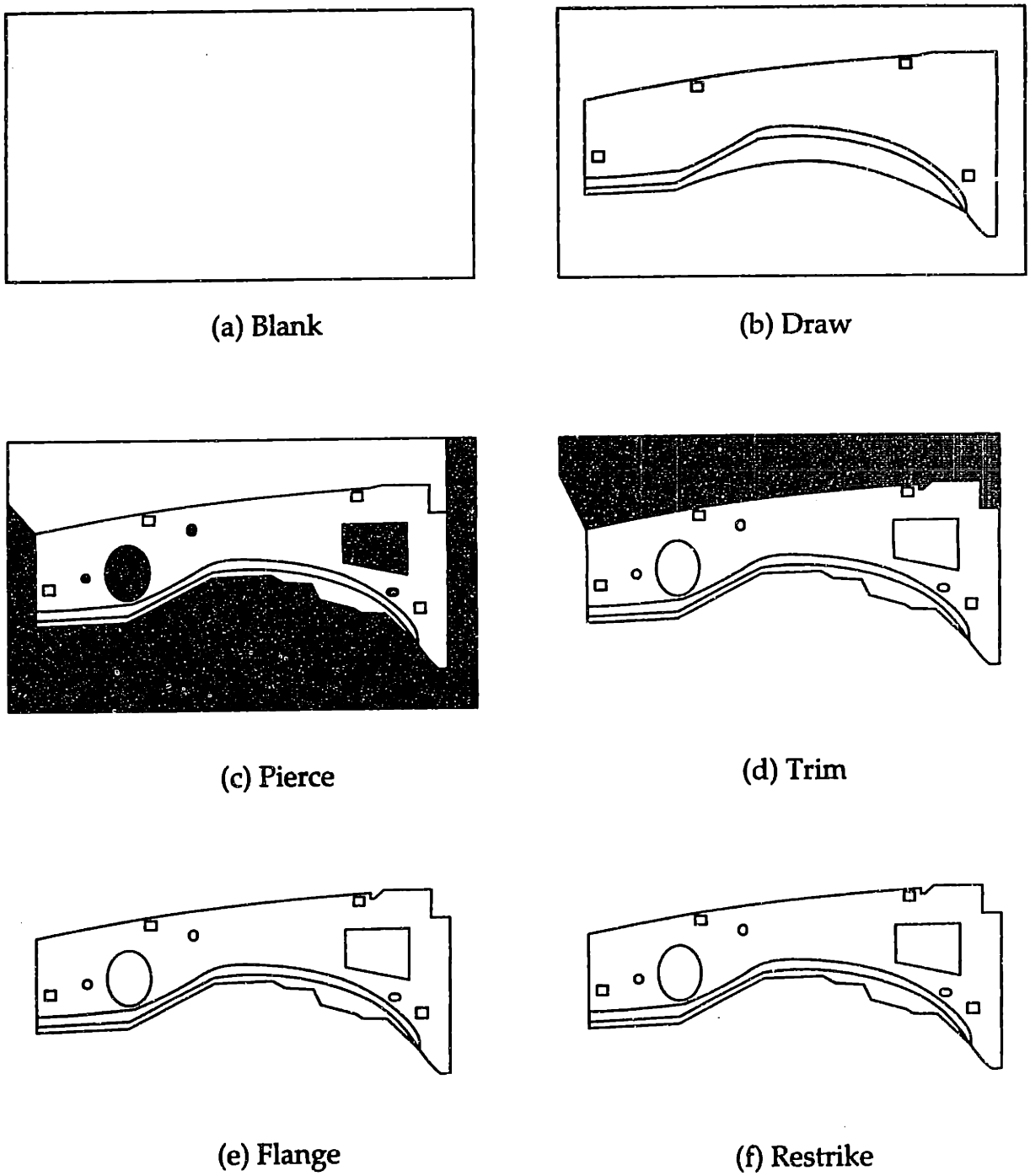

(a) Blank (b) Draw

(c) Pierce (d) Trim

(e) Flange (f) Restrike

Figure 3-1. Stamping of a sheet metal part

3.1.2 Assembly

A typical complete automobile body is composed of the body-in-white (BIW) and the hang-on panels. A BIW, also known as "body as framed," is assembled by welding together major components including the underbody, side frames, roof, shelves, and back panels (see Figure 3-2). The underbody is made by welding together the motor compartment, floor pan and rear seat compartment. The underbody is located in the body framing fixture by its locator holes and surfaces. Then the body-sides, roof, lower back panel, package tray and cowl top are located in relation to the underbody. These components are then welded together to form the body-in-white (BIW).

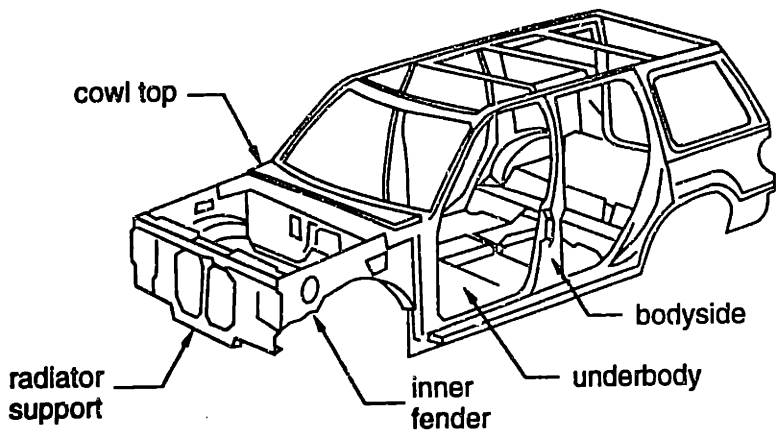

Figure 3-2. The body-in-white

When the body-sides and underbody are assembled in the body framing process, the locators of each assembly are used to precisely locate and orient them to each other.

For the side frame, different structures have been used, but it generally includes the door ring, quarter panel, motor rail and the wheel house. The side frames determine the size of the door openings. Together with the roof, the side frames also provide the size of the windshield and back-light openings. After the completion of a BIW, hang-on panels such as doors, hood, and deck-lid are attached to the BIW. This is usually called the *panel hanging process*. Finally, the complete BIW goes to the paint shop, and general assembly (trim) operations.

Most sub-assemblies consist of a main panel and 3-4 reinforcements. These reinforcements are welded on to the main panel in welding stations. At every subsequent assembly station, the sub-assembly is positioned into the fixture using the locator scheme of the main panel. Dimensional variation of a BIW is influenced by every stage of the entire body manufacturing and the assembly process.

3.2 Locator Schemes

At every station (an assembly or inspection station), parts are positioned on the fixtures by *locators*. Locators are features on parts that mate with corresponding features on the fixtures to position the part with respect to the fixture. Locator features on sheet metal parts are holes, slots and surfaces. Locator features on fixtures are pins and clamps. A pin on a fixture mates with a hole or a slot on the part. A clamp on the fixture mates with a surface on the part.

Locator schemes are the number, type and position of locators. There are two generic locator schemes used in the automobile industry: hole-slot-surface scheme and the n-2-1 scheme. Both these locator schemes are based on the conventional 3-2-1 principle (Boyes89). The following sections discuss the two locator schemes in detail.

3.2.1 The hole-slot-surface scheme

The hole-slot-surface scheme is the most commonly used locator scheme in the automobile industry for assembling structural parts in an automobile body. This scheme consists of a main locator hole, a slot and a number of surfaces on the part (see **Figure 3-3**). The main locator hole establishes the position of the part in two directions, in this case (up/down and fore/aft). The slot, also called the secondary locator hole, prevents the part from rotating about the main locator hole. Now, the part remains free to move in the in/out direction. Locator surfaces establish the position of the part in the in/out direction, and complete the location and orientation of the part with respect to the fixture.

Depending upon the configuration, size and flexibility of the part, additional locator surfaces and secondary locator holes are used to ensure that all areas of the part are positioned properly and consistently throughout the manufacture and assembly processes.

3.2.2 The n-2-1 locator scheme

The n-2-1 locator scheme (Cai94) uses only surfaces to position the part. First, a number of clamps are used as primary locators to position the part on a plane. Two secondary and one tertiary locators are then used to position the part accurately. Since this scheme involves only surfaces of the part to be used as locators, it does not require any additional holes or slots in the part. For parts that are visible to an automobile customer and cannot have locator holes or slots on them, the n-2-1 locator scheme is often used.

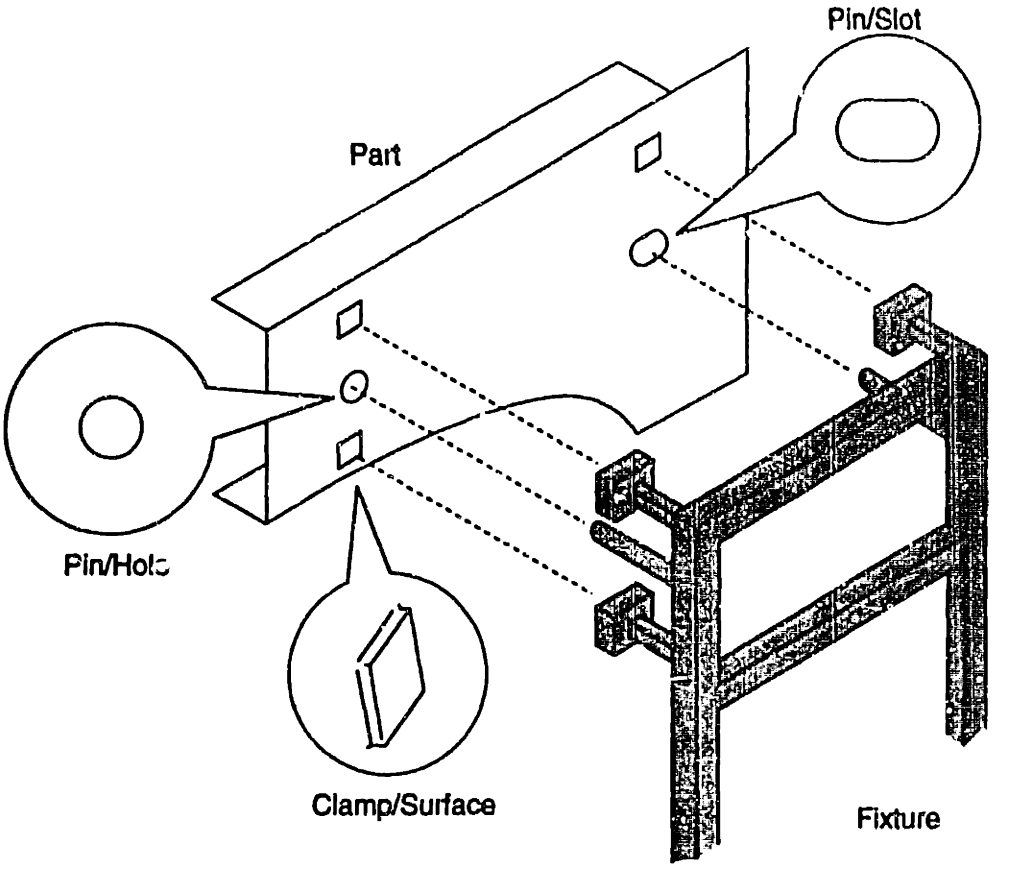

(a) 3-D Scenario

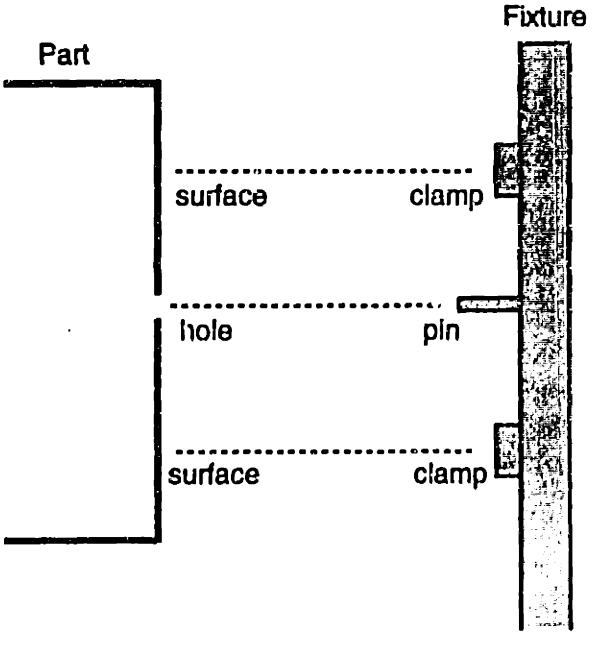

(b) 2-D Scenario

Figure 3-3. The hole-slot-surface locator scheme

3.3 The PCFRR Cycle

An assembly station is a unit of the assembly process. At every assembly station the following operations are performed. Parts are placed on the fixtures. Clamps are activated to clamp the parts to the fixtures. Parts are welded (fastened), weld guns are retracted and finally the clamps are released and the sub-assembly is removed from the fixture. This is the PCFRR cycle (place, clamp, fasten, retract and release). A typical sub-assembly goes through about five PCFRR cycles before it is finally assembled to the BIW. These operations are discussed in detail in the following sections (Figure 3-4):

3.3.1 Place

Parts are first placed in their respective fixtures. Both parts have their own locator schemes with which they are positioned on the fixtures. In the place operation, pins on fixtures engage with the corresponding holes or slots on parts.

3.3.2 Clamp

After placing the parts in the fixtures, they are clamped. Clamps are surfaces on the fixture that hold a locator surface on the part. After the part is clamped, the positioning of the part is complete. Ideally, the clamping sequence for all assembly stations is the same. Clamps on inspection fixtures are also activated in the same clamping sequence as those on assembly fixtures.

Clamps usually over-constrain the parts. i.e. the clamps constraint more than six degrees of freedom, making it a statically indeterminate system. This is done to keep the deformation of the parts under external forces to a minimum.

3.3.3 Fasten

After clamping, welding guns are activated and parts are fastened (welded) at mating surfaces. The weld gun is either positioned with respect to a stationary sheet metal part or the sheet metal part is positioned with respect to a stationary weld gun. Table 3-2 summarizes the different scenarios. Once parts are fastened, they form a sub-assembly. In the presence of intentional gaps between parts, the weld guns close these gaps during welding. This causes deformation of the parts.

parts, due to geometric incompatibility during the PCFRR cycle. These forces cause parts to deform. Forces are exerted as a result of

(i) Intentional gaps in product design,

(ii) Non-nominal geometry,

(iii) Gravity.

3.4.1 Intentional gaps in product design

Often, gaps are intentionally designed between mating surfaces of two parts in an assembly. This is done to facilitate loading and unloading of parts into fixtures. Also, intentional gaps act as buffers to "absorb" the imperfections in geometry (of parts, fixtures and weld guns). These intentional gaps are closed by the weld guns during the fastening operation of the PCFRR cycle. Hence, there exists deformation in spite of nominal geometry of incoming parts, fixtures and weld guns.

Figure 3-5 shows the behavior of parts during a PCFRR cycle for an assembly with intentional gaps between mating surfaces. Here, all parts, fixtures and weld guns have nominal geometry. Since the geometry is nominal, there is no part deformation during the place and clamp operations. When the weld guns close the intentional gap between the mating surfaces, they exert forces that deform the parts. The parts partially spring back when weld guns retract and then completely when the sub-assembly is released.

3.4.2 Non-nominal geometry

Non-nominal geometry is deviation of actual geometry from its nominal value. Nominal value of geometry is the geometry represented in its design. i.e. in engineering drawings and CAD representations.

$$\begin{Bmatrix} Non\text{-}nominal \\ geometry \end{Bmatrix} = \begin{Bmatrix} Nominal \\ geometry \end{Bmatrix} + \begin{Bmatrix} Manufacturing \\ variation \end{Bmatrix} \qquad \text{Equation 3-1}$$

Non-nominal geometry can cause part deformation as parts propagate through the assembly line. Non-nominal geometry can be classified into three categories as follows:

3.4.2.1 Non-nominal part geometry

Non-nominal part geometry is also referred to as manufacturing variation in the part geometry. These variations are inevitable and depend on the manufacturing

Table 3-2. Positioning of weld gun with respect to the part in different types of assembly processes

Type of assembly process	Weld gun	Sheet Metal Part
Robotic assembly	Positioned by robot	Stationary
Manual assembly	Positioned by operator	Stationary
Fixture assembly	Stationary	Stationary

Welding guns provide constraints to the parts in addition to those provided by the clamps and pins. Parts deform under the resulting weld gun, clamping and positioning constraints. Thickness of parts is small (about 1 mm), and deformation is primarily due to bending. So, part deformation is mostly out-of-plane and not within the plane of the sheet metal.

3.3.4 Retract

After fastening, the weld guns are retracted. In the presence of non-nominal geometry or intentional gaps, the sub-assembly partially springs back due to release of the constraint from the weld gun.

3.3.5 Release

After retraction of the weld guns, the clamps are released and the sub-assembly is removed from the assembly fixture. Since all constraints on the part are now released, the sub-assembly completely springs back. The sub-assembly has stresses locked in, which manifest as deformation of the sub-assembly. The resulting geometry is different from the intended geometry of the sub-assembly in the presence of non-nominal geometry (of weld guns, fixtures or incoming parts) and/or intentional gaps.

3.4 Causes of Part Deformation

If parts, fixtures and welding guns have ideal geometry and there are no intentional gaps, then (in a gravity-free environment) there are no forces exerted during the PCFRR cycle. When there are no forces acting, there is no part deformation. i.e. no spring back (see Figure 3-4). If there are intentional gaps in the product design, or if there exists non-nominal geometry (of incoming parts, weld guns or fixtures) or if gravity effects are significant, forces are exerted by the fixture and/or welding guns on the

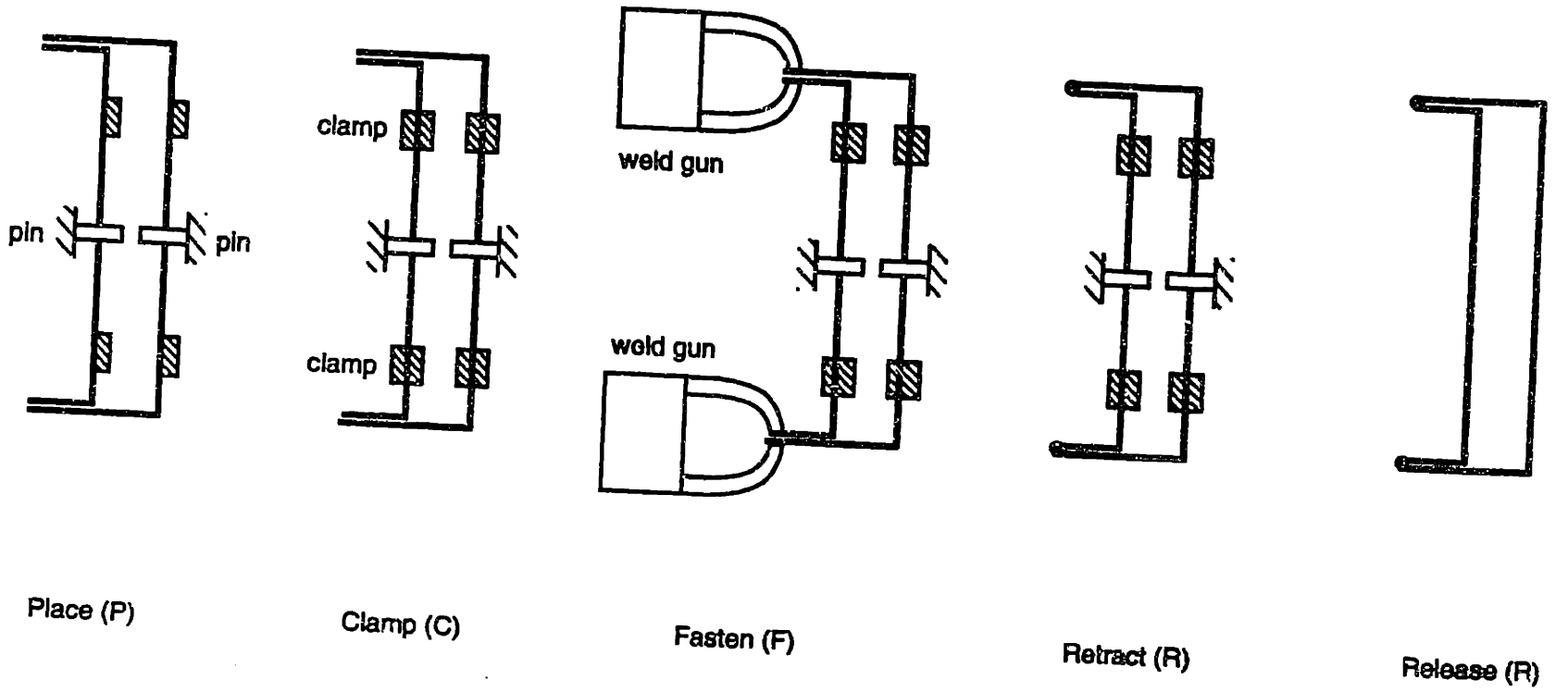

Figure 3-4. The PCFRR cycle

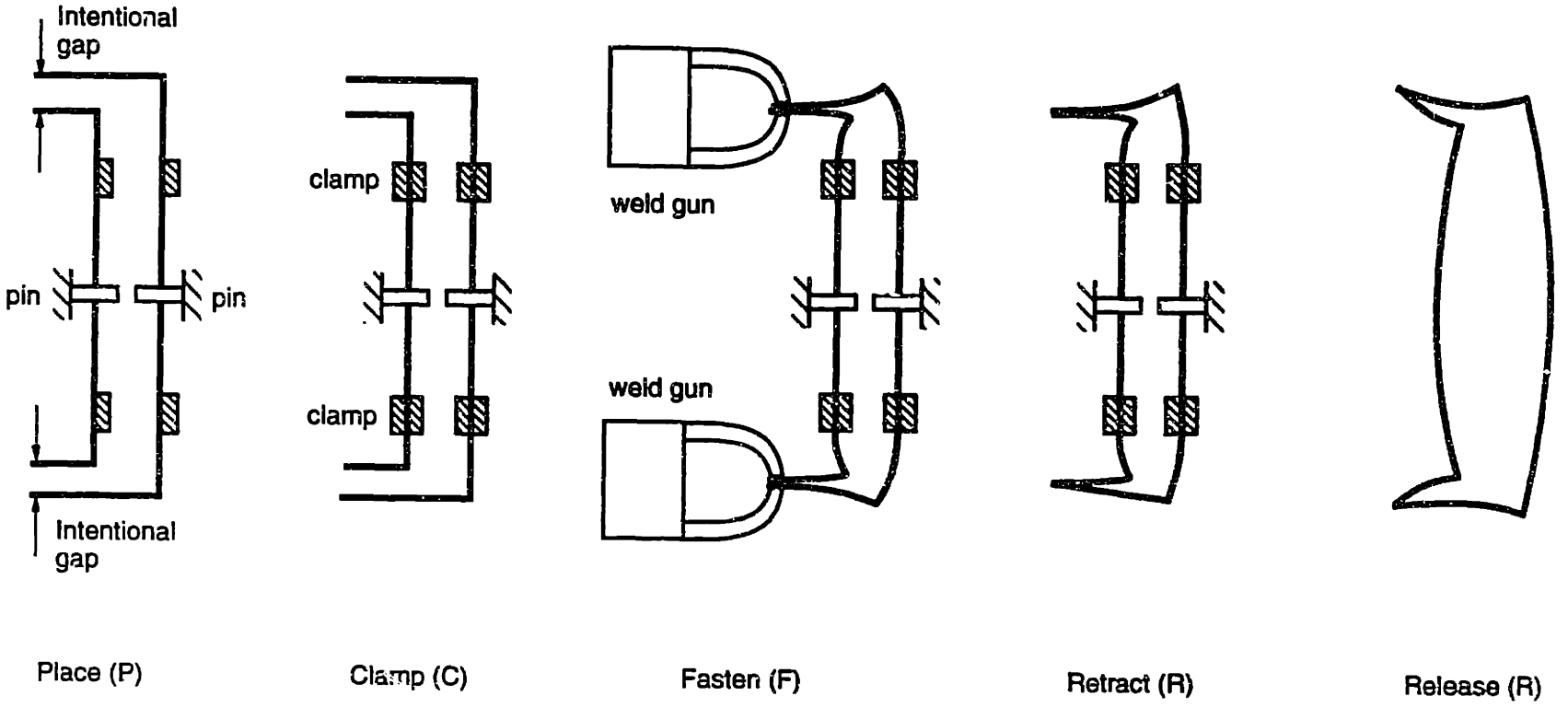

Figure 3-5. The PCFRR cycle for an assembly with intentional gaps between mating surfaces and parts with nominal geometry

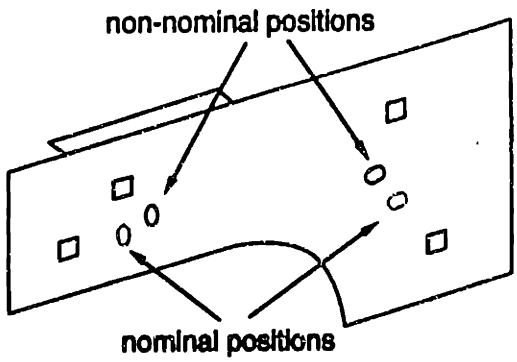

Figure 3-6. Examples of non-nominal part geometry

process. Figure 3-6 shows an example of a non-nominal part where the locator hole and slot are mislocated.

3.4.2.2 Non-nominal fixture geometry

Non-nominal fixture geometry refers to mislocation of locators on fixtures. If pins and clamps on the fixtures are not at the nominal position, they can cause parts to deform. Figure 3-7 shows an example of a non-nominal fixture where a clamp is mislocated.

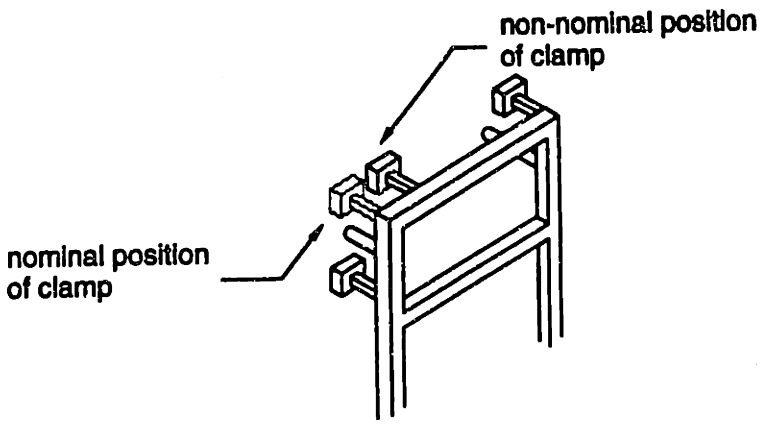

Figure 3-7. Example of a non-nominal fixture

3.4.2.3 Non-nominal position of weld guns

Welding guns are positioned with respect to the part as shown in Table 3-2. A non-nominal position of a weld gun refers to a mislocated weld gun. A welding gun welds the parts at their mating features (part/part interface which is always a surface/surface interface). Mislocation of the welding gun is measured normal to this welding surface.

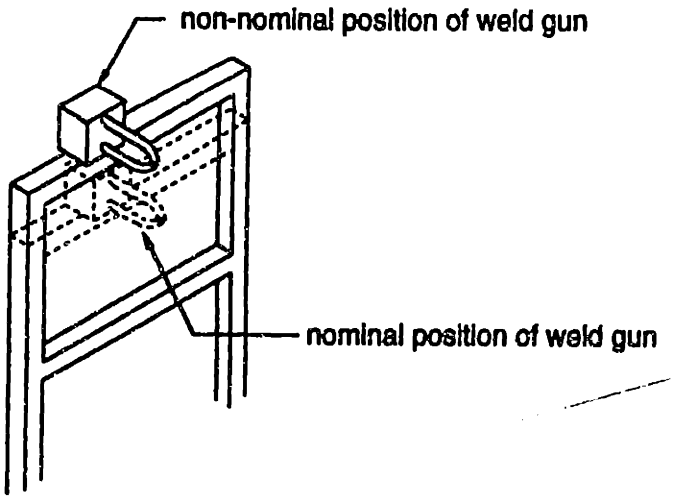

Figure 3-8. Example of non-nominal position of a weld gun

Figure 3-9 shows the behavior of parts for a PCFRR cycle for an assembly with intentional gaps between mating surfaces and parts with non-nominal geometry. Parts deform when the parts are clamped to the fixture. They undergo further deformation when they are welded (fastened), when weld guns retract and when clamps are released.

3.4.3 Gravity

Large sheet metal parts, like the roof, undergo deformation under the influence of gravity. Unlike the reaction forces at weld guns and locators, which are point forces (i.e. forces applied at one point on the part), gravity is a body force and acts on every point on the part. Although large parts can deform significantly under gravity, its influence is negligible for small-sized parts.

3.5 Model Overview

We want to predict the geometry of the assembly at any stage in the assembly process[3]. This section discusses the development of an analytical model that takes geometry of incoming parts, positions of weld spots, weld guns and fixtures as inputs and predicts the geometry of the out-going assembly.

Figure 3-10 shows an overview of the model, the inputs and the outputs. The procedure to predict the geometry of parts after any operation (such as place, clamp,

---

[3] The geometry of the sub-assembly is measured on the inspection fixture. This is done by first releasing the sub-assembly from its assembly fixture and then placing/clamping it on its inspection fixture. The inspection operation is similar to the assembly operation (PCFRR cycle). In the inspection process, however, the fasten-release operations in assembly process are replaced by "inspect" operation. However, this difference does not affect our analysis.

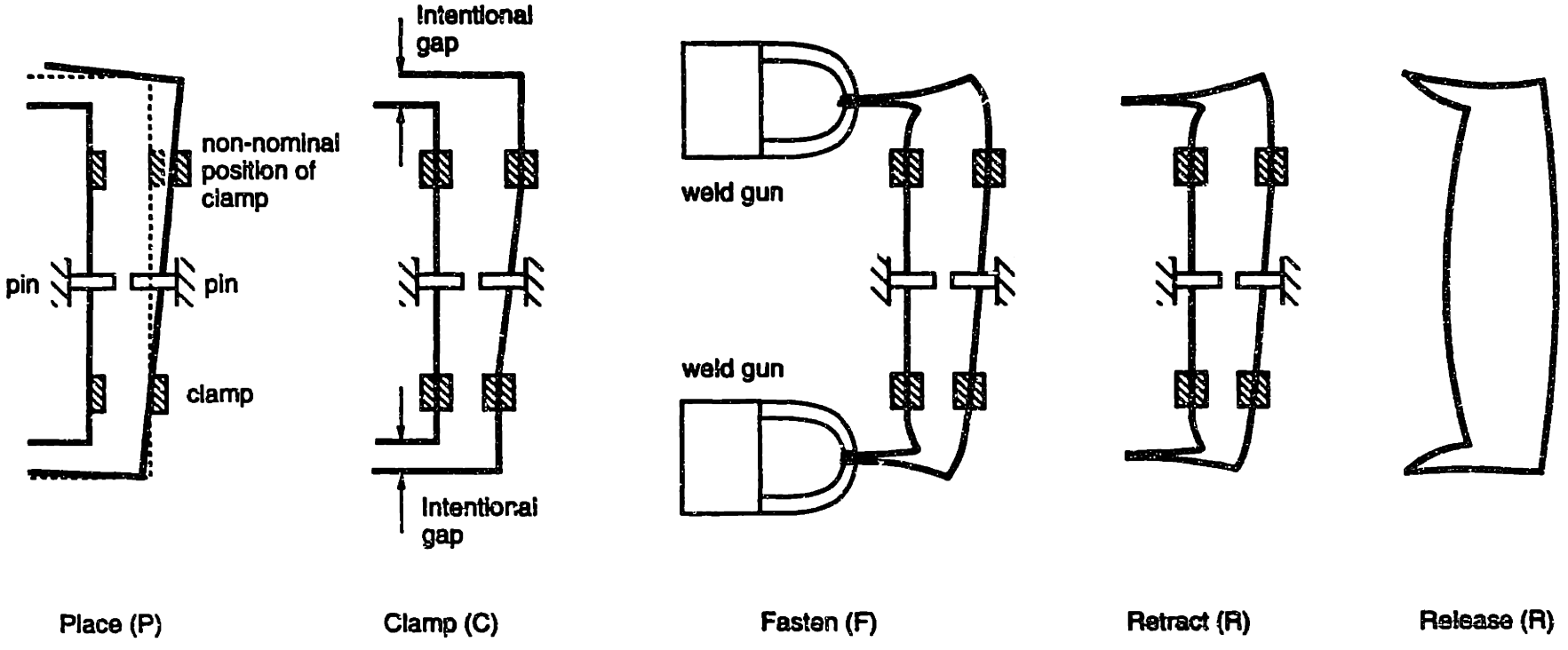

Figure 3-9. The PCFRR cycle for assembly with intentional gaps and non-nominal geometry

fasten, retract or release) and to predict the geometry of the final assembled product is described in section 3.8.

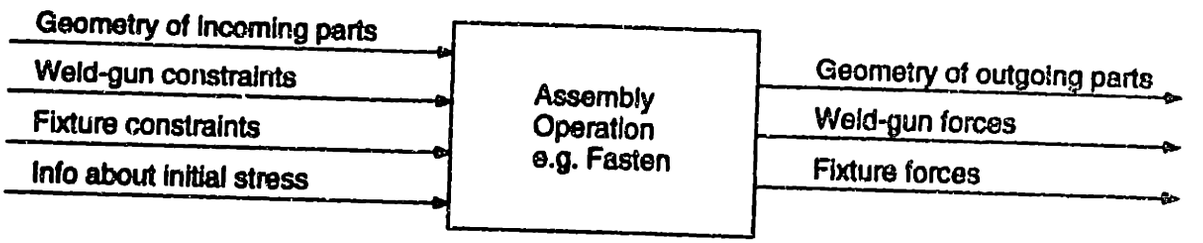

Figure 3-10. Model overview

The mathematical abstraction of different components of the assembly process is done to use existing numerical techniques to simulate the assembly process. Finite element analysis is used as the primary computational tool (Figure 3-11). Our problem is formulated and the entire assembly process is represented so as to use finite element analysis. We will start with the geometry of incoming parts and use the appropriate boundary conditions to calculate the geometry of out-going assembly. In the following sections we will discuss modeling assumptions and the representations of all components of the assembly process.

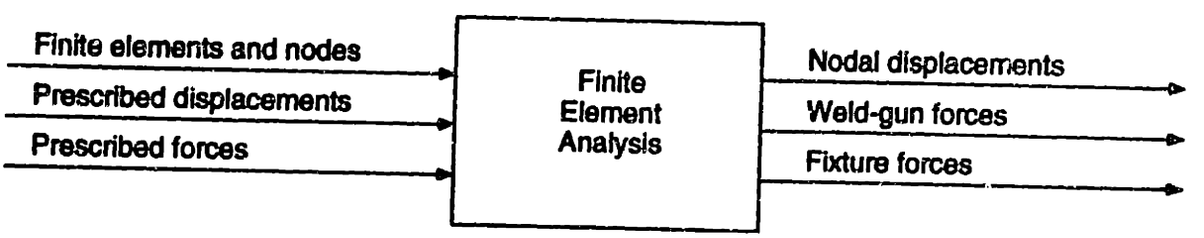

Figure 3-11. Schematic of finite element analysis

3.6 Modeling Assumptions

The modeling assumptions and justifications used to develop the analytical framework for predicting the geometry of assembled product are discussed in detail. Modeling assumptions specific to certain assembly representations are described in section 3.7.

3.6.1 Material is isotropic and linearly elastic

All parts are assumed to be compliant and that their material is isotropic and linearly elastic. The sheet metal is steel with elastic constants, E = 210 GPa and ν = 0.3. Parts are assumed to undergo elastic deformation only and that there is no plastic

deformation. Although the stamping operation introduces anisotropy in the sheet metal part, it affects only the plastic behavior of the parts and so can be neglected.

3.6.2 Fixtures and weld guns are rigid

Fixtures and weld guns are much stiffer than the sheet metal parts. Pins and clamps on the fixtures and weld tips have a much larger cross section as compared to the sheet metal parts, which are around 1-2 mm thick. The fixtures and weld guns are assumed to be rigid and undergo no deformation.

3.6.3 Friction is negligible

During the stamping operation, blanks are coated with oil to reduce friction between the part and the die. After stamping, the parts are assembled. The oil on the surface of the parts acts as a lubricant to reduce friction between the part and the assembly fixtures. Effects of friction on the assembly process are neglected.

3.7 Representation

This section presents the representation used for different components of the assembly process, such as, parts, sub-assemblies, fixtures, weld guns etc.

3.7.1 Parts

3.7.1.1 Part geometry

Geometry of parts is defined in engineering drawings or as CAD drawings. For sheet metal parts, only one of the two surfaces of the part is stored digitally. The other surface is obtained by off-setting this surface by the thickness of the sheet metal. The stored surface is represented in a parametric form. Most CAD software use a surface representation of the parts such as a B-spline surface.

The stamping process causes the thickness of the sheet metal part to be different at different points on the part. This variation in thickness is usually very small and for our model, we can assume that the thickness of the sheet metal is the same everywhere on the part.

We will represent the geometry of the part as a set of finite elements and nodes. The parametric representation of the part in the CAD software is used to generate finite elements and nodes (Figure 3-12). The finite element mesh should be dense enough to provide sufficiently accurate results, but parse enough for fast computation. The aspect

ratio for the elements should be of the order 1 to avoid spurious results. The choice of the type of finite elements affects the accuracy and speed of the analysis. The type of finite element should be chosen so as to capture all anticipated modes of deformation. We used shell elements, since they can capture the out-of-plane deformation modes of the sheet metal quite well.

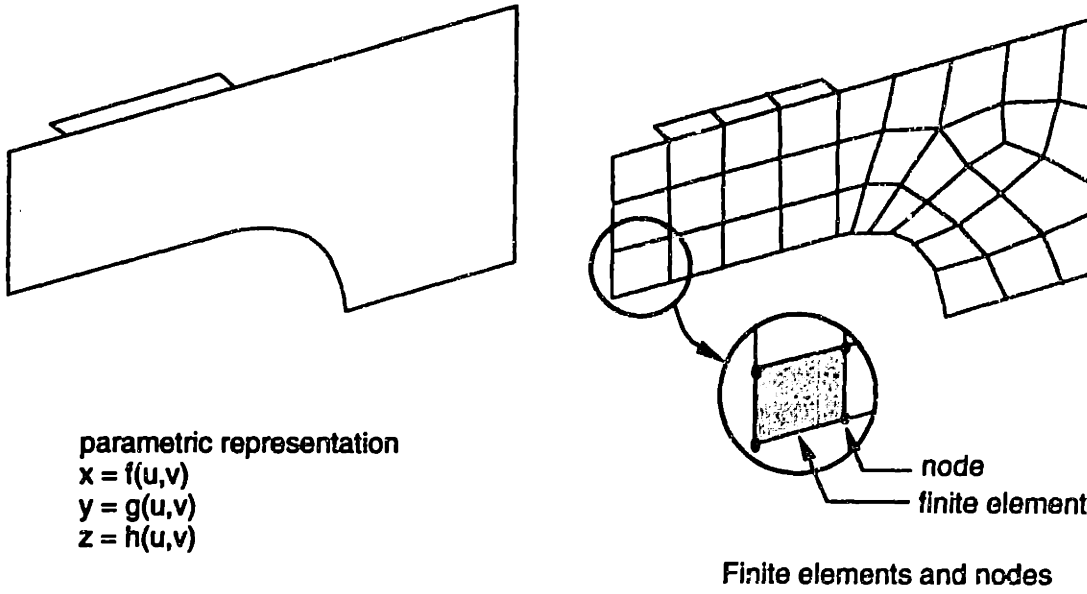

Figure 3-12. Representation of reference geometry of a part

3.7.1.2 Part features

Part features refer to locators (holes, slots, surfaces) and position of weld spots on the part. Locators and weld spots are represented as nodes (Figure 3-13). A nodal coordinate frame is associated with these features.

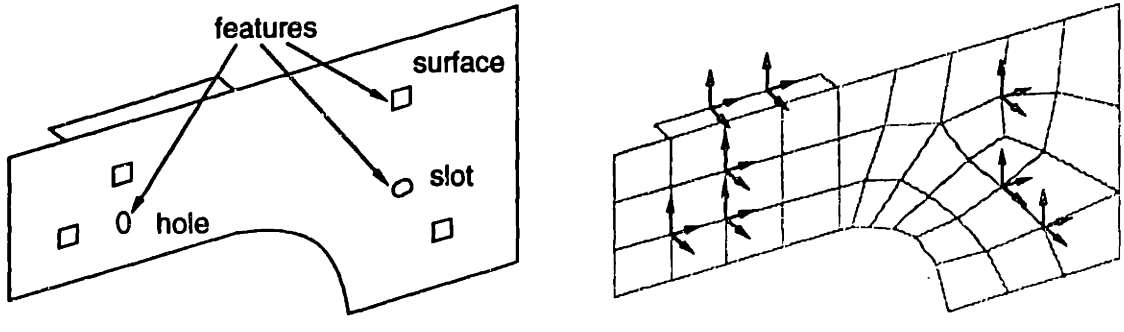

Figure 3-13. Representation of part features

3.7.1.3 Reference geometry of a part

We will use the undeformed nominal geometry of the part as reference. Part deformation is measured with respect to this geometry. Figure 3-12 shows the reference geometry. Every node on the reference geometry can have up to six degrees of freedom. Coordinates of a point on the reference geometry are denoted as (X_x, X_y, X_z) and the normal to the surface at that point is denoted as $(X_\theta, X_\phi, X_\varphi)$. Both can be concisely denoted as a vector, $\vec{X}_{part} = (X_x, X_y, X_z, X_\theta, X_\phi, X_\varphi)_{part}$.

3.7.1.4 Deformed geometry of a part

As the part propagates through the assembly line, it deforms. The coordinates of a point on the deformed part geometry and the normal to the surface at that point, are concisely denoted by a vector, $\vec{Y}_{part} = (Y_x, Y_y, Y_z, Y_\theta, Y_\phi, Y_\varphi)_{part}$. Similarly, the deformation is denoted by a vector, $\vec{U}_{part} = (U_x, U_y, U_z, U_\theta, U_\phi, U_\varphi)_{part}$. So,

$$\vec{Y}_{part} = \vec{X}_{part} + \vec{U}_{part} \qquad \text{Equation 3-2}$$

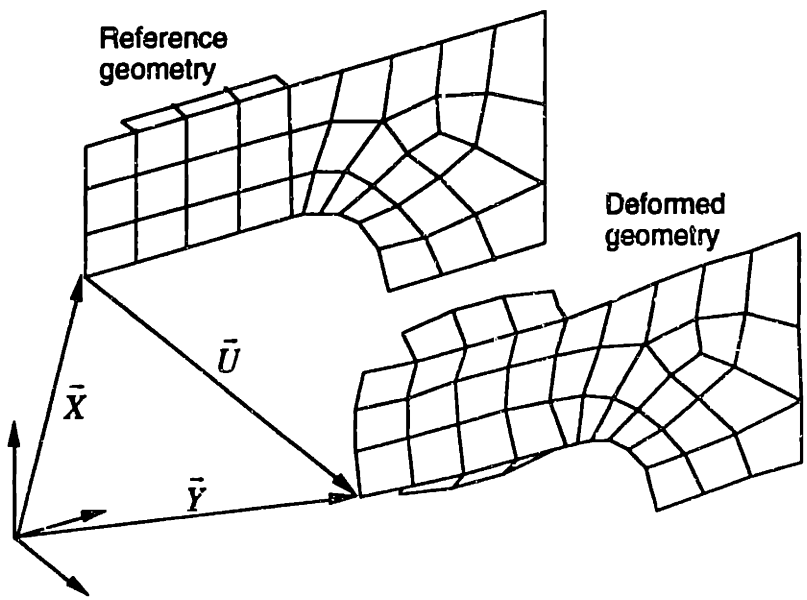

Figure 3-14. Representation of deformed geometry

Since we represent the geometry as a set of finite elements and nodes, $\vec{U}$ is the nodal displacement. Displacement of a point lying in the interior of the finite element can be obtained by using the interpolating function for the finite element.

3.7.2 Sub-assemblies

After parts are fastened, they form a sub-assembly. After parts are fastened, there is no relative rigid body motion between the parts. The weld spots hold together the two corresponding points on the two parts (Figure 3-15). This is modeled as a total constraint on all degrees of freedom of those two points. i.e. their corresponding displacements and rotations are the same.

Reference geometry for sub-assembly and the deformed geometry of the sub-assembly is represented similar to that of the part geometry (see section 3.7.1.3).

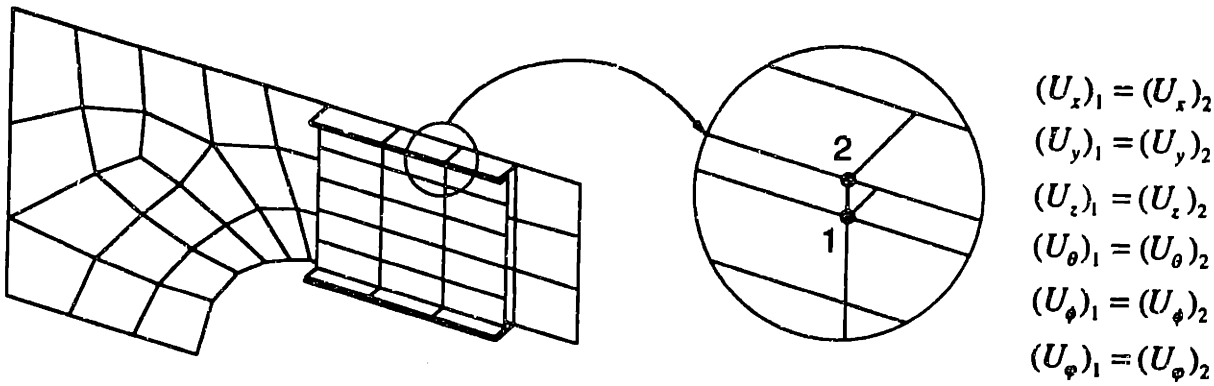

Figure 3-15. Representation of sub-assemblies

3.7.3 Fixtures

A fixture uses pins and clamps to position the part[4] during the assembly or inspection process. The *assembly fixture* positions the part during the assembly process and the *inspection fixture*, also called the gage fixture, positions the part during inspection. The inspection operation is similar to the assembly process, but for the difference that instead of the "fasten" operation, there is the "inspect" operation.

We represent the position of any point on the fixture and the corresponding normal, as a vector $\vec{X}_{fixture} = (X_x, X_y, X_z, X_\theta, X_\phi, X_\varphi)_{fixture}$. Since the fixtures are rigid, they do not undergo any deformation. The flexible parts, however, deform so as to conform to the corresponding features of the fixture. This can be represented mathematically as,

$$\vec{Y}_{part\ feature} = \vec{X}_{fixture\ feature} \qquad \text{Equation 3-3}$$

When we substitute Equation 3-2 in Equation 3-3 we get,

---

[4] We assume that after the part is placed and clamped on the fixture, there is no uncertainty in its position. Position uncertainty is discussed in detail by Fleming (Fleming88) and Inui (Inui91).

$$\vec{X}_{part\ feature} + \vec{U}_{part\ feature} = \vec{X}_{fixture\ feature}$$

$$\vec{U}_{part\ feature} = \vec{X}_{fixture\ feature} - \vec{X}_{part\ feature} \qquad \text{Equation 3-4}$$

The following sections describe special cases of fixture-part mating conditions and constrain equations corresponding to Equation 3-4.

3.7.3.1 Representation of a pin/hole mating condition

As Figure 3-16 shows, a pin restricts motion of the hole in the plane perpendicular to the axis of the pin (say, the z axis). It permits linear movement along the axis of the pin, and also all angular movements. For a pin/hole mating condition, from Equation 3-4,

$$\vec{U}_{hole} = \vec{X}_{pin} - \vec{X}_{hole} \qquad \text{Equation 3-5}$$

Writing Equation 3-5 in scalar form we get,

$$(U_x)_{hole} = (X_x)_{pin} - (X_x)_{hole} \qquad \text{Equation 3-6}$$

$$(U_y)_{hole} = (X_y)_{pin} - (X_y)_{hole}$$

3.7.3.2 Representation of pin/slot

As Figure 3-17 shows, a pin restricts motion of a slot in the plane perpendicular to the axis of the pin (say, the z axis). For a pin/slot mating condition, from Equation 3-4,

$$\vec{U}_{slot} = \vec{X}_{pin} - \vec{X}_{slot} \qquad \text{Equation 3-7}$$

Writing Equation 3-7 in scalar form we get,

$$(U_y)_{slot} = (X_y)_{pin} - (X_y)_{slot} \qquad \text{Equation 3-8}$$

Equation 3-6 and Equation 3-8 describe the displacement boundary conditions imposed by the pin on the fixture on the corresponding feature on the part, a hole and a slot respectively.

3.7.3.3 Representation of a clamp

Clamps consists of two flat surfaces between which a locator surface of a part is positioned. When clamp is closed, there is a gap of 0.01 mm between the sheet metal and the clamp surface (Figure 3-18). Clamps maintain the angle made by the part the same on both sides. i.e. the clamps can apply a moment to maintain a zero slope at the clamp. A clamps allows no movement normal to the clamp surface (say the z axis). We can represent the constraints imposed by the clamp on the part using Equation 3-4,

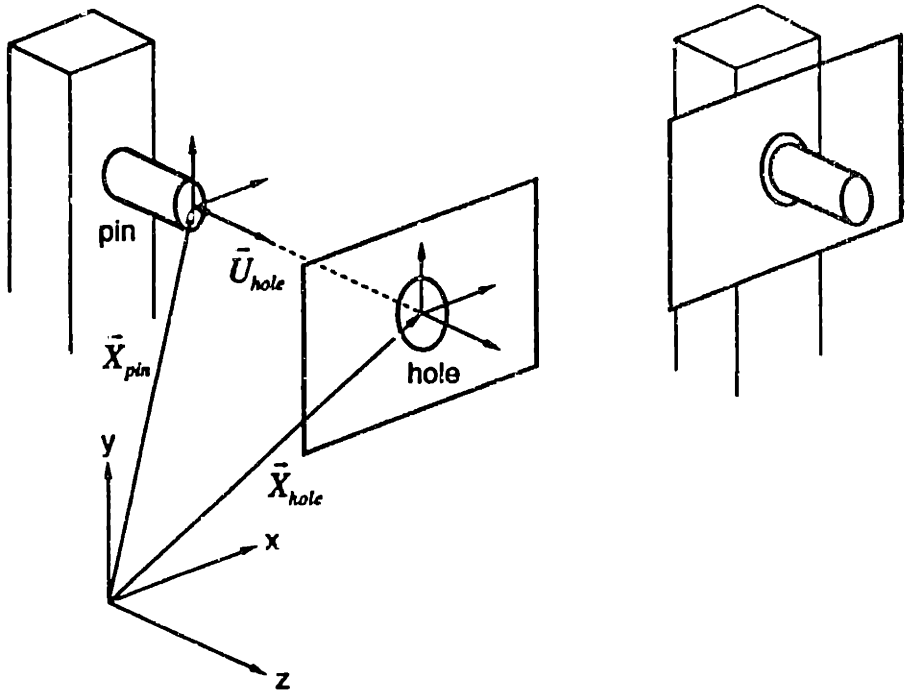

Figure 3-16. Representation of a pin/hole mating condition

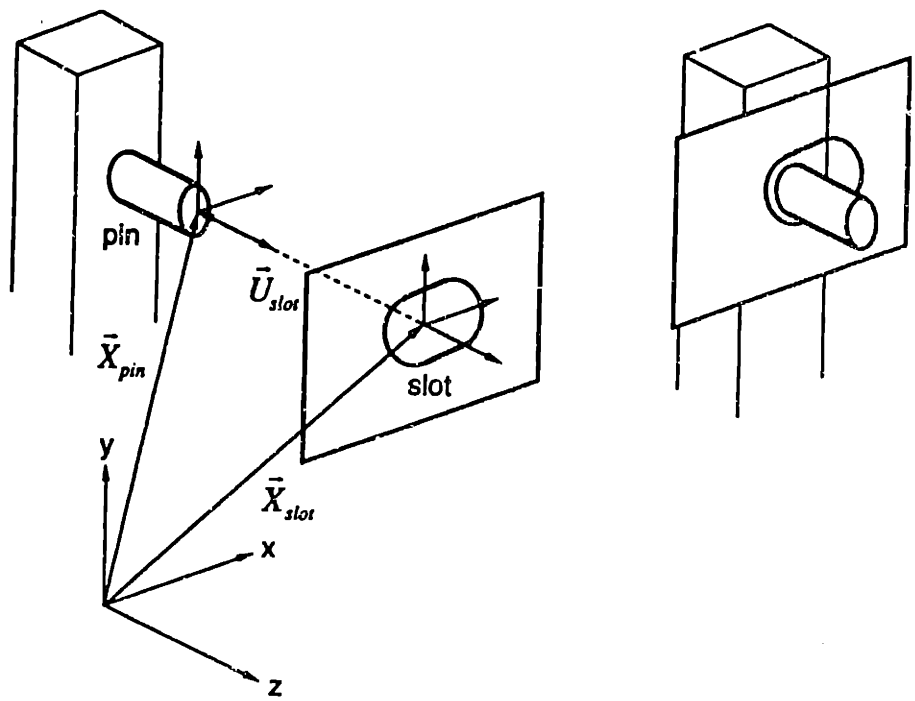

Figure 3-17. Representation of a pin/slot mating condition

Equation 3-9

$$\vec{U}_{surface} = \vec{X}_{clamp} - \vec{X}_{surface}$$

Writing Equation 3-7 in scalar form we get,

Equation 3-10

$$(U_z)_{surface} = (X_z)_{clamp} - (X_z)_{surface}$$
$$(U_\theta)_{surface} = (X_\theta)_{clamp} - (X_\theta)_{surface}$$
$$(U_\phi)_{surface} = (X_\phi)_{clamp} - (X_\phi)_{surface}$$

Equation 3-19 describes the displacement boundary conditions imposed by the clamp on the corresponding locator surface on the part.

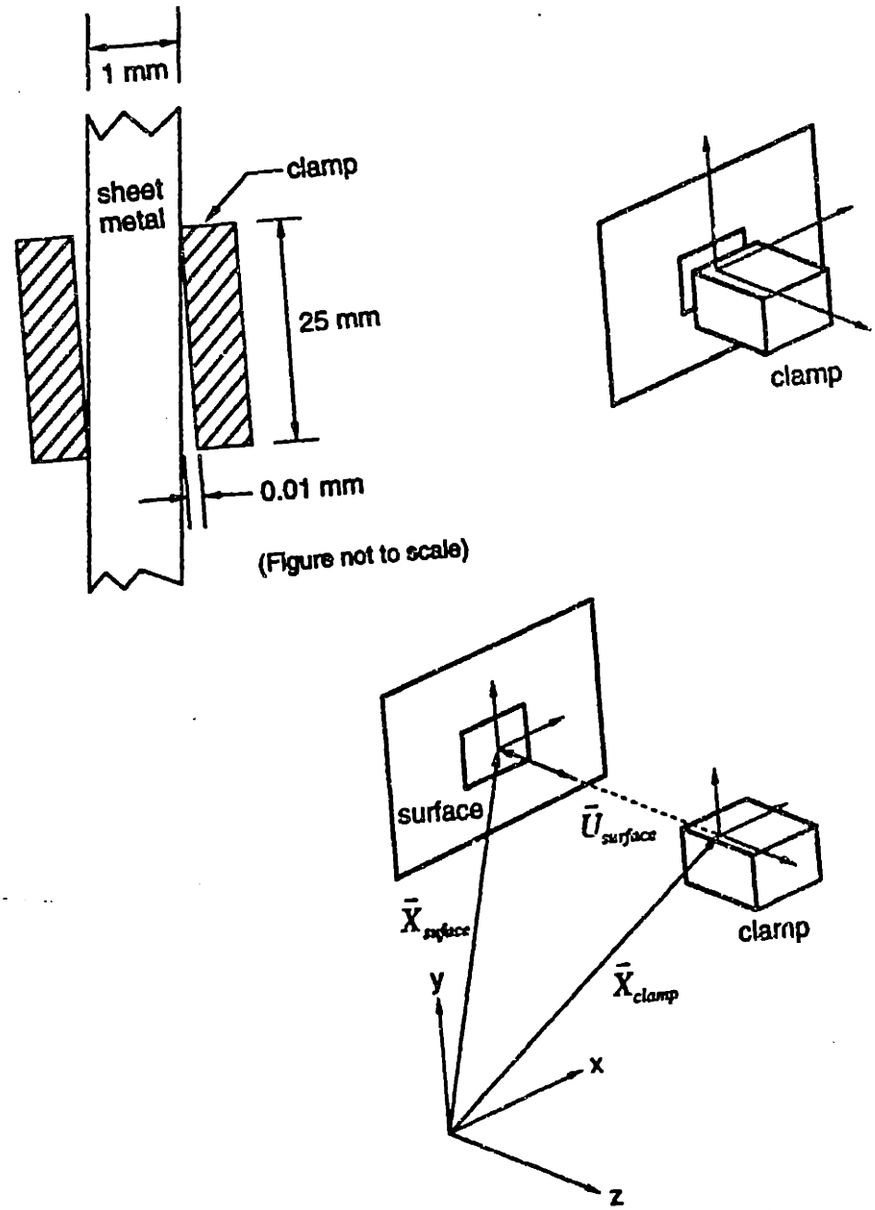

Figure 3-18. A clamp and its representation

3.7.4 Weld guns

A weld gun is a simple mechanical device that creates a weld spot to a sheet metal assembly. There are only a few distinctively different styles of weld guns used in resistance welding (Koltuniak96). These are summarized in Figure 3-19. Although the weld gun components can vary in size and shape from one design to another, components share the same basic functions in all designs (Figure 3-20).

The primary function of a weld gun is to fasten two sheet metal parts together by creating a *weld spot* (also called a *weld nugget*). This is accomplished by first positioning the weld gun with respect to the parts to be welded at a pre-specified location. Then the sheet metal parts are squeezed together with a tip force (generated either by a pneumatic or a hydraulic cylinder) and then applying electrical current through the weld caps causing enough heat to melt the metal together. This is how a weld nugget is formed.

If there is a gap between the two parts that are to be welded, the cylinder provides sufficient pressure to cause the weld tips to close the gap. If the gap is large and the cylinder pressure is not sufficiently high to close the gap, a weld nugget cannot be formed. We are interested in the scenario where a weld spot is formed. This can be modeled as a displacement boundary condition as shown in

Figure 3-21.

Let us represent the position of the weld guns and the normal at the weld tips, by a vector $\vec{X}_{weld\,gun} = (X_x, X_y, X_z, X_\theta, X_\phi, X_\varphi)_{weld\,gun}$. Since the weld guns are rigid, they do not undergo any deformation. They pull the parts so that they deform and thus conform to the weld gun's position (e.g. when there exists an intentional gap). This can be represented mathematically as,

$$\vec{Y}_{weld\,spot} = \vec{X}_{weld\,gun} \qquad \textbf{Equation 3-11}$$

where $\vec{Y}_{weld\,spot}$ is a vector representing the location of the weld spot on the part.

Substitute Equation 3-2 in Equation 3-20,

$$\vec{X}_{weld\,spot} + \vec{U}_{weld\,spot} = \vec{X}_{weld\,gun}$$
$$\vec{U}_{weld\,spot} = \vec{X}_{weld\,gun} - \vec{X}_{weld\,spot} \qquad \textbf{Equation 3-12}$$

Writing Equation 3-23 in scalar form we get,

$$(U_z)_{weld\,spot} = (X_z)_{weld\,gun} - (X_z)_{weld\,spot}$$
$$(U_\theta)_{weld\,spot} = (X_\theta)_{weld\,gun} - (X_\theta)_{weld\,spot} \qquad \textbf{Equation 3-13}$$
$$(U_\phi)_{weld\,spot} = (X_\phi)_{weld\,gun} - (X_\phi)_{weld\,spot}$$

Equation 3-24 describes the displacement boundary conditions imposed by the weld gun on the part.

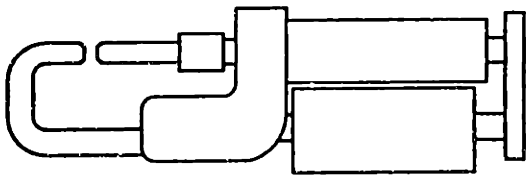

(a) Straight gun

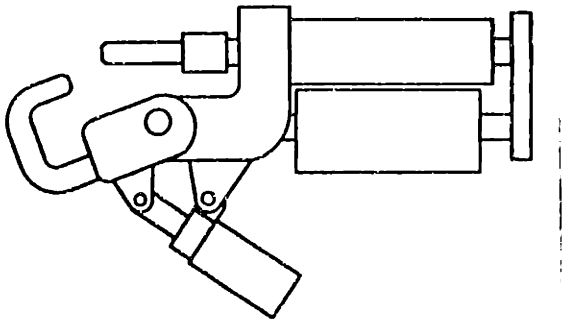

(b) Break-away gun

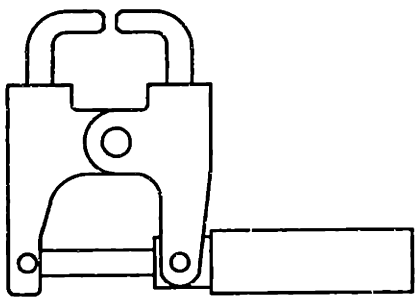

(c) Scissor gun

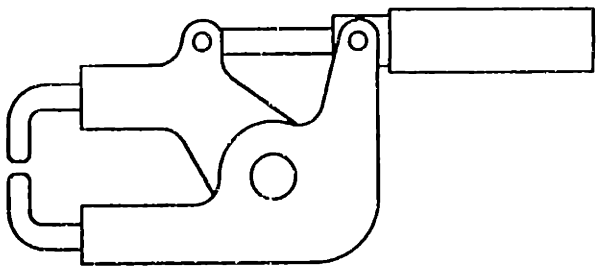

(d) Pinch gun

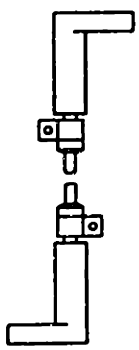

(e) Push/Pull gun

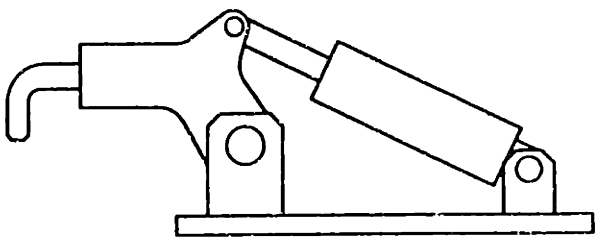

(f) Rocker gun

Figure 3-19. Types of weld guns

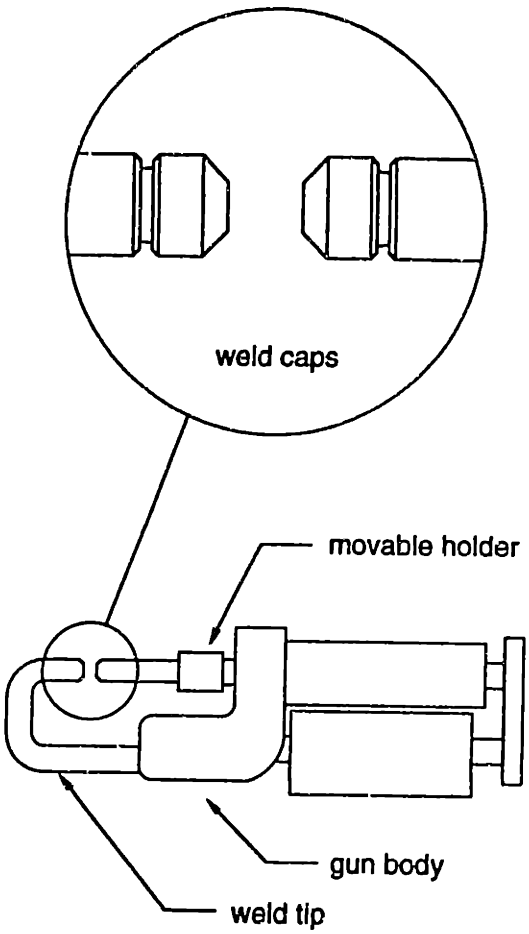

Figure 3-20. Components of a weld gun

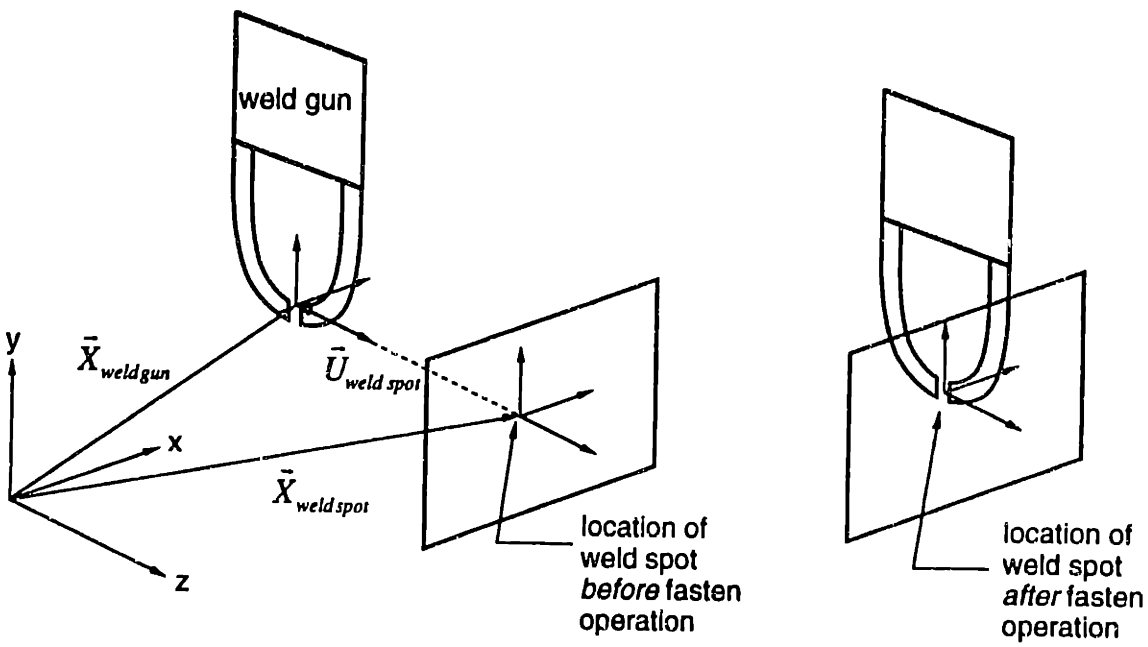

Figure 3-21. Representation of a weld gun

During the fastening operation, metal is melted locally by the heat generated by the electric current passing through the weld tips. The metal then solidifies to bond the two parts together at the weld spot. This change of phase results in change of material properties and locally different deformation. But since this effect is local, we will ignore its effects on global deformation.

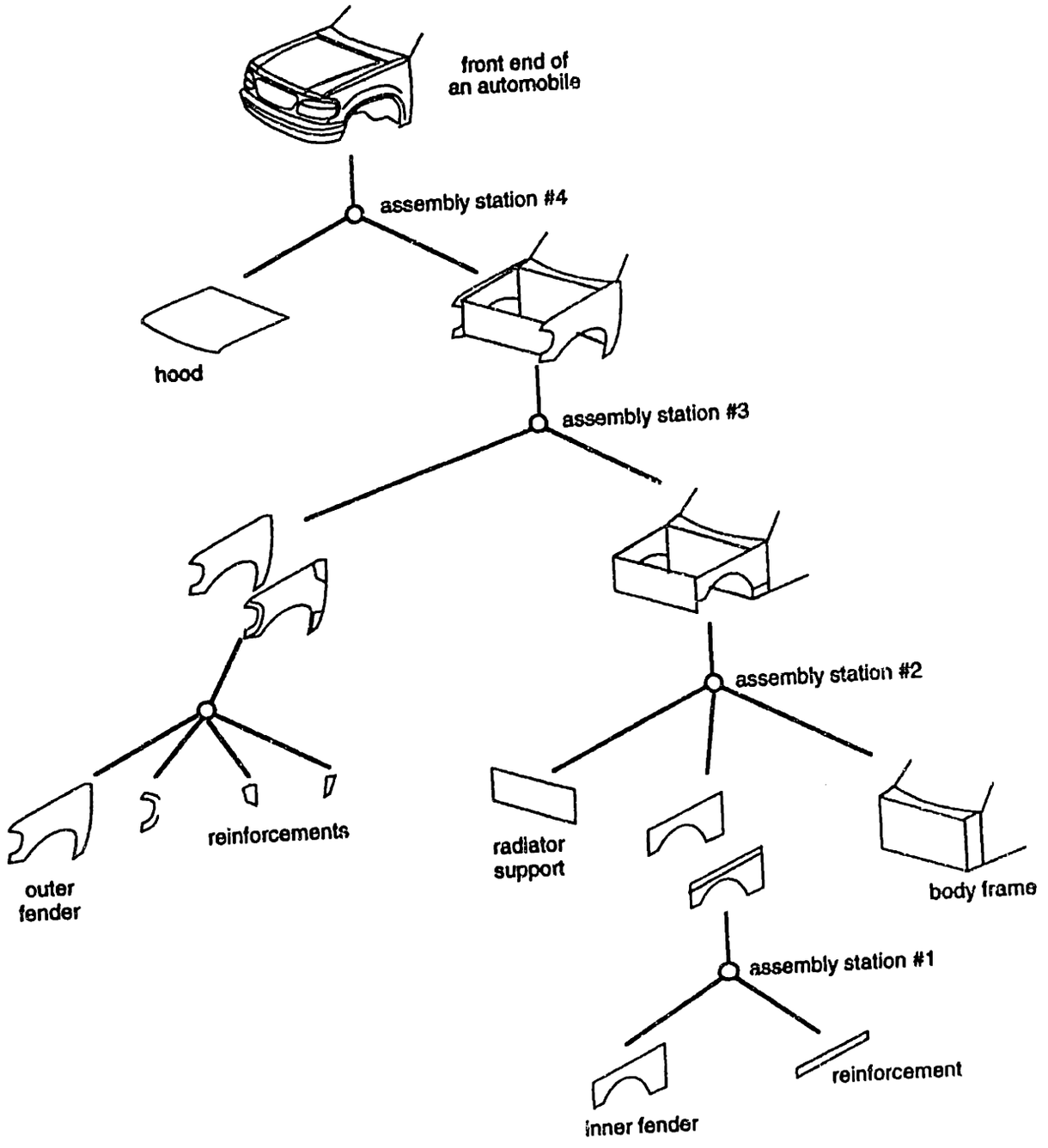

Figure 3-22. The part map showing the assembly process for the front end of an automobile body

3.7.5 Assembly sequence

The assembly sequence can be shown pictorially as a *part map*. (Figure 3-22). The part map also shows the parts that make up the product. Individual parts are shown in the bottom and the assembled product is shown at the top. Individual parts are fastened to make sub-assemblies. Sub-assemblies are then put together to make the final product. The part map shows this process step by step. Every node represents one assembly station. Individual parts (or sub-assemblies) go into an assembly station and a sub-assembly comes out.

3.7.6 Connectivity

Connectivity describes a detailed view of the interactions between parts, fixtures and weld guns. Specifically, connectivity describes the relationships between different components of the assembly process. e.g. locators on parts, locators on fixtures, and weld guns etc. This connectivity information can be represented in a graph form. We have seen such connectivity arcs in Figure 3-16, Figure 3-17, Figure 3-18, and

Figure 3-21.

A connectivity graph also be drawn for each of the individual operations in a PCFRR cycle as shown in Figure 3-23. It is difficult to show this graph in an assembled state, so Figure 3-23 shows an exploded view.

During the PCFRR cycle, constraints are imposed on the part by weld guns, pins and clamps on fixtures. The connectivity graph shows these constraints in graph form. Every node of the connectivity graph represents a coordinate frame (see section 3.7.1.2). An arc represents constraints imposed by one node on the other.

Connectivity graphs represent two kinds of constraints: displacement constraints and degree-of-freedom constraints.

Displacement constraints are constraints where a pre-specified displacement is imposed on a node. Fixtures and weld guns impose displacement constraints on the part as described in section 3.7.3 and section 3.7.4 respectively. Displacement constraints are denoted by a single-headed arrow. The arrowhead points to the node on which a displacement constraint is imposed.

The second type of constraint is a degree-of-freedom constraint. Degree-of-freedom constraint refers to the condition where two nodes have dependent degrees of freedom. For example, consider the points on two parts that are welded together. Before welding, these points can move independent of each other. i.e. they have independent degrees of freedom. After welding, their degrees of freedom are constrained and there is

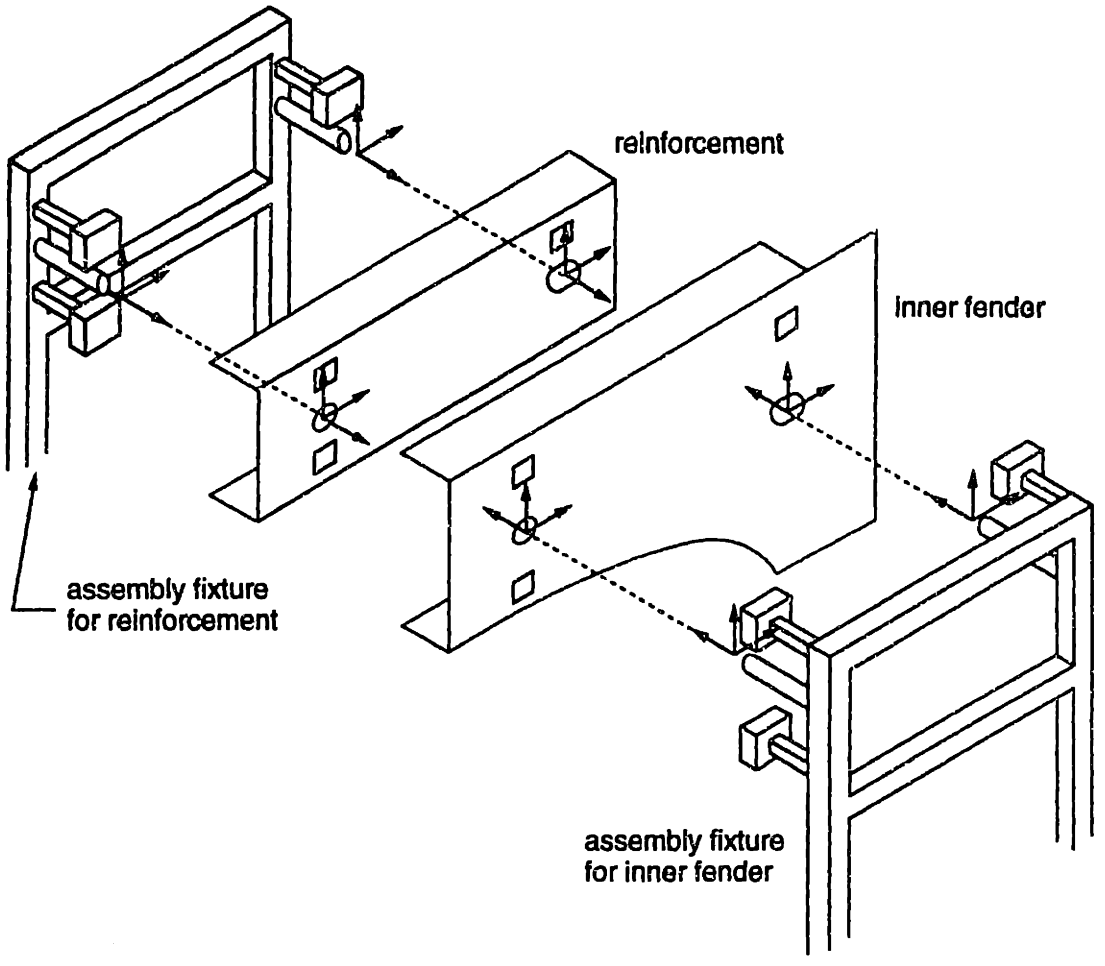

The connectivity graph for the place operation of a PCFRR cycle

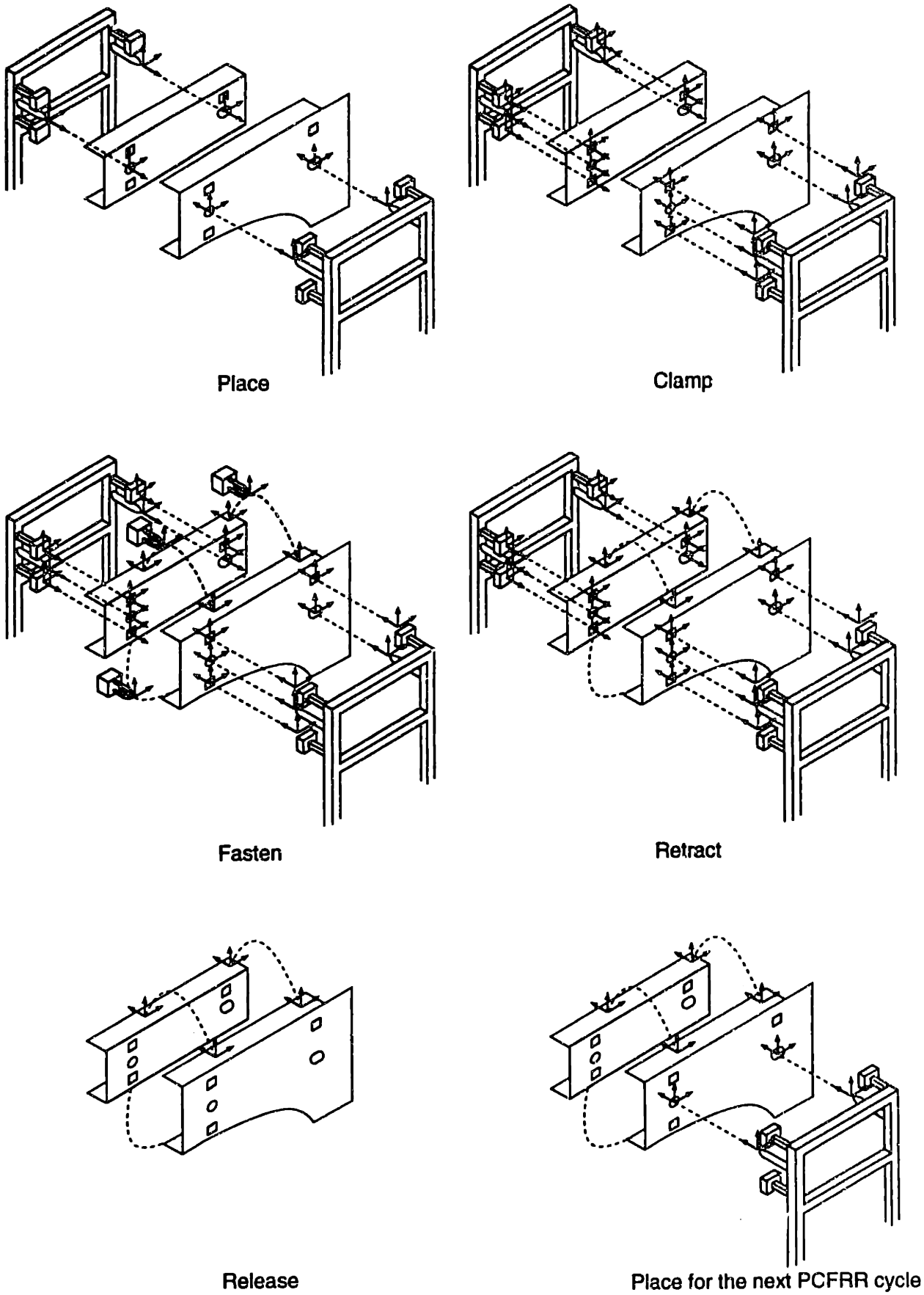

Figure 3-23. Connectivity graphs for the PCFRR cycle

no relative motion between them. i.e. they have a degree-of-freedom constraint imposed on them (see Figure 3-15).

The connectivity graphs show the connectivity and constraint information in graphical form. These graphs are a focal point of our analysis of the assembly.

3.7.7 Non-nominal geometry

As described in section 3.4.2.1, non-nominal geometry can be classified into three categories: part geometry, fixture geometry, weld guns. Note that the non-nominal geometry is measured with respect to the reference geometry.

Let us represent the non-nominal undeformed geometry as $\vec{X}_{non-nominal} = (X_x, X_y, X_z, X_\theta, X_\phi, X_\varphi)_{non-nominal}$. Equations in section 3.7.3 and section 3.7.4 hold for non-nominal geometry also.

3.7.7.1 Non-nominal part geometry

Due to the inherent nature of manufacturing processes, parts are produced that have non-nominal geometry. This part geometry can be classified into three groups: mating features, locator features, non-functional geometry.

3.7.7.1.1 Mating features

Mating features are part/part interfaces. There are several mating constraints like spot welding, nut-bolt, hinge, latch (e.g. hood, door) etc. In an automobile body, all mating features in which we are interested are surface/surface interfaces. A mating feature is non-nominal when the surface/surface interface does not occur at its nominal position. This error is measured normal to the nominal position of surface/surface interface.

3.7.7.1.2 Locator features

Locator features are part/tool interfaces on the part. There are three types of locators features: hole, slot and surface. Error in location of a hole (or slot) is the in-plane displacement of the hole (or slot). The error in location of the surface is the out-of-plane displacement of the surface.

3.7.7.1.3 Non-functional geometry

If the non-functional geometry is non-nominal, its effect on the geometry of the assembled product is small and we will ignore it.

3.7.7.2 Non-nominal fixture geometry

The locator features on the fixture can be non-nominal. Error in location of a pin is measured in the plane to which the pin axis is a normal. The error in location of a clamp is the displacement measured normal to the surface of the clamp. The displacement boundary conditions imposed by non-nominal fixture are similar to that described in section 3.7.3.

For a non-nominal pin in a pin/hole mating condition,

$$(U_x)_{hole} = (X_x)_{non-nominal\ pin} - (X_x)_{hole}$$
$$(U_y)_{hole} = (X_y)_{non-nominal\ pin} - (X_y)_{hole} \qquad \text{Equation 3-14}$$

For a non-nominal pin in a pin/slot mating condition,

$$(U_y)_{slot} = (X_y)_{non-nominal\ pin} - (X_y)_{slot} \qquad \text{Equation 3-15}$$

For a non-nominal clamp in a clamp/surface mating condition,

$$(U_z)_{surface} = (X_z)_{non-nominal\ clamp} - (X_z)_{surface}$$
$$(U_\theta)_{surface} = (X_\theta)_{non-nominal\ clamp} - (X_\theta)_{surface} \qquad \text{Equation 3-16}$$
$$(U_\phi)_{surface} = (X_\phi)_{non-nominal\ clamp} - (X_\phi)_{surface}$$

3.7.7.3 Non-nominal position of weld guns

A welding gun welds the parts at their mating features (part/part interface which is always a surface/surface interface for an automobile body). Mislocation of the welding gun is measured perpendicular to this welding surface. The displacement boundary conditions imposed by a weld gun which has non-nominal position are similar to that described in section 3.7.4,

$$(U_z)_{weld\ spot} = (X_z)_{non-nominal\ weld\ gun} - (X_z)_{weld\ spot}$$
$$(U_\theta)_{weld\ spot} = (X_\theta)_{non-nominal\ weld\ gun} - (X_\theta)_{weld\ spot} \qquad \text{Equation 3-17}$$
$$(U_\phi)_{weld\ spot} = (X_\phi)_{non-nominal\ weld\ gun} - (X_\phi)_{weld\ spot}$$

3.8 The Assembly Model

In this section, we will discuss the assembly model to predict the geometry of parts and sub-assemblies as they propagate through the assembly line. We will use finite element analysis for this purpose. To perform a finite element analysis, we need the reference geometry, displacement boundary conditions and force boundary conditions. In the following sections, we will discuss different aspects of this model.

3.8.1 Constant topology cycles

The entire assembly process is comprised of multiple assembly stations. In every assembly station, the parts go through the PCFRR operations. The assembly process can be viewed as a series of assembly operations as: PCFRRPCFRR.... and so on. The topology of parts and sub-assemblies stays constant till the they are fastened to each other. i.e. between two consecutive fasten operations the topology of the sub-assembly stays the same. This is called a *constant topology cycle* (see Figure 3-24).

Within a constant topology cycle, the topology of parts and sub-assemblies stays constant. This means that although constraints are added and released during operations of a constant topology cycle, the part compliance (characterized by the stiffness matrix *K*) stays constant. Since the geometry stays linear during every cycle and there is no positioning uncertainty, the behavior of the sub-assembly can be considered to be linear[5] within a constant topology cycle. Notice that although two consecutive constant topology cycles are linear, the entire assembly process is *piecewise linear*. The change of topology occurs when parts are fastened. A constant topology cycle typically has Fasten-Retract-Release from one assembly station, followed by Place-Clamp from the next assembly station.

Once parts are fastened, the topology, and hence, the compliance of the sub-assembly changes. We can view the assembly process as a series of constant topology cycles. The model is linear within a constant topology cycle. Thus, we can model the assembly process as a piecewise linear process made up of a series of constant topology cycles shown in Figure 3-24.

To simulate the assembly process, we subdivide it into constant topology cycles. We represent every constant topology cycle by the connectivity graph for its fasten operation. After the last fasten operation, the entire product is assembled. Notice that the last constant topology cycle would have only the Fasten-Retract-Release from last assembly station. We can thus represent the entire assembly process as a series of connectivity graphs (one for every constant topology cycle). We then perform a finite element analysis of these connectivity graphs to obtain the final geometry of the assembled product as shown in Figure 3-25.

---

[5] If friction effects are not negligible, they can introduce non-linear effects. For our purpose, we will assume that friction effects can be ignored.

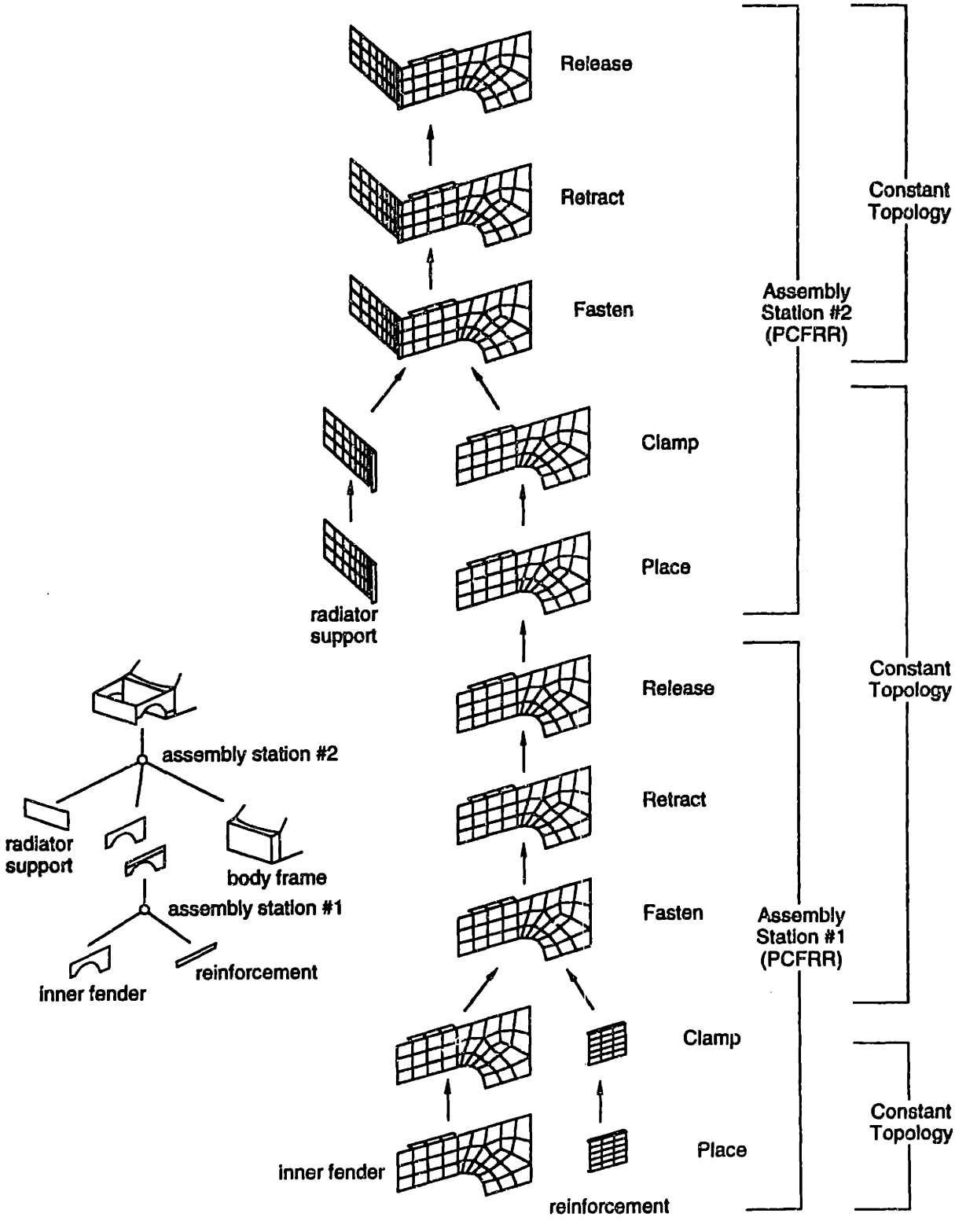

Figure 3-24. Constant topology cycles

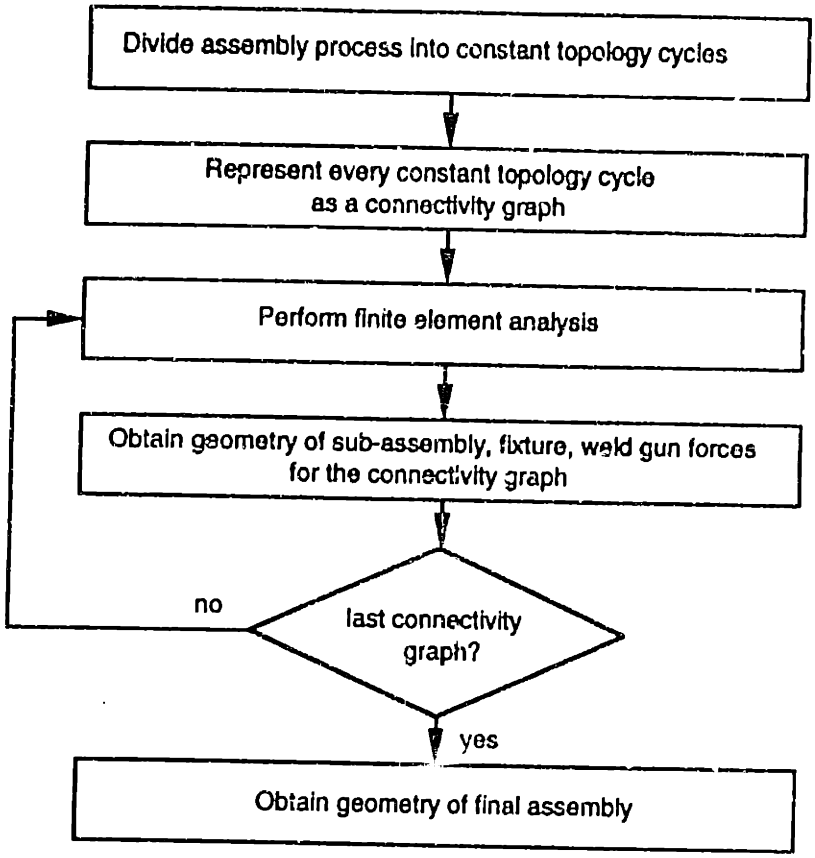

Figure 3-25. Flow chart for predicting geometry after the entire assembly process

3.8.2 Simulation of a constant topology cycle

A constant topology cycle is characterized by the connectivity graph for its fasten operation. To simulate a constant topology cycle, we need to simulate only the fasten operation of that cycle. The out-going geometry for one constant topology cycle becomes the incoming geometry for the subsequent cycle. If a part or sub-assembly is deformed during an operation, this deformed part or sub-assembly goes in as incoming geometry for the next operation where it is deformed further. Let,

$\vec{X}$ = $(X_x, X_y, X_z, X_\theta, X_\phi, X_\varphi)$ be the coordinates of a point and a normal at that point, on the reference part geometry

$\vec{Y}_n$ = $(Y_x, Y_y, Y_z, Y_\theta, Y_\phi, Y_\varphi)_n$ be the coordinates of a point and a normal at that point, on the outgoing geometry for the n th operation,

$\vec{Y}_{n-1}$ = incoming geometry for the n th operation (which is also the outgoing geometry for the n-1 th operation),

$\vec{u}_n$ = $(u_x, u_y, u_z, u_\theta, u_\phi, u_\varphi)_n$ be the deformation or nodal displacement during the n th operation,

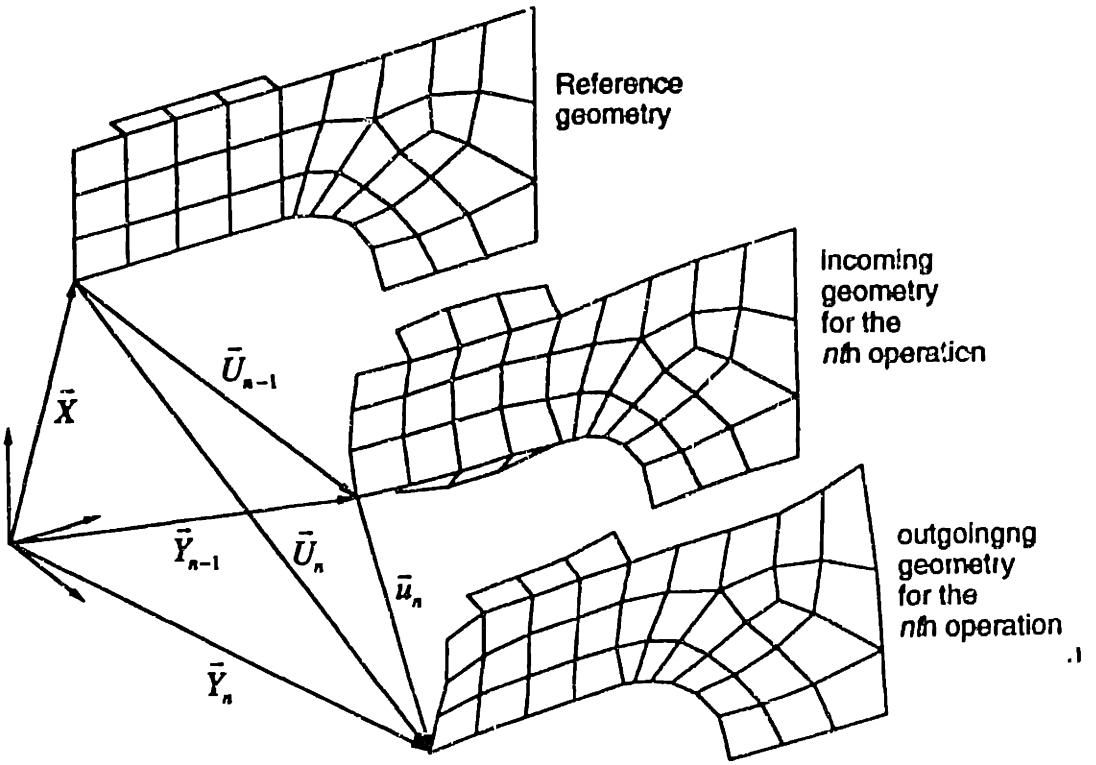

Figure 3-26. Simulation of the *n* th assembly operation

From Figure 3-26 we get,

$$\vec{Y}_n = \vec{Y}_{n-1} + \vec{u}_n$$

$$\vec{Y}_n = (\vec{Y}_{n-2} + \vec{u}_{n-1}) + \vec{u}_n$$

$$\vec{Y}_n = \vec{X} + \vec{u}_1 + \ldots + \vec{u}_{n-1} + \vec{u}_n \qquad \because \vec{Y}_1 = \vec{X} + \vec{u}_1$$

$$\vec{Y}_n = \vec{X} + \sum_i^n \vec{u}_i \qquad \text{Equation 3-18}$$

if we define $\vec{U}_n$ such that,

$$\vec{U}_n = \sum_i^n \vec{u}_i \qquad \text{Equation 3-19}$$

then Equation 3-18 becomes,

$$\vec{Y}_n = \vec{X} + \vec{U}_n \qquad \text{Equation 3-20}$$

Equation 3-20 says that the total deformation of the part after any operation is the sum of the deformation in every operation before it. Note that when we perform a finite element analysis of the *n* th operation, we get the deformation $\vec{u}_n$ in that operation (not to be confused with $\vec{U}_n = \sum_i^n \vec{u}_i$).

3.8.3 Reference geometry

We will use the nominal part geometry as the reference geometry. This is a stress-free, undeformed state. Using the nominal part geometry as the reference geometry obviates the necessity to re-mesh the part for every finite element analysis. We will calculate the part compliance (characterized by the stiffness matrix K) based on this reference geometry. To do so, we make the following assumptions:

3.8.3.1 Compliance of deformed part is same as that of the undeformed part

As the part propagates through the assembly line, it deforms. Although, the out-going geometry for one operation becomes the incoming geometry for the subsequent operation, we will characterize the deformation of the part during an operation with respect to the reference geometry and not with respect to the previously-deformed incoming geometry. We will assume that the part deformation is small enough, so that the compliance of the deformed part is the same as that of the undeformed (or reference) geometry. i.e. the stiffness matrix K of the deformed geometry in Figure 3-27 (a) is the same as that of Figure 3-27 (b).

3.8.3.2 Compliance of a non-nominal part is the same as that of a nominal part

Manufacturing variations cause non-nominal geometry. We use the nominal geometry as reference geometry. When part geometry is non-nominal, the undeformed geometry is different from the nominal geometry. We will assume this deviation from nominal is small enough, so that the part compliance of the non-nominal part is the same as that of a nominal part. i.e. stiffness matrix K of the non-nominal part is the same as that of the nominal part.

3.8.3.3 Part geometry stays linear during an operation

When boundary conditions are applied to the part to simulate its behavior during an operation, the part deforms. We assume that this deformation is small so that it does not affect the part compliance while the boundary conditions are being applied. i.e. the stiffness matrix (K) of the part does not change during the application of boundary conditions. In other words, geometry of the part stays linear during an operation.

In the finite element formulation, we will assume that the displacements of the finite element assemblage are infinitesimally small and that the material is linearly elastic. In addition, we also assume that the nature of boundary conditions remains

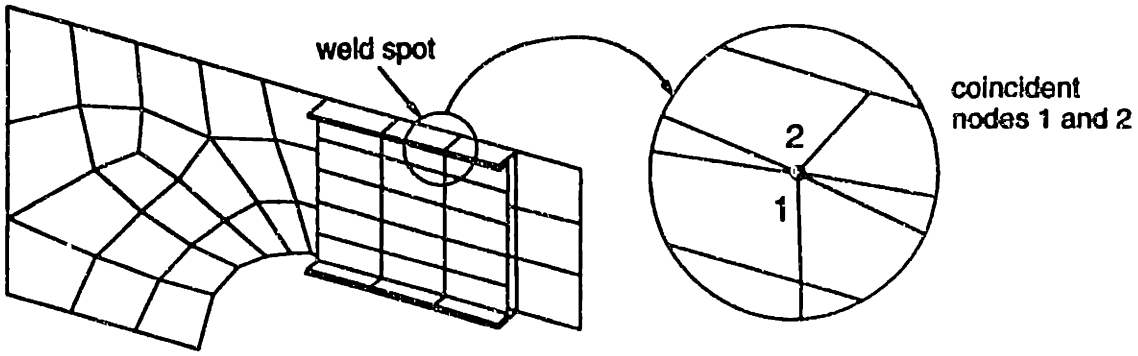

(a) Deformed geometry with degrees of freedom constrained for nodes 1 and 2

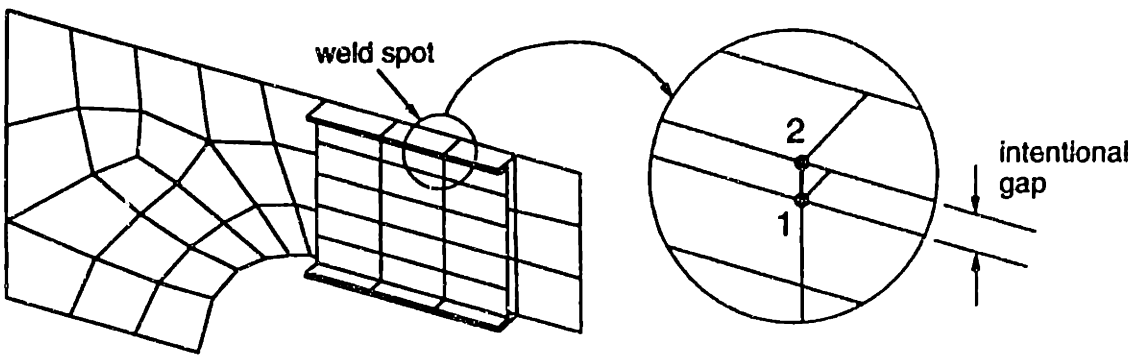

(b) Undeformed geometry with degrees of freedom constrained for nodes 1 and 2

Figure 3-27. Reference geometry and deformed geometry

unchanged during the application of the loads on the finite element assemblage. With these assumptions, the finite element equilibrium equations for static analysis can be expressed as,

$$\mathbf{K}\mathbf{u} = \mathbf{F} \qquad \text{Equation 3-21}$$

These equations correspond to a linear[6] analysis.

---

[6] This analysis would become nonlinear if geometric nonlinearities exist. Geometry is considered non-linear for large rotations. Large rotations are defined as those that exceed 10° (Kardestuncer87). For our analysis, the maximum rotations are about 2-3°, and hence our linearity assumption is justified. This was also confirmed by comparing the stress distributions for small and large deformations. The stress distributions matched closely, thus validating the assumption of "small deformations."

3.8.4 Displacement boundary conditions

The connectivity graphs shows the constraints imposed by the weld guns and fixtures on the part. As described in section 3.7.3 and section 3.7.4, these can be modeled as displacement boundary conditions. Note that these constraints are defined in terms of $\vec{U}_n = (U_x, U_y, U_z, U_\theta, U_\phi, U_\varphi)_n$ and not in terms of $\vec{u}_n = (u_x, u_y, u_z, u_\theta, u_\phi, u_\varphi)_n$ For example, a pin on a fixture in Figure 3-16 imposes the displacement boundary conditions $U_x = U_y = 0$ and not $u_x = u_y = 0$. To simulate the n th operation, we need the displacement boundary conditions $\vec{u}_n$.

From previous analyses we know the displacement field, $\vec{U}_{n-1}$. The connectivity graphs show the displacement constraints $\vec{U}_n$. We can determine the displacement boundary conditions for the n th operation using From Equation 3-19,

$$\vec{U}_n = \sum_i^n \vec{u}_i$$
$$\vec{U}_n = \vec{U}_{n-1} + \vec{u}_n$$
$$\vec{u}_n = \vec{U}_n - \vec{U}_{n-1} \qquad \text{Equation 3-22}$$

Figure 3-28 shows connectivity graph and the imposed displacement constraints $\vec{U}_n$. The displacement boundary conditions can be found using Figure 3-28 and Equation 3-22.

3.8.5 Force boundary conditions

For simulating the n th constant topology cycle (i.e. its fasten operation), we calculate the deformation incurred in that operation, $\vec{u}_n$. This means that the reaction forces for the n-1 th constant topology cycle (i.e. n-1 th fasten operation) become the force boundary conditions for the n th operation. The reaction forces include weld gun forces and fixture forces (forces exerted by the pins and clamps).

3.9 Method

We want to predict the geometry after any operation, say the n th constant topology cycle. This method can be applied over and over again for every constant topology cycle. Finally, we can use it to predict the geometry of the final product.

	Connectivity graph	Constraints
pin/slot 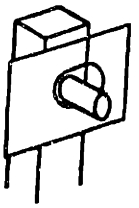	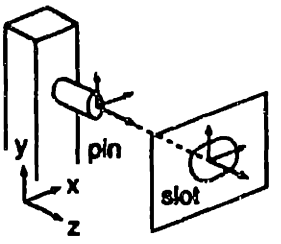	$(U_y)_{slot} = (X_y)_{pin} - (X_y)_{slot}$
pin/hole 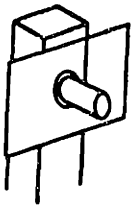	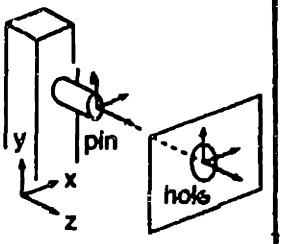	$(U_x)_{hole} = (X_x)_{pin} - (X_x)_{hole}$ $(U_y)_{hole} = (X_y)_{pin} - (X_y)_{hole}$
clamp/surface 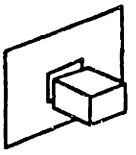	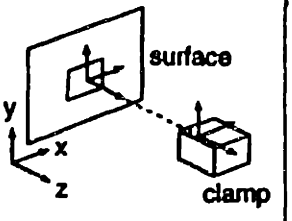	$(U_z)_{surface} = (X_z)_{clamp} - (X_z)_{surface}$ $(U_\theta)_{surface} = (X_\theta)_{clamp} - (X_\theta)_{surface}$ $(U_\phi)_{surface} = (X_\phi)_{clamp} - (X_\phi)_{surface}$
weld gun 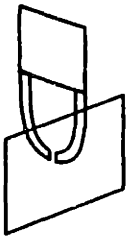	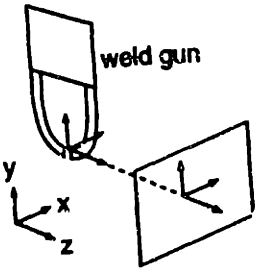	$(U_z)_{weld\ spot} = (X_z)_{weld\ gun} - (X_z)_{weld\ spot}$ $(U_\theta)_{weld\ spot} = (X_\theta)_{weld\ gun} - (X_\theta)_{weld\ spot}$ $(U_\phi)_{weld\ spot} = (X_\phi)_{weld\ gun} - (X_\phi)_{weld\ spot}$
weld spot of sub-assembly 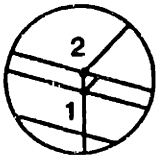	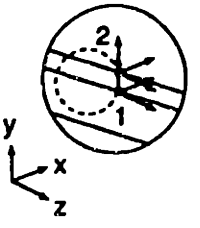	$(U_x)_1 = (U_x)_2$ $(U_y)_1 = (U_y)_2$ $(U_z)_1 = (U_z)_2$ $(U_\theta)_1 = (U_\theta)_2$ $(U_\phi)_1 = (U_\phi)_2$ $(U_\varphi)_1 = (U_\varphi)_2$

Figure 3-28. Connectivity graph and the imposed displacement constraints

The method is as follows:

Step 1: Represent the reference or nominal geometry of incoming parts as a set of finite elements and nodes.

Step 2: Use the connectivity graph to determine the constraints imposed by fixtures and weld guns on the parts (see Figure 3-28). These are prescribed displacement boundary conditions ($\mathbf{u}_\beta$).

Step 3: Denote the reaction forces from the *n-1* th constant topology cycle as a force displacement boundary condition ($\mathbf{F}_\alpha$) for the *n* th constant topology cycle.

Step 4: Formulate the problem in the form,

$$\mathbf{K}\mathbf{u}_n = \mathbf{F}_n \qquad \textbf{Equation 3-23}$$

$$\begin{bmatrix} \mathbf{K}_{\alpha\alpha} & \mathbf{K}_{\alpha\beta} \\ \mathbf{K}_{\beta\alpha} & \mathbf{K}_{\beta\beta} \end{bmatrix} \begin{Bmatrix} \mathbf{u}_\alpha \\ \mathbf{u}_\beta \end{Bmatrix} = \begin{Bmatrix} \mathbf{F}_\alpha \\ \mathbf{F}_\beta \end{Bmatrix} \qquad \textbf{Equation 3-24}$$

where,

$\mathbf{F}_\alpha$ = applied nodal forces

$\mathbf{F}_\beta$ = unknown reactions

$\mathbf{u}_\alpha$ = unknown nodal displacements

$\mathbf{u}_\beta$ = prescribed displacements

Solve Equation 3-24, to get unknowns $\mathbf{F}_\beta$ and $\mathbf{u}_\alpha$. This is done as follows,

By matrix multiplication, Equation 3-24 yields,

$$\mathbf{F}_\alpha = \mathbf{K}_{\alpha\alpha}\mathbf{u}_\alpha + \mathbf{K}_{\alpha\beta}\mathbf{u}_\beta \qquad \textbf{Equation 3-25}$$

$$\mathbf{F}_\beta = \mathbf{K}_{\beta\alpha}\mathbf{u}_\alpha + \mathbf{K}_{\beta\beta}\mathbf{u}_\beta \qquad \textbf{Equation 3-26}$$

Unknown nodal displacements $\mathbf{u}_\alpha$ are obtained from Equation 3-25,

$$\mathbf{u}_\alpha = \mathbf{K}_{\alpha\alpha}^{-1}(\mathbf{F}_\alpha - \mathbf{K}_{\alpha\beta}\mathbf{u}_\beta) \qquad \textbf{Equation 3-27}$$

Substituting Equation 3-27 into Equation 3-26 yields the unknown reactions $\mathbf{F}_\beta$,

$$\mathbf{F}_\beta = \mathbf{K}_{\beta\alpha}\mathbf{K}_{\alpha\alpha}^{-1}\mathbf{F}_\alpha - (\mathbf{K}_{\beta\alpha}\mathbf{K}_{\alpha\alpha}^{-1}\mathbf{K}_{\alpha\beta} - \mathbf{K}_{\beta\beta})\,\mathbf{u}_\beta \qquad \textbf{Equation 3-28}$$

Step 5:

(a) Calculate the deformation *after* the *n* th operation using Equation 3-19,

$$\mathbf{U}_n = \mathbf{U}_{n-1} + \mathbf{u}_n \qquad \textbf{Equation 3-29}$$

where, the deformation *during* the *n* th operation $\mathbf{u}_n$ is,

$$\mathbf{u}_n = \begin{Bmatrix} \mathbf{u}_\alpha \\ \mathbf{u}_\beta \end{Bmatrix} \qquad \textbf{Equation 3-30}$$

$\mathbf{U}_n$ will be used for step 2 of the next operation.

(b) Reaction forces $\mathbf{F}_\beta$ are used as prescribed force boundary conditions for step 3 of the $n+1$ th operation.

3.10 Example: Predicting geometry after one assembly station

Let us consider a simple example where two parts are fastened on one assembly station and the geometry of the resulting assembly is inspected in an inspection station. This process can be divided into two constant topology cycles as shown in Figure 3-29.

Let us assume that all geometry is nominal and that there exists an intentional gap between the mating surfaces. We number the constant topology cycles as, 1 and 2 as shown in Figure 3-29.

Now let us examine constant topology cycle #1. We will look at the fasten (weld) operation. When the weld guns are activated, they close the intentional gap between the two mating surfaces of the parts by deforming them. We want to find this deformed shape, when the weld guns have been activated, but not yet retracted. They exert forces (and moments) on the parts which help close the intentional gap between the parts. We want to find out $\mathbf{u}_1$, the deformation during the fasten operation. Let the intentional gap be d, and the weld guns meet midway between the gap.

Also, note that just before the two parts are fastened together, they can move independent of each other.

3.10.1 Simulation of constant topology cycle #1

For this simulation, we consider constant topology cycle #1, which is characterized by the connectivity graph of the fasten operation in the assembly station.

Step 1: Represent the reference geometry of the incoming parts as a set of finite elements and nodes (see Figure 3-30)

Step 2: Using the connectivity graph, we can determine the constraints imposed by the fixtures and the weld guns on the parts.

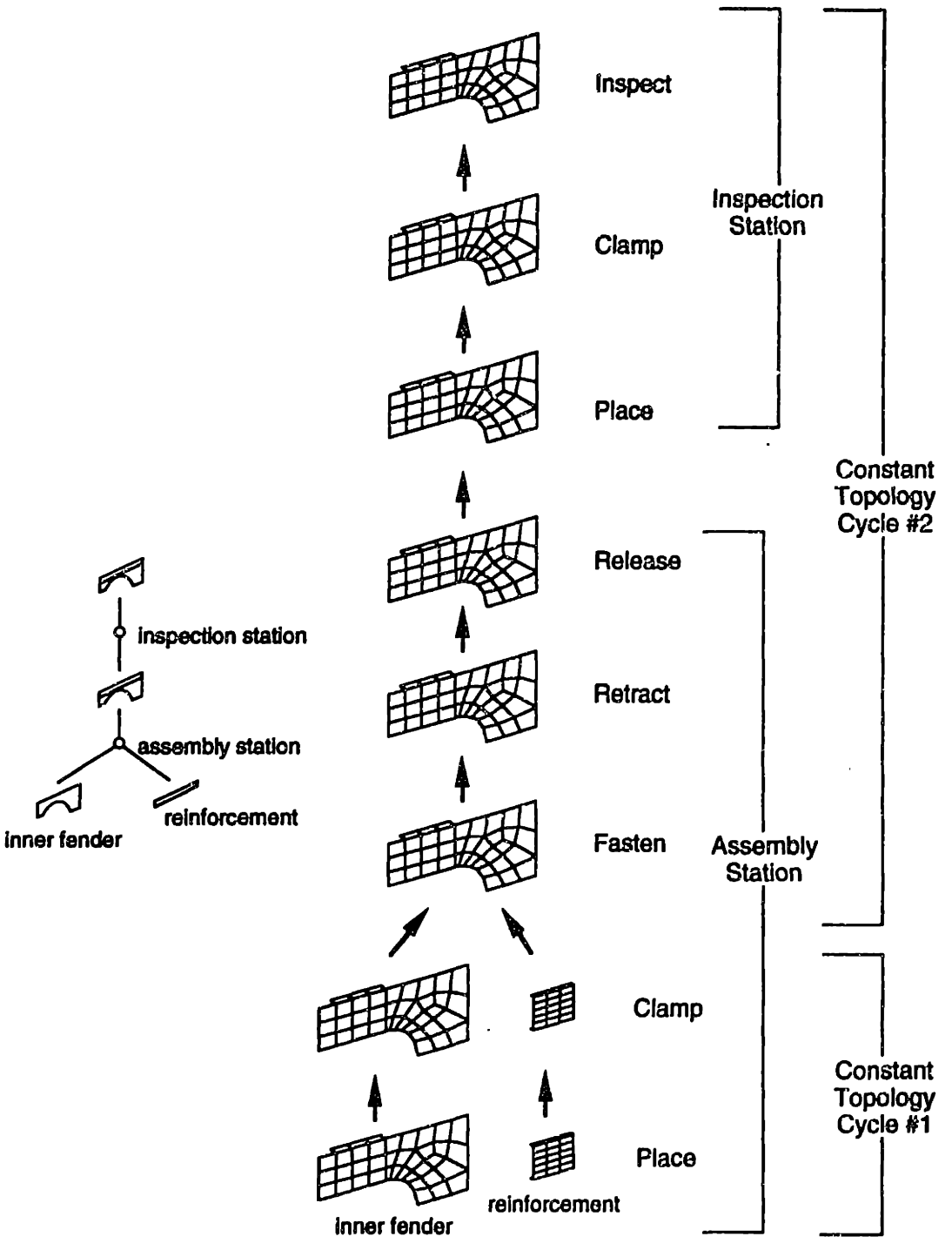

Figure 3-29. Assembly process for example in section 3.10

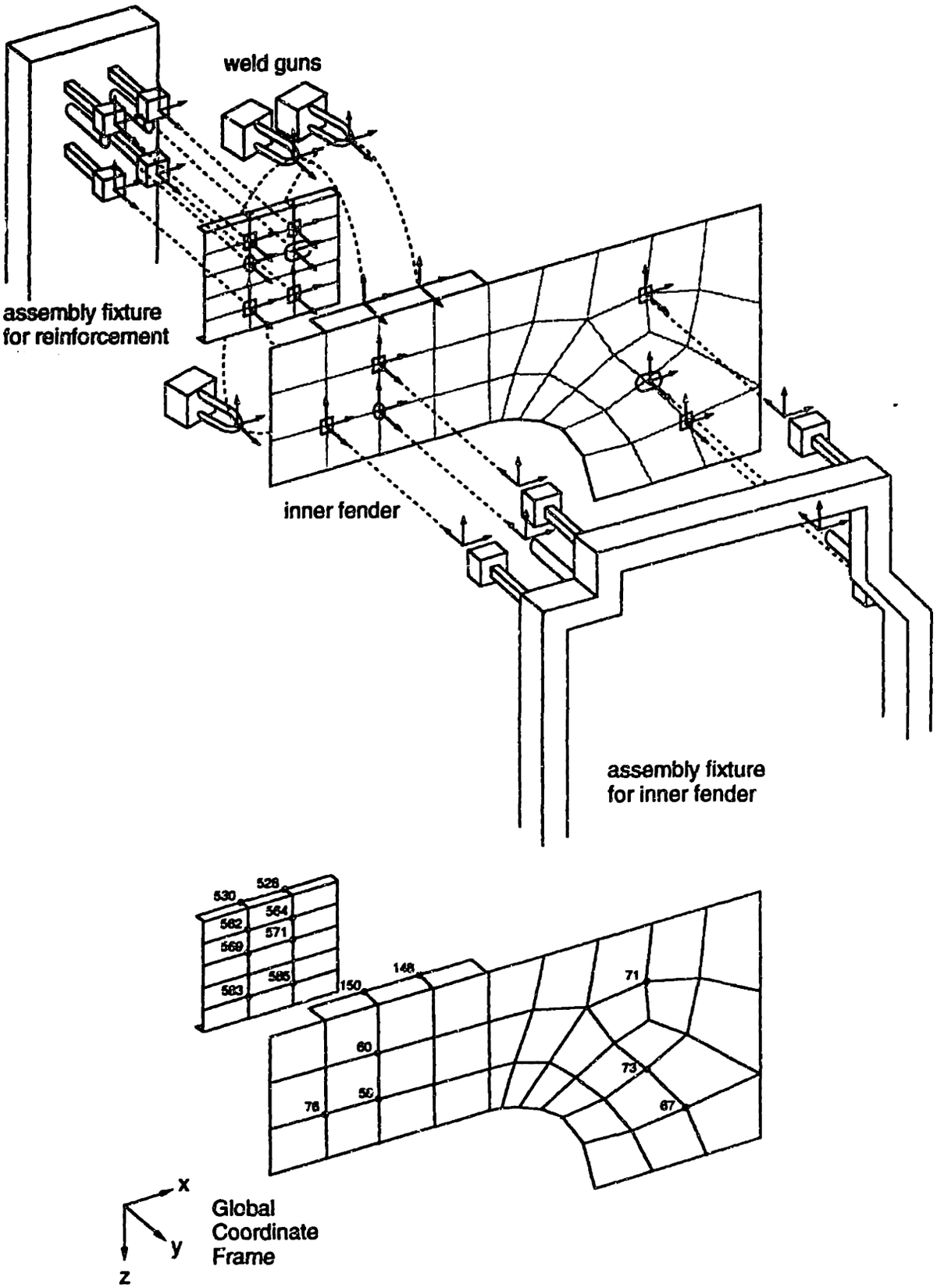

Figure 3-30. Connectivity graph for fasten operation (example of section 3.10)

For the weld guns,

$$(u_z)_{148} = (u_z)_{150} = \frac{d}{2}$$

$$(u_z)_{528} = (u_z)_{530} = -\frac{d}{2}$$

$$(u_z)_{488} = (u_z)_{486} = \frac{d}{2}$$

$$(u_z)_{171} = (u_z)_{173} = -\frac{d}{2}$$

Equation 3-31

For the pin/hole of the reinforcement,

$$(u_z)_{569} = (u_z)_{569} = 0$$

Equation 3-32

For the pin/slot of the reinforcement,

$$(u_z)_{571} = 0$$

Equation 3-33

For clamp corresponding to node 564,

$$(u_y)_{564} = 0$$

$$(u_\theta)_{564} = 0$$

$$(u_\varphi)_{564} = 0$$

Equation 3-34

Similarly we can get constraint equations for all fixture points. These equations together define $\mathbf{u}_\beta$.

Step 3: Since the incoming parts are undeformed,

$$\mathbf{F}_\alpha = 0$$

Equation 3-35

Step 4: From Equation 3-27 and Equation 3-28 we get,

$$\mathbf{u}_\alpha = \mathbf{K}_{\alpha\alpha}^{-1}(\mathbf{F}_\alpha - \mathbf{K}_{\alpha\beta}\mathbf{u}_\beta)$$

$$\mathbf{F}_\beta = \mathbf{K}_{\beta\alpha}\mathbf{K}_{\alpha\alpha}^{-1}\mathbf{F}_\alpha - (\mathbf{K}_{\beta\alpha}\mathbf{K}_{\alpha\alpha}^{-1}\mathbf{K}_{\alpha\beta} - \mathbf{K}_{\beta\beta})\,\mathbf{u}_\beta$$

Equation 3-36

Step 5: From Equation 3-30,

$$\mathbf{u}_1 = \begin{Bmatrix} \mathbf{u}_\alpha \\ \cdots \\ \mathbf{u}_\beta \end{Bmatrix}$$

Equation 3-37

Using Equation 3-29 and Equation 3-36 , we get,

$$\mathbf{U}_1 = \mathbf{u}_1$$

Equation 3-38

Also, $\mathbf{F}_\beta$ describes the weld gun forces and reactions forces at the fixtures. Let us define ${}^{fasten}\mathbf{F}$ to be used in step 3 for the next simulation,

$${}^{fasten}\mathbf{F} = \mathbf{F}_\beta$$

Equation 3-39

3.10.2 Simulation of constant topology cycle #2

For this simulation, we consider constant topology cycle #2, which is characterized by the connectivity graph for the inspection operation in the inspection station.

We will continue from the previous section. The weld guns retract after fastening the two part to form a sub-assembly. Since the weld gun forces are no longer present, the sub-assembly springs back. Then it is placed and clamped on to the inspection fixture. We want to determine the geometry $\mathbf{u}_2$ of the sub-assembly at this stage.

Step 1: Represent the reference geometry of the incoming parts as a set of finite elements and nodes (see Figure 3-31)

Step 2: Using the connectivity graph, we can determine the constraints imposed by the fixtures on the parts.

For the pin/hole of the inner fender,

$$(u_x)_{58} = (u_z)_{58} = 0 \qquad \textbf{Equation 3-40}$$

For the pin/slot of the inner fender,

$$(u_z)_{73} = 0 \qquad \textbf{Equation 3-41}$$

For clamp corresponding to node 564 of the inner fender,

$$(u_y)_{76} = 0 \qquad \textbf{Equation 3-42}$$
$$(u_\theta)_{76} = 0$$
$$(u_\varphi)_{76} = 0$$

The connectivity graph shows that weld spots have constrained degrees of freedom. For the weld spot corresponding to 148 and 528,

$$(u_x)_{148} = (u_x)_{528} \qquad \textbf{Equation 3-43}$$
$$(u_y)_{148} = (u_y)_{528}$$
$$(u_z)_{148} = (u_z)_{528}$$
$$(u_\theta)_{148} = (u_\theta)_{528}$$
$$(u_\phi)_{148} = (u_\phi)_{528}$$
$$(u_\varphi)_{148} = (u_\varphi)_{528}$$

Similarly we can get constraint equations for all locators and weld spots. These equations together define $\mathbf{u}_\beta$.

Step 3: From Equation 3-39, the force boundary conditions are the reaction forces from the previous simulation. This can be characterized as,

$$\mathbf{F}_\alpha = {}^{fasten}\mathbf{F} \qquad \textbf{Equation 3-44}$$

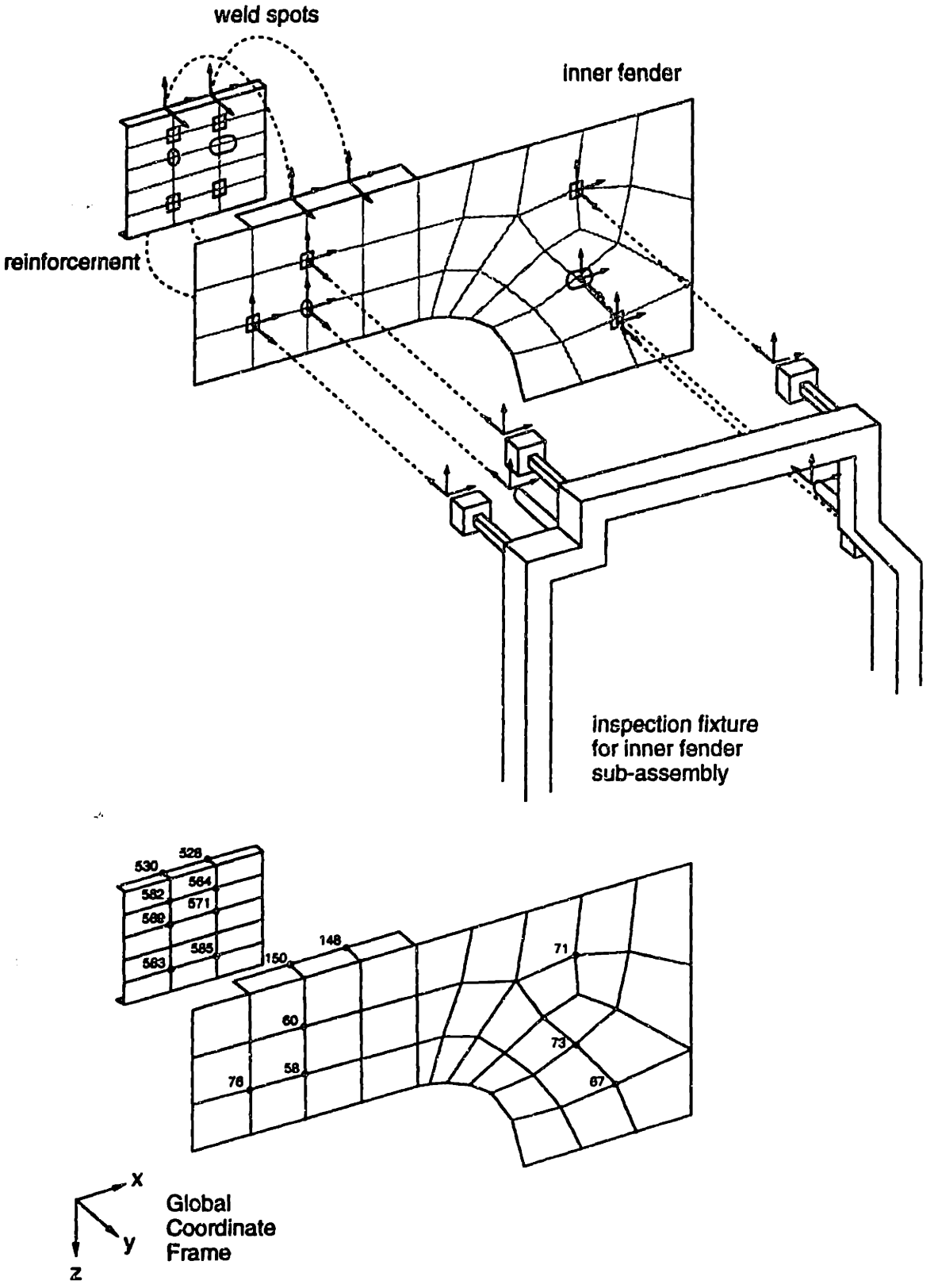

Figure 3-31. Connectivity graph for inspection operation (example of section 3.10)

Step 4: From Equation 3-27 and Equation 3-28 we get,

$$\mathbf{u}_\alpha = \mathbf{K}_{\alpha\alpha}^{-1}(\mathbf{F}_\alpha - \mathbf{K}_{\alpha\beta}\mathbf{u}_\beta) \qquad \text{Equation 3-45}$$

$$\mathbf{F}_\beta = \mathbf{K}_{\beta\alpha}\mathbf{K}_{\alpha\alpha}^{-1}\mathbf{F}_\alpha - (\mathbf{K}_{\beta\alpha}\mathbf{K}_{\alpha\alpha}^{-1}\mathbf{K}_{\alpha\beta} - \mathbf{K}_{\beta\beta})\mathbf{u}_\beta$$

Step 5: From Equation 3-30,

$$\mathbf{u}_2 = \begin{Bmatrix} \mathbf{u}_\alpha \\ \cdots \\ \mathbf{u}_\beta \end{Bmatrix} \qquad \text{Equation 3-46}$$

Using Equation 3-29 and Equation 3-36 , we get,

$$\mathbf{U}_2 = \mathbf{U}_1 + \mathbf{u}_2 \qquad \text{Equation 3-47}$$

Thus, the geometry of the sub-assembly can be calculated.

3.11 Summary

In this chapter we represented the different components of the assembly process. The geometry of parts and sub-assemblies is represented as a set of finite elements and nodes. The assembly process is represented as a set of connectivity graphs. We use these connectivity graphs to obtain prescribed displacements and prescribed force boundary conditions for the finite element analysis. The outgoing geometry for one connectivity graph is used as the incoming geometry for the next one. In this way, the geometry of the sub-assembly can be predicted after any assembly operation.

4.

Implementation

In this chapter, we will implement the assembly model to predict the geometry of a outer fender for a front end of an automobile. This chapter discusses the assembly process, its model, the analysis procedure and the analysis results. All geometry is nominal. Here, we will examine the effect of intentional gaps on final geometry of product as parts propagate through the assembly line.

4.1 The front end of an automobile

The assembly in question is the front end of an automobile. The assembly dimensions of our interest are the margins and flushness values for the fender outer. e.g. fender-to-hood or fender-to-door margins and flushness as shown in Figure 1-1. To determine these values, we need to predict the geometry of the outer fender after it is assembled on to the front end. The major parts of the front end of an automobile are: inner fenders, outer fenders, reinforcements, radiator support, and the body frame.

4.1.1 The assembly process

The assembly process for the front fender is shown in Figure 4-1. It has three assembly stations (numbered 1 to 3). In every assembly station, parts are placed and clamped into assembly fixtures, welding guns fasten the parts, weld guns retract and finally, parts are released from the assembly fixtures. Table 4-1 shows the incoming parts and outgoing sub-assemblies for the assembly stations.

Table 4-1. Incoming parts and outgoing sub-assemblies for assembly stations

Assembly Station	Incoming parts	Outgoing sub-assembly
1	inner fender reinforcement	inner fender sub-assembly
2	inner fender sub-assembly radiator support body frame	body-in-white (BIW)
3	body-in-white outer fender	body-in-white+outer fender

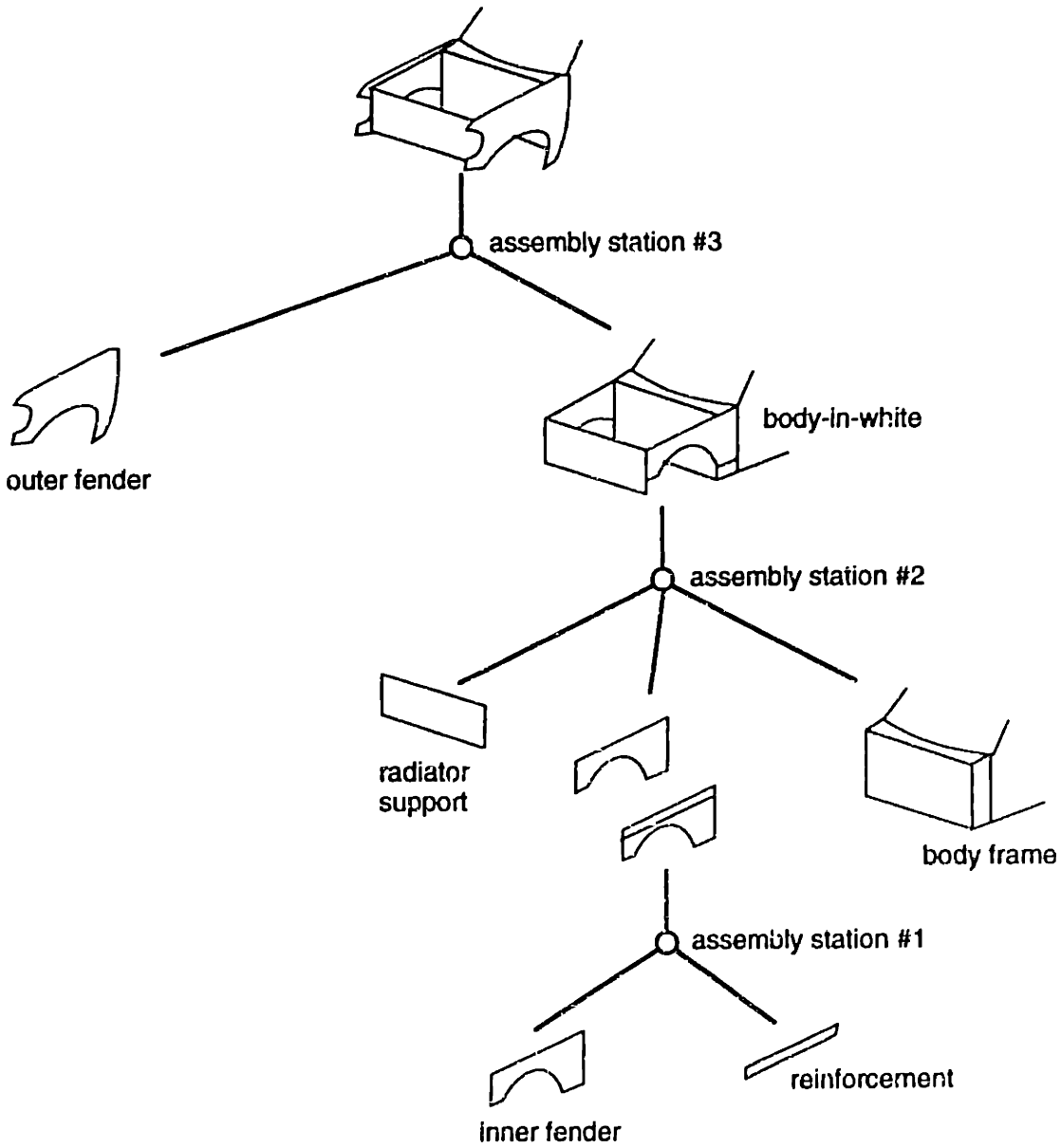

Figure 4-1. The part map showing the assembly process for the outer fender

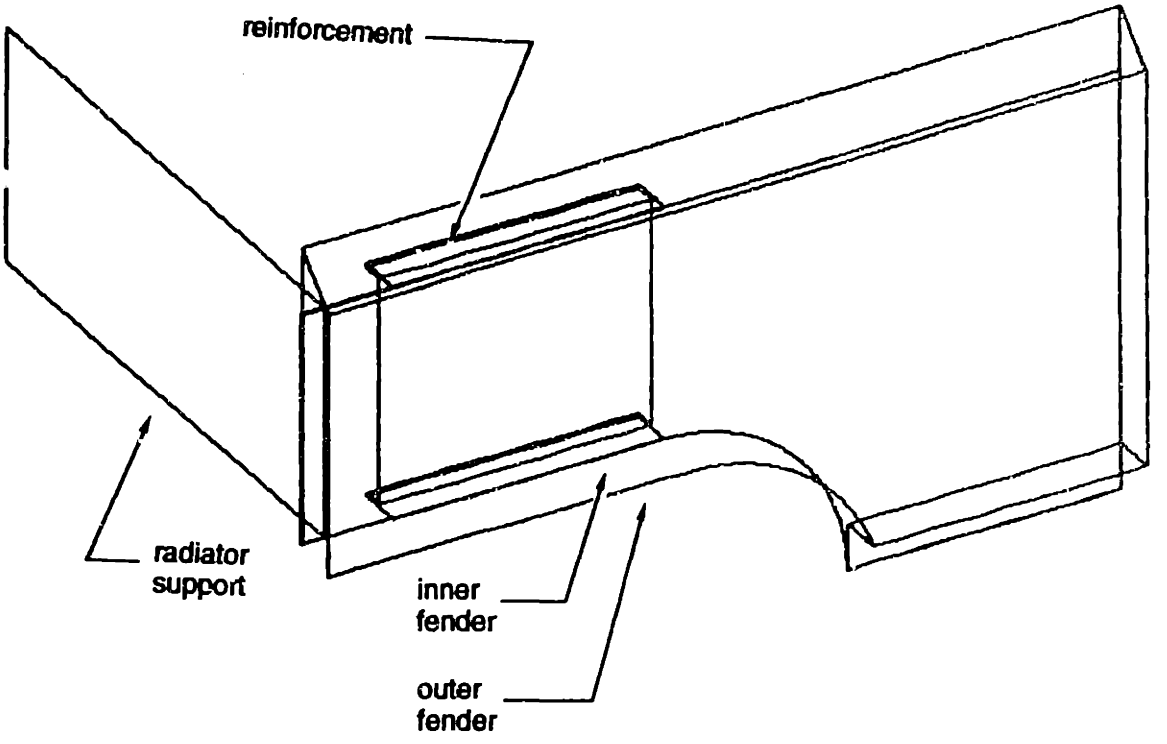

Figure 4-2. Part geometry

4.1.2 The inspection process

After the outer fender is fastened to the BIW in assembly station #3, it is measured to verify if it complies with its engineering design (its nominal geometry). This is done by placing and clamping the assembly into an inspection fixture. The assembly is then measured using a CMM (Coordinate Measuring Machine). We want to predict the geometry of the front fender when the assembly is in its inspection fixture.

4.2 The Assembly Model

We want to predict the geometry of the outer fender during the inspection operation, after the outer fender has been fastened to the BIW. Hence, our model will simulate three assembly stations and one inspection station for an assembly of six parts (inner fender, reinforcement, radiator support, body frame and the outer fender).

4.2.1 Simplified Geometry

We will use simplified geometry for parts. The front end can be considered to have lateral symmetry. To reduce the computational complexity of our analysis, we will consider only the left half of the front end. In this model, we will simulate a scenario where all parts have nominal geometry, but there exists intentional gap of 2 mm between parts as shown in Figure 4-2. The weld guns meet midway between the intentional gap.

The body frame has a number of reinforcements welded to it prior to assembly station #2. At this point, the body frame can be considered to be fairly rigid. We will use a three dimensional representation for the geometry of the inner fender, reinforcement, radiator support and the outer fender. These parts are meshed using 8-noded shell elements as shown in Figure 4-3.

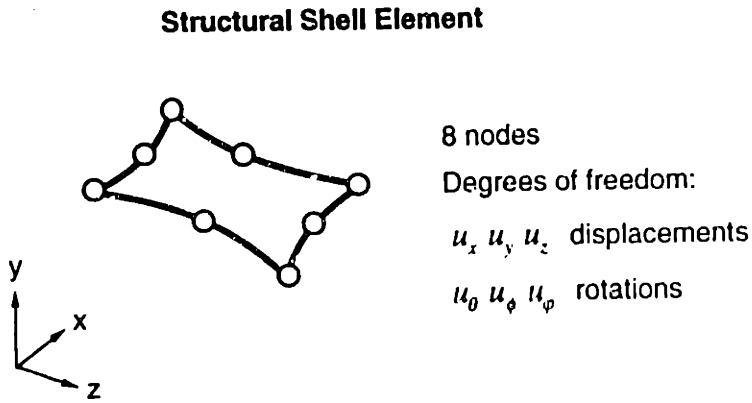

Figure 4-3. The shell element used to model part geometry

4.2.2 Connectivity graphs

As discussed in the previous chapter, we will analyze only the fasten operation in every assembly station. The connectivity graphs for the three assembly stations are shown in Figure 4-4. During the inspection process, the front end is positioned by the body and no fixture is used. So, no connectivity graph is shown for the inspection station.

4.2.3 The Assembly

The assembly consists of five parts: the inner fender, reinforcement, radiator support, body and the outer fender. There exists an intentional gap of 2 mm between the mating surfaces of the inner fender and the reinforcement and the body. The sheet metal parts are 1 mm thick.

4.3 Method

Let sub-scripts 1,2, 3 and 4 refer to assembly stations 1, 2, 3 and the inspection station respectively. For the n th station, the deformation of outgoing sub-assembly with respect to incoming geometry is represented as $\mathbf{u}_n$ where $1 \le n \le 4$. The total deformation of outgoing sub-assembly with respect to reference geometry is represented by $\mathbf{U}_n$. From Chapter 3,

$$\vec{U}_n = \sum_{i=1}^{n} \vec{u}_i, \; for \; 1 \le n \le 4$$

For this model, the nominal geometry of the parts was defined using the commercial solid modeler, ProEngineer®. The geometry was then imported to Ansys® in IGES revision 5.1 format. The finite element analysis for every station was simulated in Ansys®. For every station, displacement constraints and degree-of-freedom constraints were applied using their corresponding the connectivity graph (The nodal displacements $\mathbf{u}_n$'s and reaction forces $\mathbf{F}_\beta$'s were found. The output of the analysis of one station was used as an input to the next station. The geometry of the final assembly is found using $\vec{U}_4 = \sum_{i=1}^{4} \vec{u}_i$.

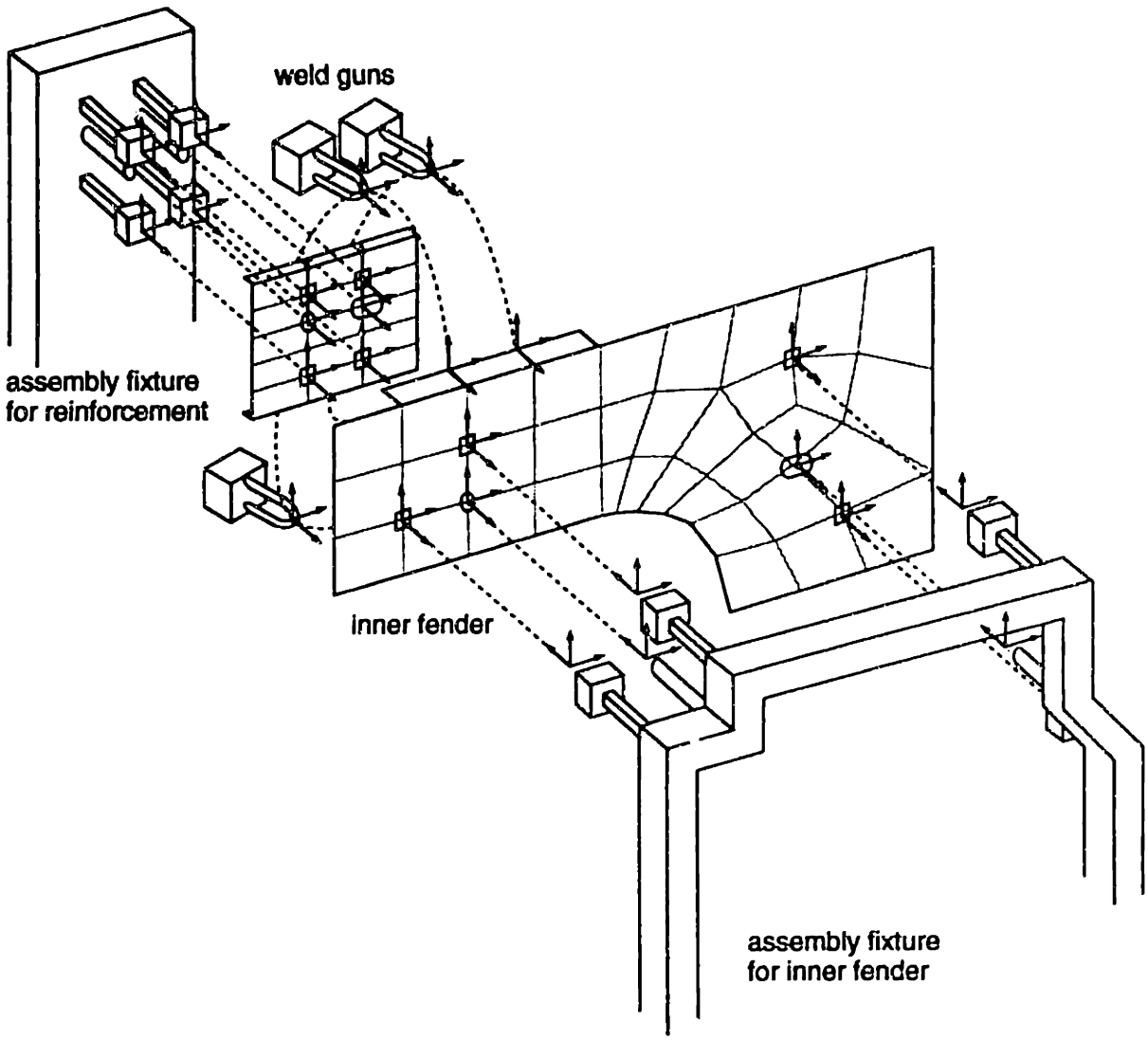

(a) Connectivity graph for assembly station #1

Figure 4-4. Connectivity graphs

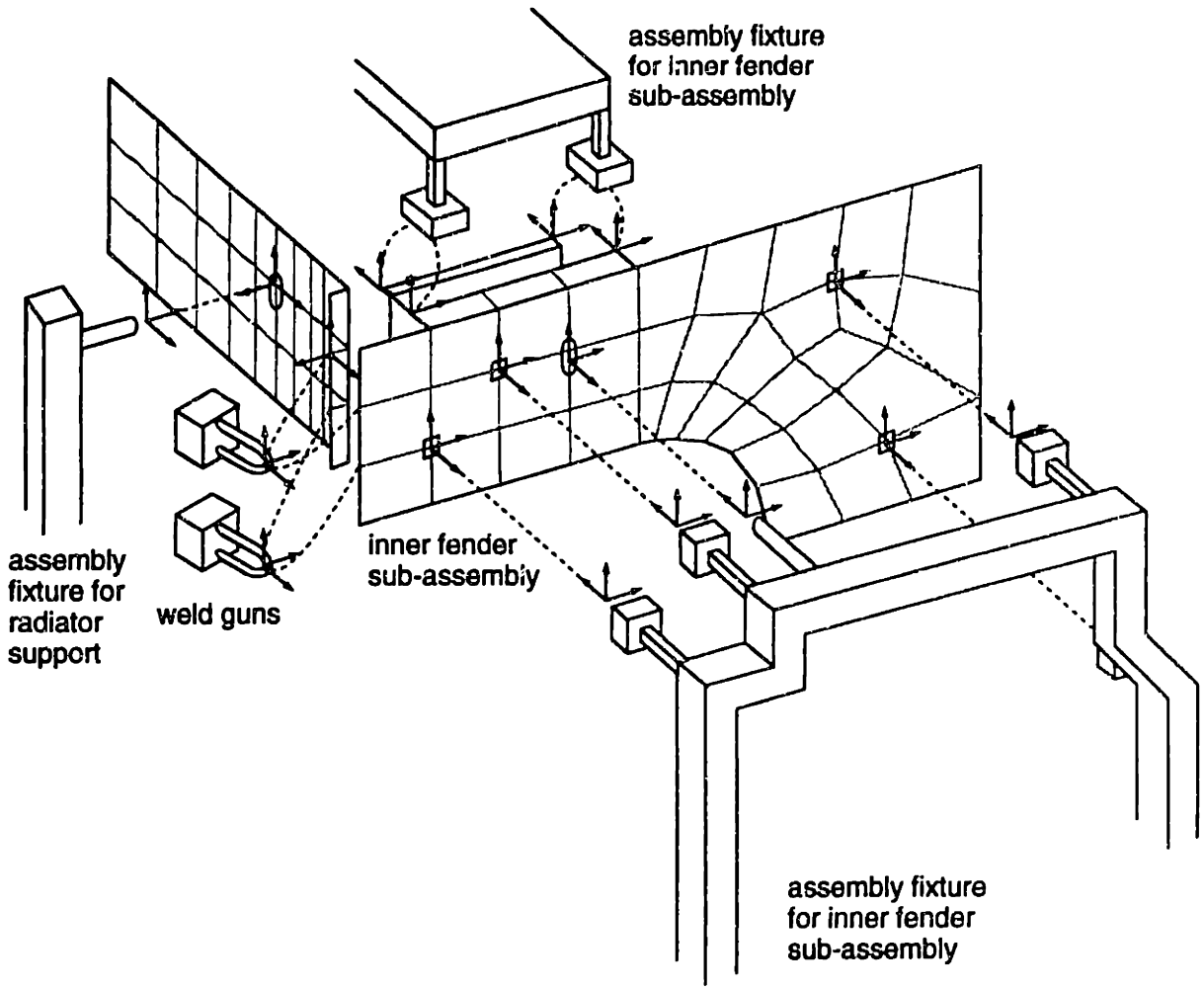

Figure 4.4 (b) Connectivity graph for assembly station #2

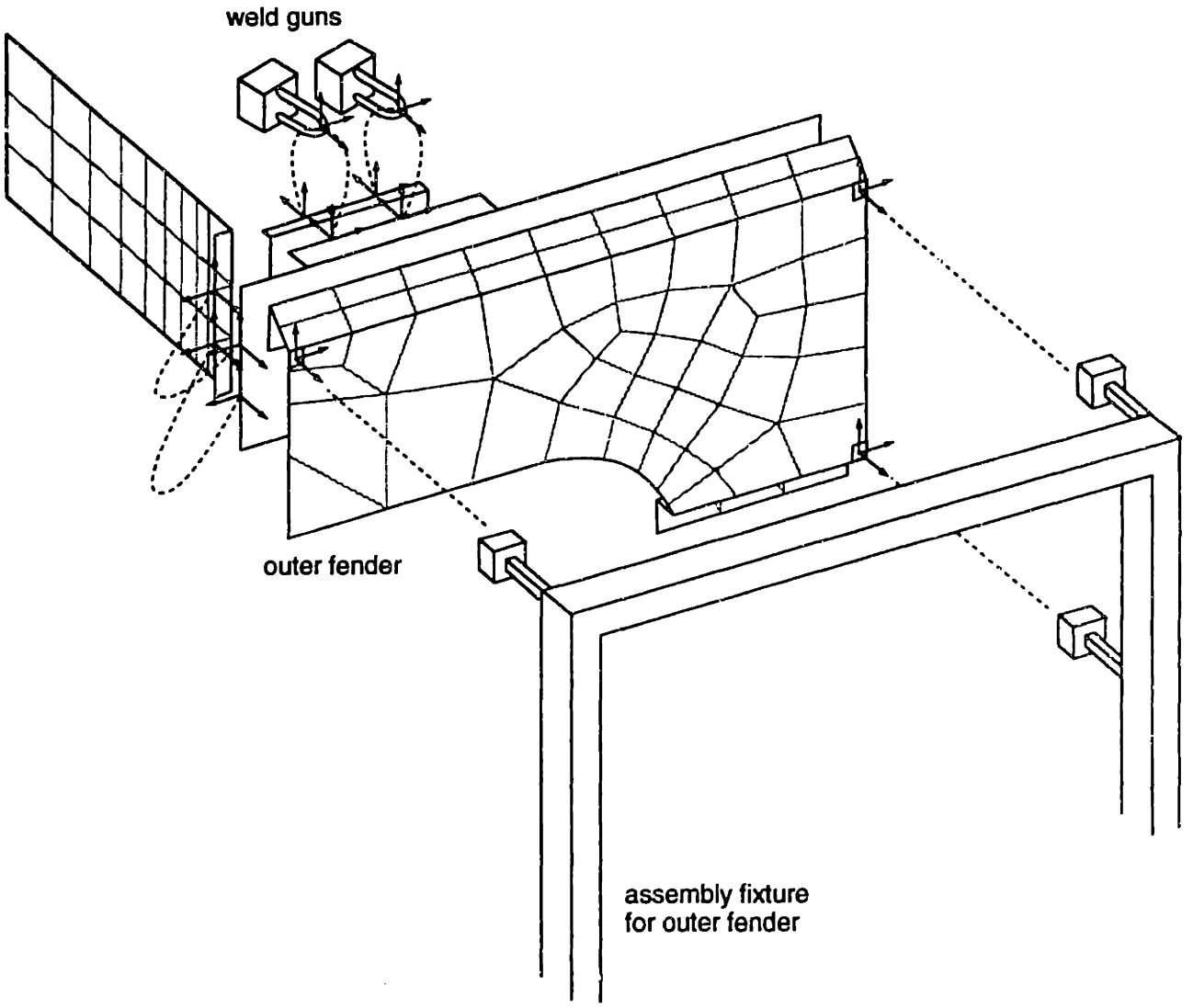

Figure 4.4 (c) Connectivity graph for assembly station #3

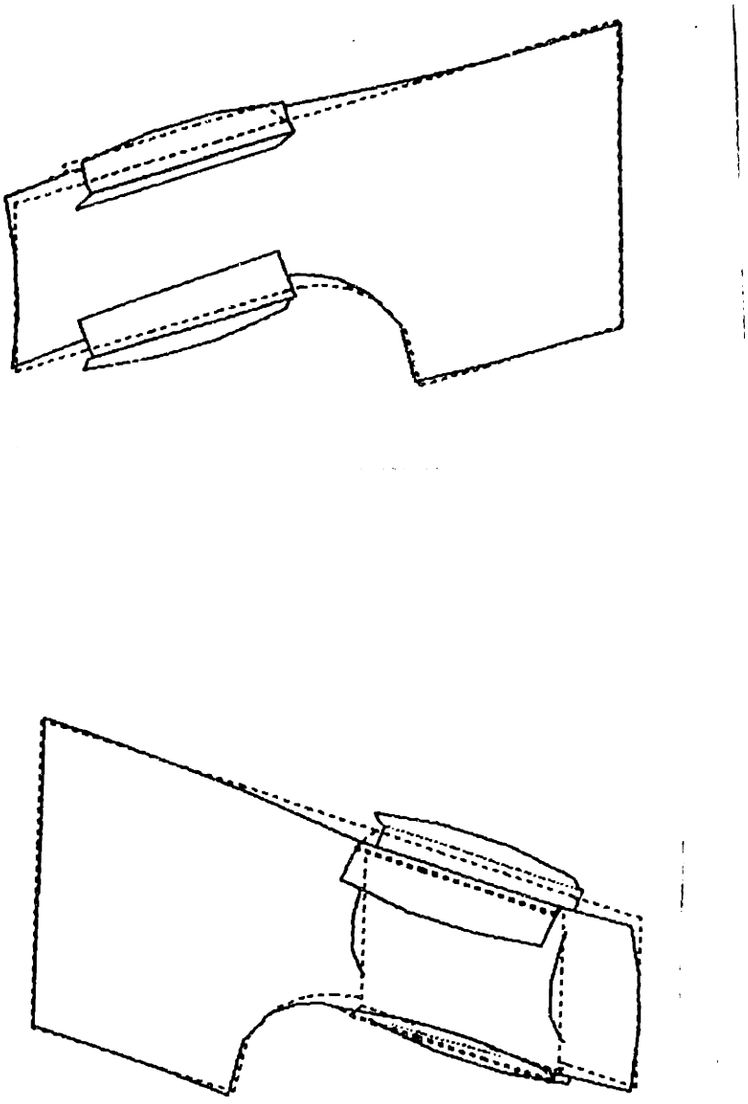

Figure 4-5 (a). Deformed geometry u_i for assembly station #1 (Isometric and oblique view with deformed geometry shown in solid lines and reference geometry shown in dashed lines. Displacements are magnified 45 times)

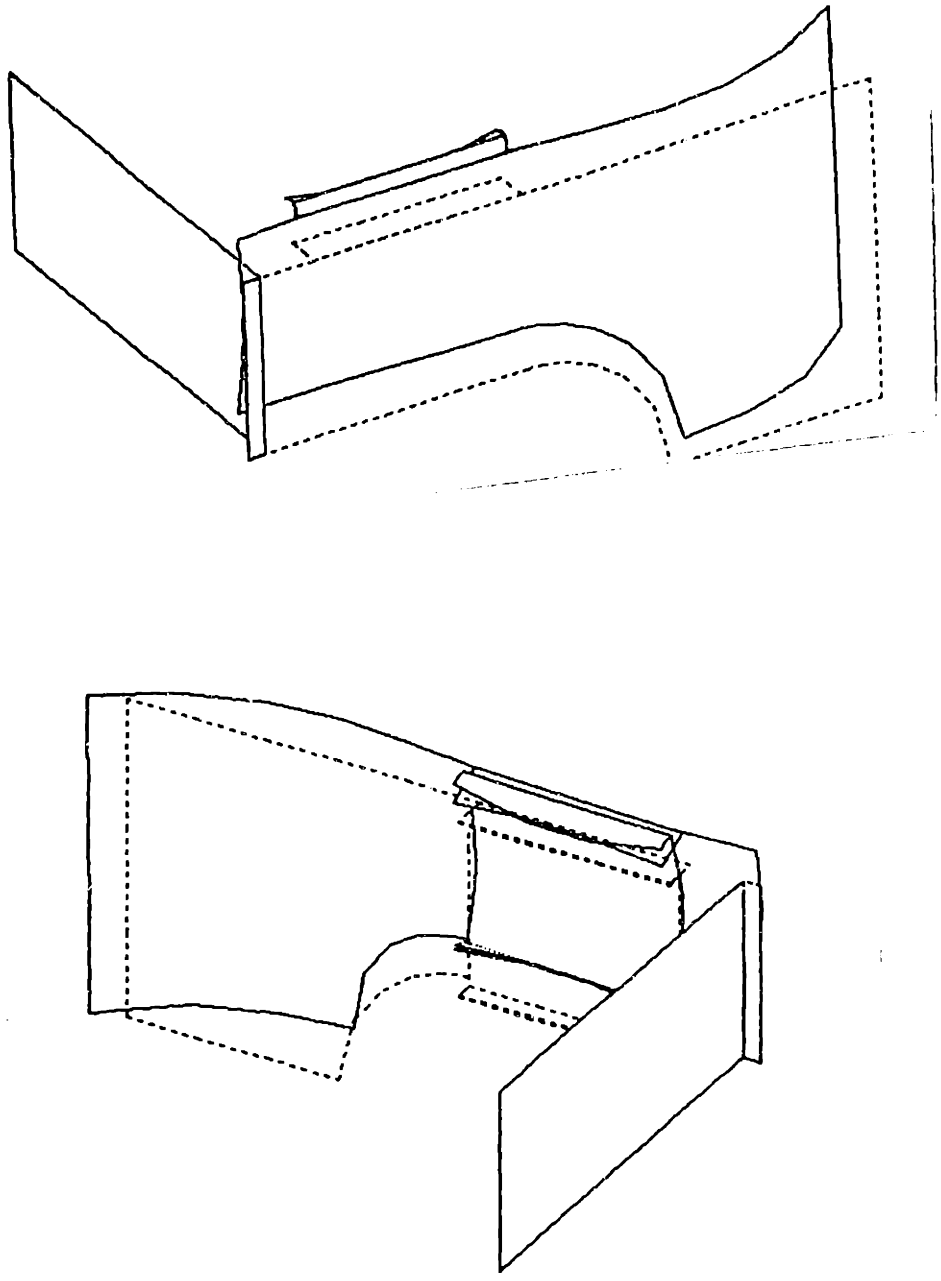

Figure 4-5 (b). Deformed geometry u_2 for assembly station #2 (Isometric and oblique view with deformed geometry shown in solid lines and reference geometry shown in dashed lines. Displacements are magnified 45 times)

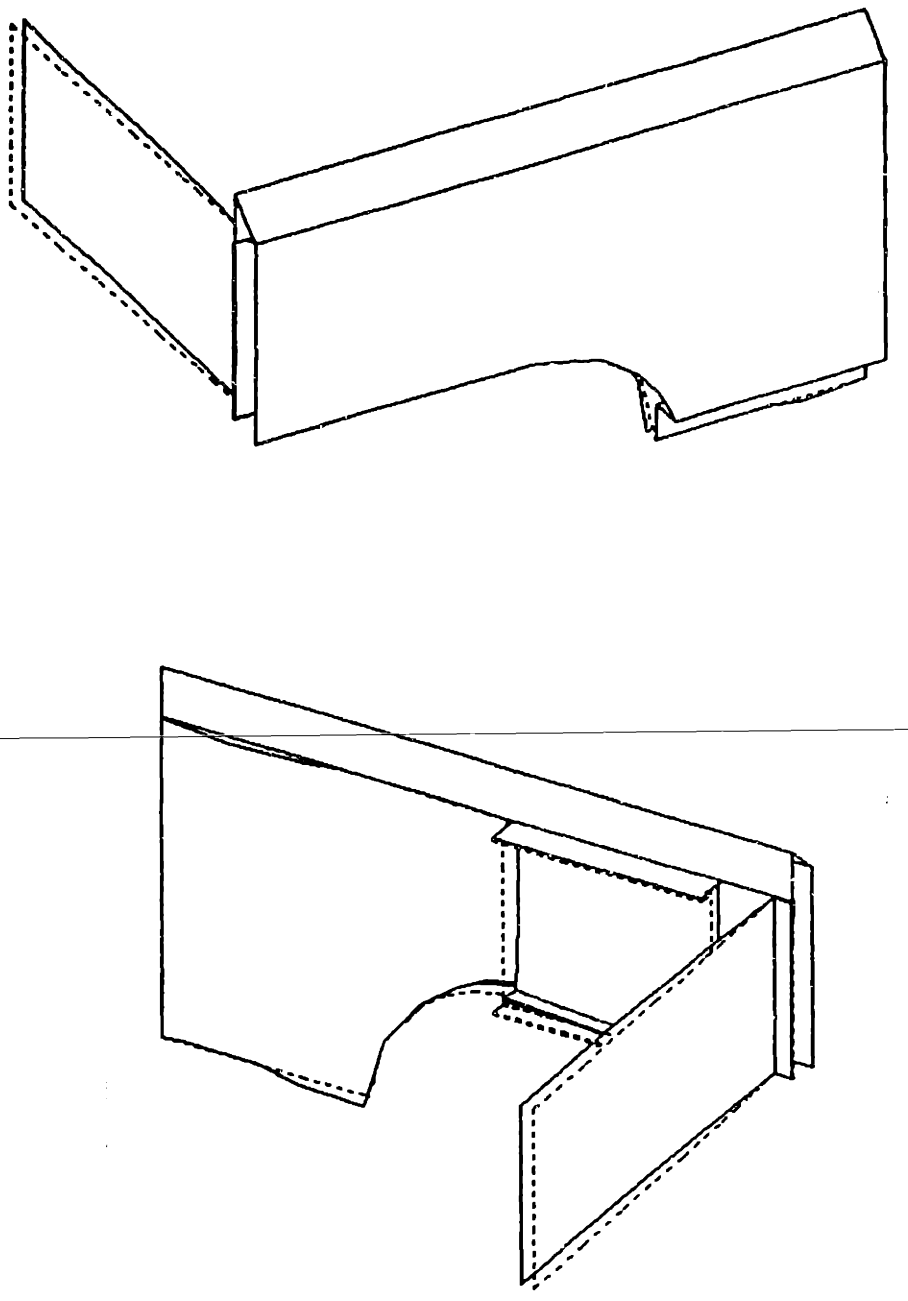

Figure 4-5 (c). Deformed geometry u_3 for assembly station #3 (Isometric and oblique view with deformed geometry shown in solid lines and reference geometry shown in dashed lines. Displacements are magnified 45 times)

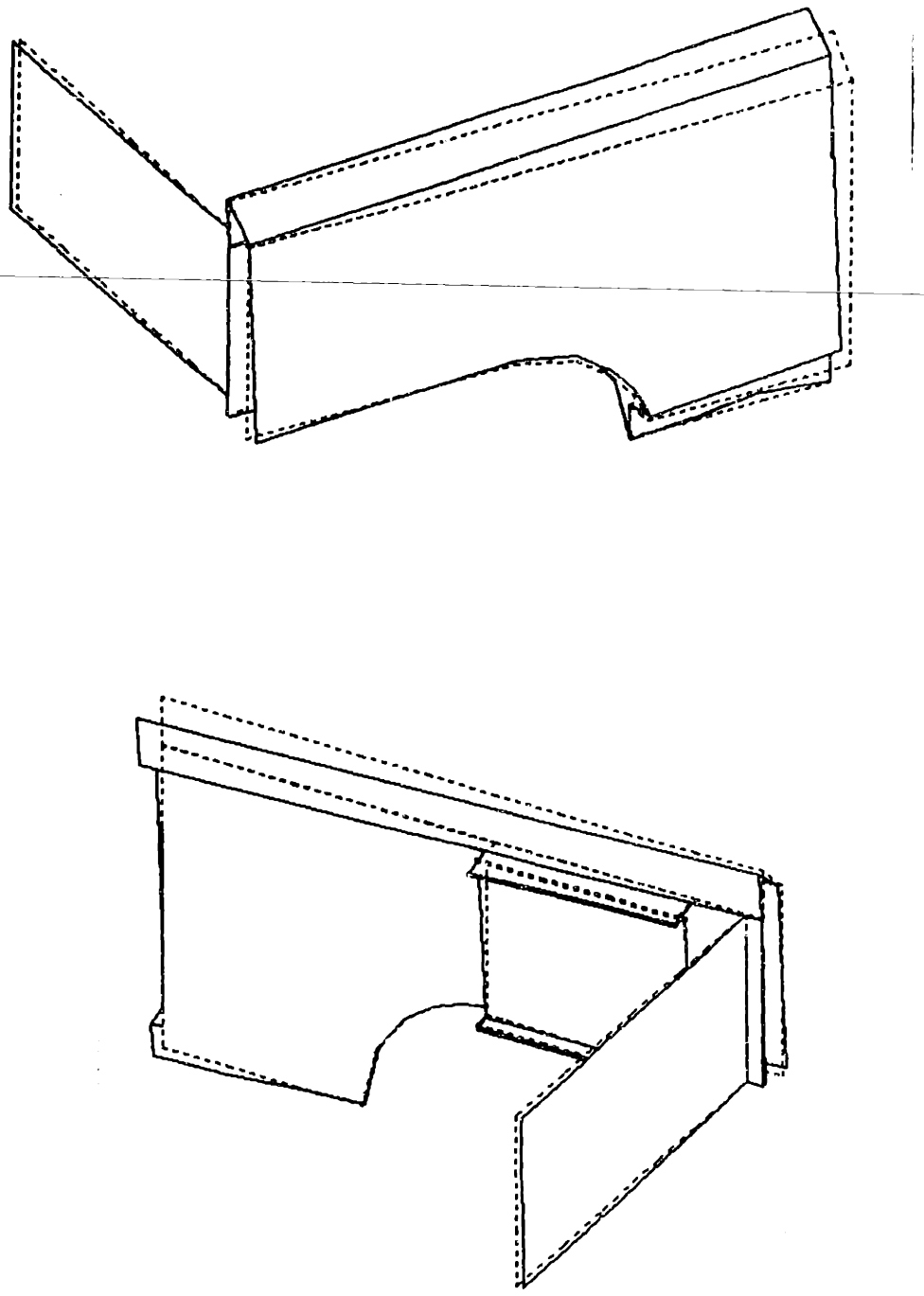

Figure 4-5 (d). Deformed geometry u_4 for inspection station (Isometric and oblique view with deformed geometry shown in solid lines and reference geometry shown in dashed lines. Displacements are magnified 45 times)

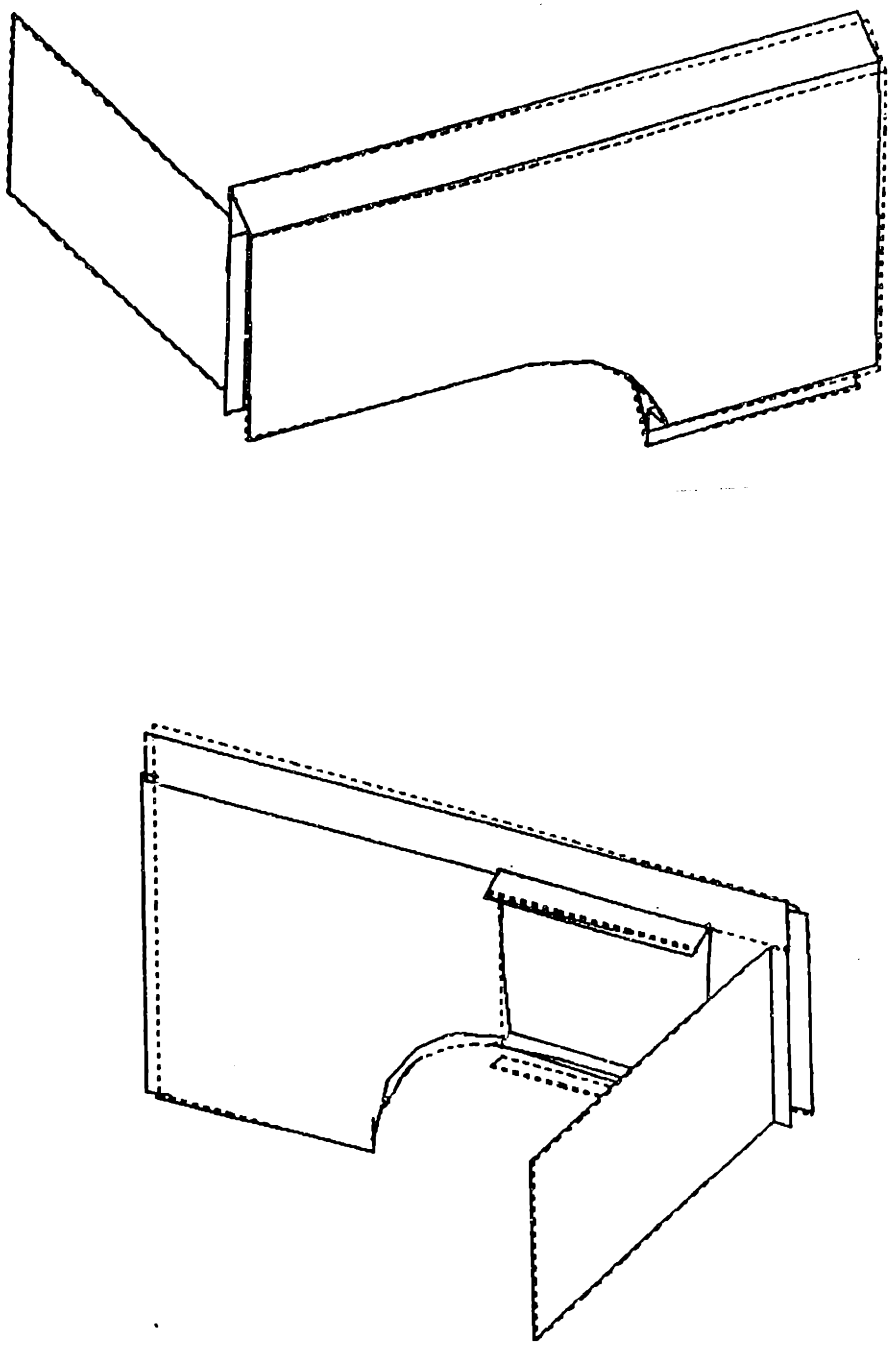

Figure 4-6. Geometry of final product in the inspection station $U_4 = \sum_{i=1}^{4} u_i$ (Isometric and oblique view with deformed geometry shown in solid lines and reference geometry shown in dashed lines. Displacements are magnified 45 times)

4.4 Results

The results of the finite element analysis for the four stations is shown in Figure 4-5. The deformed geometry is shown with the displacements magnified by a factor of 45. Although, it seems that parts penetrate each other, it is an artifact of the displacement magnification. The geometry of the final assembly $\mathbf{U}_4$ in the inspection station is shown in Figure 4-6 (note that $\vec{U}_4 = \sum_{i=1}^{4} \vec{u}_i$).

4.5 Discussion

We find that although parts, fixtures and weld guns have nominal geometry, in the presence of intentional gaps between parts, the geometry of the final product deviates form the nominal. Intentional gaps have a non-ignorable effect on the assembly process.

We also observe that the geometry of the outer fender is affected not only by its geometry, but even more profoundly by the geometry of other parts that belong to the assembly.

5.

Design of Locator Schemes

In this chapter, we will apply our assembly model to design locator schemes for compliant parts. This chapter discusses a two-dimensional case study and a three-dimensional case study for the design of locators for the inner fender.

5.1 Locator Schemes

A *locator scheme* positions a part with respect to a fixture. A locator scheme is characterized by the number, type and position of locators for a part. A locator scheme is required for every part/sub-assembly at every assembly/inspection station. Locator schemes determine the position $\vec{X}_{part}$ and compliant body deformation $\vec{U}_{part}$ of a part during the entire process. They play a central role in determining the dimensional integrity of the assembled product.

Typically, a part consists of a main panel and 3-4 reinforcements that are welded to it. After reinforcements are welded to the main panel, it forms a reinforced part. Many such reinforced parts as assembled to form a sub-assembly. Multiple sub-assemblies are put together to form an automobile body. Before the fasten operation in an assembly station, all incoming parts require a locator scheme to position them. After the fasten operation, parts form a sub-assembly and only one locator scheme is required to position the sub-assembly in the subsequent stations. As a part propagates through the assembly process, it is positioned in stations using the locator scheme for the main panel. Design of a locator schemes refers to designing a locator scheme for this main panel (see Figure 5-1).

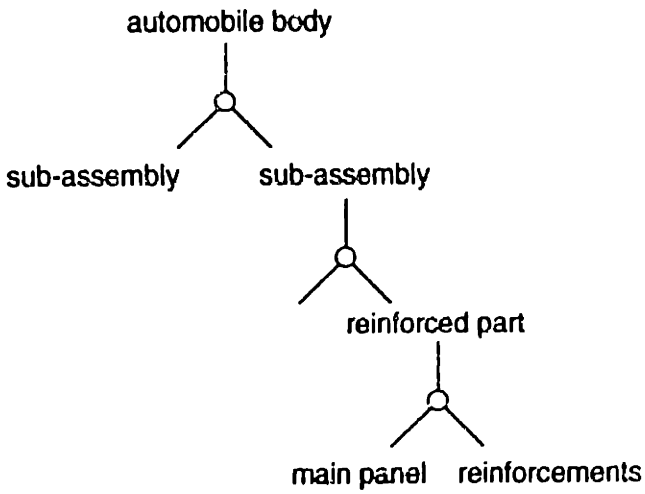

Figure 5-1. Schematic of assembly process

Ideally, one locator scheme should be used to position a part in all stations. But there are circumstances under which the part has to be positioned in a station using a locator scheme different from the one used in other stations. This happens due to the following reasons:

Accessibility: All locators might not be accessible at a certain station. After parts are assembled, a locator of one part can get obscured by the other part, thus, making it inaccessible. Weld guns, clamps, and other assembly tooling can also make locators inaccessible at a station. In such cases, a different locator is often used to position the part.

Extra support: In addition to the clamps designed for a locator scheme, extra clamps are added to the assembly fixture, to provide additional support to the part during welding. After a reinforcement is welded on to a part, the part becomes stiff and the extra clamp is no longer in subsequent stations.

Longevity of locators: Locators (on both, the part and the fixture) can get damaged due to repeated use. If the part needs to be positioned at a large number of stations, another set of locators is used to reduce the possibility of erroneous positioning due to damaged locators.

5.2 Requirements of a Locator Scheme

These are the requirements that a locator scheme must satisfy.

5.2.1 Total restraint of part

Although there might be compliant body motion under assembly forces, there should be no rigid body motion during any operation of the assembly process. A

compliant body has infinite degrees of freedom, out of which six degrees of freedom correspond to rigid body movements (3 rotations and 3 translations). The locator scheme must completely constrain all 6 rigid body motions (Sakurai90). Very often, locator schemes constrain more than 6 degrees of freedom. This results in over-constraining of the part.

5.2.2 Accessibility

The locators should be such that there is no interference between fixture, the part and weld guns at any time during the assembly process. After parts are assembled some locators of a part might not be accessible in the sub-assembly. These locators cannot be used for subsequent stations to position the part. When locator schemes are designed, attention has to be paid to the positions of clamps, weld guns, power transformers for weld guns, electrical wiring, pneumatic actuators, and other components of the assembly tooling.

5.2.3 Acceptable part deformation and stresses

Parts deform during the assembly operation. To ensure good dimensional integrity, the locator scheme should be designed in such as way so as to minimize part deformation and stresses. During the assembly process, parts are subject to two kinds of external forces: gravity and assembly forces. Assembly forces include weld gun forces and forces exerted by the clamps and pins of a fixture. Under extreme uniaxial compression, parts can buckle.

Assembly forces and gravity cause stresses to be developed in the parts. These stresses should be within acceptable limits. Locked in stresses can lead to stress-induced corrosion. Also, if stresses exceed the yield strength of the material, parts deform plastically. Locator schemes should be designed to keep part deformation and stresses within acceptable limits.

5.2.4 Variation stackup

A locator scheme, when artfully designed, can reduce sensitivity of the dimensions of the assembled product to variations in geometry of parts, fixtures and weld guns.

Locator schemes are designed so that variations are "pushed" to one side. As an example, consider the fender-to-hood flushness. The high-low position of the outer fender is determined by the high-low position of the surface on the inner fender on which

the outer fender rests. So, the high-low position of this surface is important. To ensure the correct location of this surface, the inner fender is positioned in assembly station #2 using surface locators that lie on this surface (as discussed in the previous chapter). This way imperfections on the fender inner are "pushed downward." Any variation in the height of the inner fender does not affect the position of the outer fender. This reduces the sensitivity of the high-low position of the outer fender to variations in geometry of the inner fender.

5.2.5 Overuse of locators

If a part goes through many assembly stations, the locator scheme is used repeatedly at every assembly station. The rate of production determines how many stations there are in the assembly line. Higher rate of production, lower the cycle time, more are the number of stations, hence locators are subjected to repeated exposure to assembly forces. So, durability of a locator scheme also plays a role in its design.

5.3 Design of Locator Schemes

5.3.1 Related work

5.3.1.1 Academia

Most of the work done in academia is restricted to a one-part-one-station scenario. Existing research literature for this case is discussed in detail in Chapter 2.

5.3.1.2 Industry

Currently the design of locator schemes is experience-based. A generic part is used as a template and the locator scheme for the new part in question is derived from this template. Designers use "recommended practices" to derive a locator scheme for the new part starting from the generic part. Some examples of these recommended practices are: (a) pins and slots should be square to the xyz grid (b) angle between pin and slot on a part should not be more than 25 (d) whenever possible, locator surfaces should be placed on 100mm body coordinate lines.

Although these recommended practices have developed over the years based on experience, the reasoning behind the choice of number, type and position of locators is lost. Also, the geometry of parts changes significantly from one model to the next.

Locator scheme design is strongly influenced by the part geometry and hence, designing a locator scheme for the new part is more art than science.

5.3.1.3 Commercial software

Commercial software (e.g. VSA®, 3-Dcs®, Mechanical Advantage®) exists to calculate to evaluate the sensitivity of an assembly dimension to incoming part dimensions by performing a variation stack-up analysis. This analysis is based on rigid body geometry. These software cannot evaluate the sensitivity of product dimension to variation in position of weld gun and variations in locator position.

5.3.2 Locators and Mating surfaces

The behavior of a part during the assembly process depends on all interfaces (part/part and part/fixture interfaces) that come in contact with it during the assembly process. Locators are part/fixture interfaces. Mating surfaces are part/part interfaces between two adjacent parts of an assembly. Both of these interfaces affect the geometry and position of the part. We have to clarify the distinction between the two.

Locators are features that are used consistently throughout the manufacturing, assembly, inspection processes. The part and its tooling make and break contact repetitively during these processes and this is shown by the connectivity graphs. On the other hand, once mating surfaces are established by welding, the contact is maintained.

There are three main types of locators: pin/hole, pin/slot, clamp/surface. There is only one type of mating surface, and it is surface/surface.

Since locators and mating surfaces both affect the part, design of locator schemes and design of mating surfaces go hand in hand.

5.3.3 Criteria for comparing locator schemes

Design of locator schemes is done by comparing two candidate locator schemes. Conceptual alternatives are derived for locator schemes. A comparison is made by evaluating these alternatives. This comparison can be done by quantifying the "goodness" of the locator scheme. The following metrics can be used for this comparison:

- Influence of intentional gaps on assembly dimensions of interest.
- Sensitivity of assembly dimension to variations in parts, fixtures and weld guns.
- Deformation and stress distribution in the part.
- Reuse of locators.

- Force required to place the part in its fixture.

In the following two sections, we will discuss two case studies for the design of locator schemes. We will consider a two-dimensional and a three-dimensional case study and design a locator scheme for the fender inner. We will generate conceptual alternatives in both case studies and then evaluate them. To illustrate the use of different metrics for evaluating locator schemes, we will consider the sensitivity of the hood-to-fender flushness to variation in weld gun position (for the two-dimensional case study), and the influence of intentional gaps on the hood-to-fender flushness/margin (for the three-dimensional case study).

5.4 2D case study

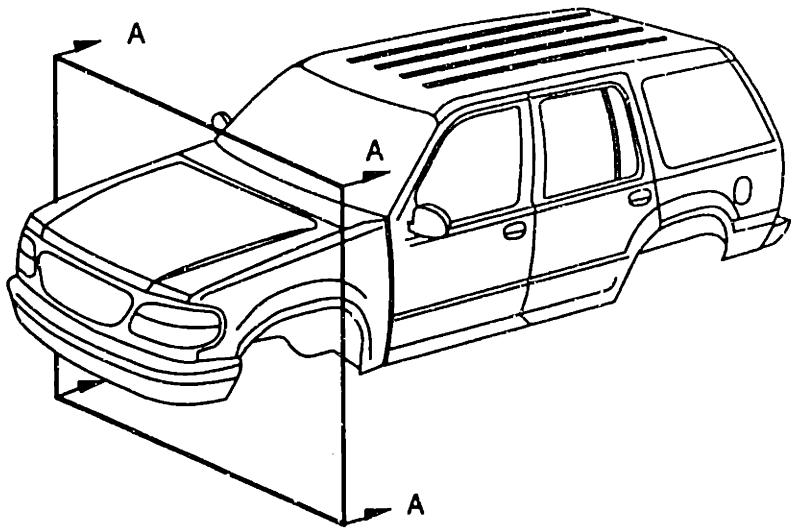

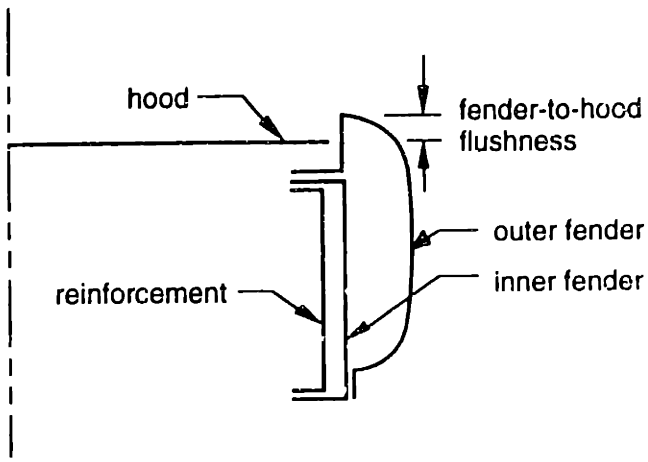

Section A-A

Figure 5-2. The 2-D case study

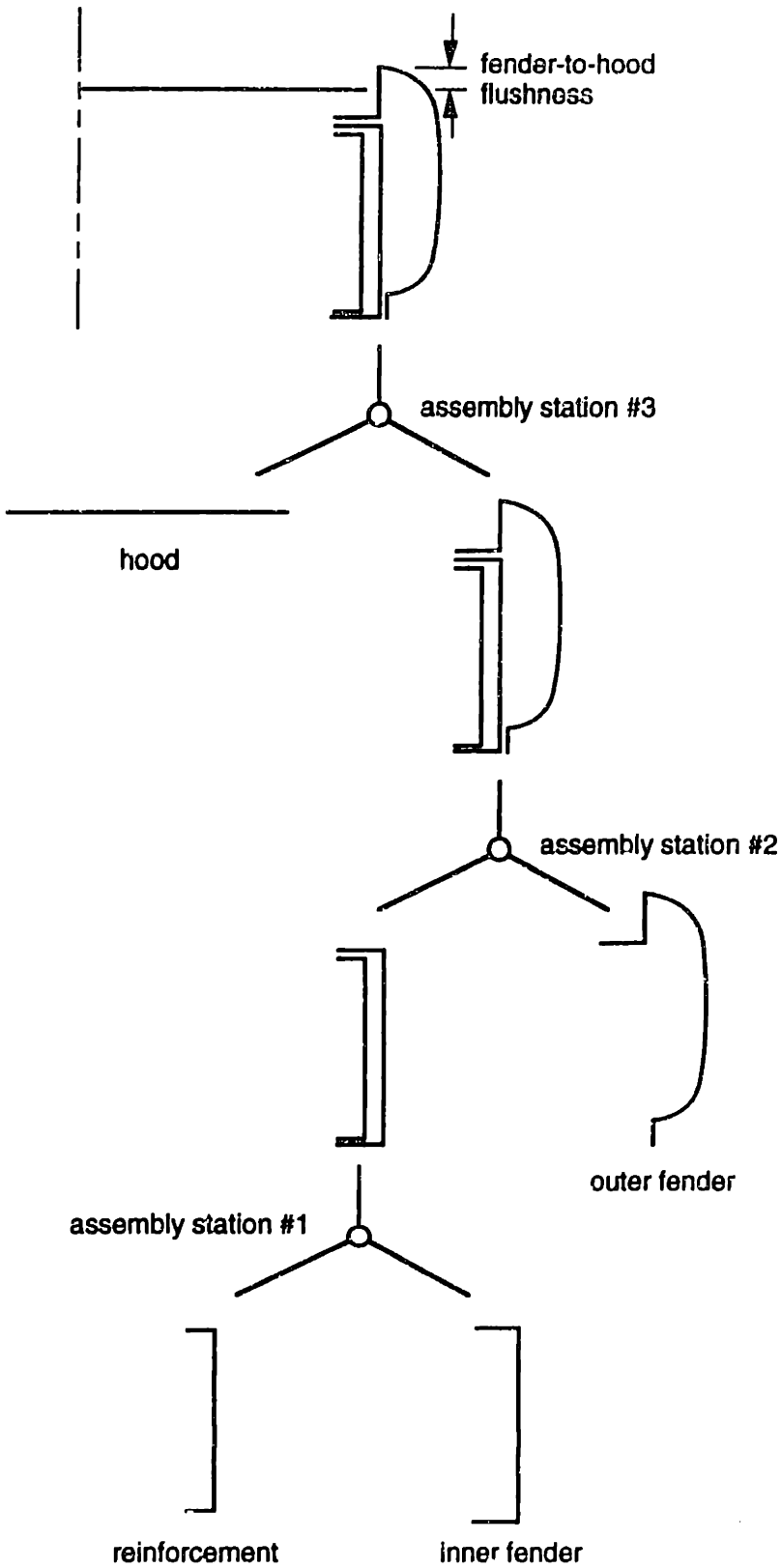

Figure 5-3. Assembly sequence for 2-D case study

In this section we will perform is a 2-D model with simplified part geometry of the inner fender and its reinforcement. Most sub-assemblies in an automobile body show the following characteristics:

1. They are comprised of a main panel and reinforcements.

2. The parts are fastened together by spot welding.

3. The weld spots are situated on flanges that branch out from the main geometry of the parts.

4. The main panel goes through a series of assembly stations. At every station, reinforcements are welded to it. The main panel, with its reinforcements welded to it, is positioned by the locator scheme of the main panel.

A sub-assembly comprised of an inner fender (the main panel) and a reinforcement can be considered as a generic sub-assembly in an automobile body for the aforementioned reasons. We will discuss the design of a locator scheme for the inner fender, the main panel of this sub-assembly.

The major parts in the assembly are: inner fender, reinforcement, outer fender and the hood (see Figure 5-2). We are interested in the flushness between the hood and the outer fender.

During the design process, the mating surfaces between parts are designed and then design of locator schemes is done.

5.4.1 Design of mating surfaces

Here, we first design the mating surfaces between the inner fender and the outer fender. The rule of thumb for designing mating surfaces is to "use slip planes." We want the analyze the hood-to-fender flushness, so we will concentrate on the mating surface that influences this assembly dimension. We generate a number of conceptual alternatives. Figure 5-4 shows three such conceptual alternatives.

Concept A maximizes the use of slip planes. Here, positioning of the outer fender can be done independent of the position of the inner fender. Thus the flushness value between the two parts can be monitored accurately. Concept A also has a simple part geometry, which makes it easy to manufacture those parts. The drawback of this concept is that the mating surfaces are not accessible for fastening.

Concept B uses two slip planes to allow monitoring the high/low position of the outer fender. Now, although the mating surface is accessible, its angle and position with respect to the front end makes it difficult for manual disassembly of the outer fender. Manual dis-assembly is required if the outer fender gets damaged in an accident and needs to be replaced manually.

Concept C has two mating surfaces perpendicular to each other. Although this concept does not allow to adjust for the high-low position of the outer fender, it is superior to concepts A and B, because it has simple part geometry. Also, both the mating surfaces are easily accessible and manual dis-assembly is possible.

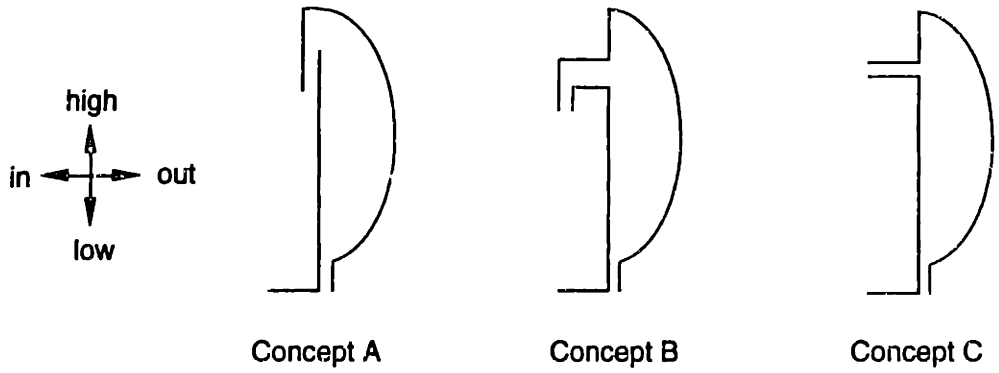

Figure 5-4. Conceptual alternatives for the mating surface between the inner fender and its reinforcement

We will choose concept C for the mating surfaces between the inner fender and the outer fender. The design of mating surfaces between the inner fender and the reinforcement is a trivial task since there is only one conceptual alternative that will provide enough structural rigidity to the inner fender.

5.4.2 Locator scheme design for the inner fender

We now proceed to the design of a locator scheme for the inner fender. For the fender inner, let us consider two locator schemes: hole-slot-surface scheme and the n-2-1 scheme. Let us call the hole-slot-surface scheme as option A and the n-2-1 scheme as option B. For a two-dimensional case, the hole-slot-surface scheme is comprised of a hole and two surface as shown in Figure 5-5. The n-2-1 scheme has two primary surfaces and one secondary surface as shown in Figure 5-6. Figure 5-5 and Figure 5-6 also show the connectivity graphs for the two options.

We will evaluate the sensitivity of the fender-to-hood flushness for the two options and choose the option that provides a robust assembly. i.e. one that makes the fender-to-hood flushness less sensitive to variation in weld gun position. As shown in Figure 5-3, the inner fender goes through a number of assembly stations. In this example, for the sake of clarity, we will discuss only the first assembly station and an inspection station. A similar analysis can be performed for other assembly stations also. Since the outer fender rests on the inner fender, for the fender-to-hood flushness to be accurate,

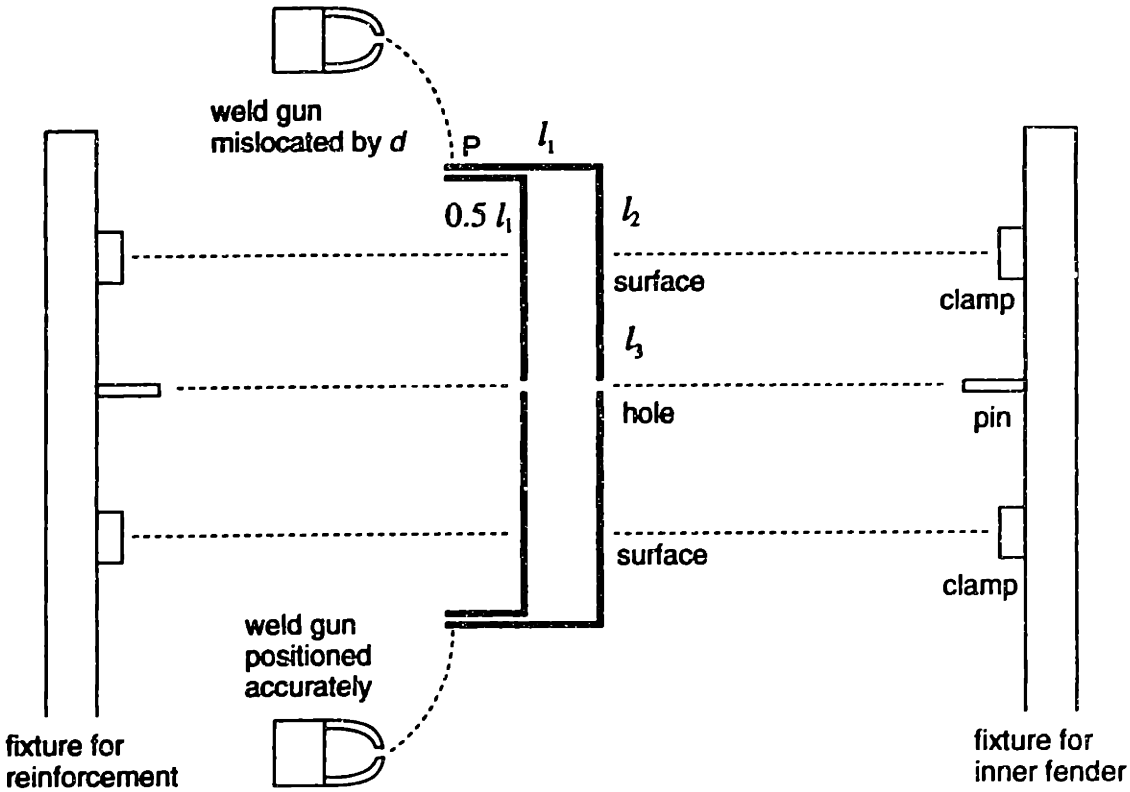

(a) Connectivity graph for the assembly station

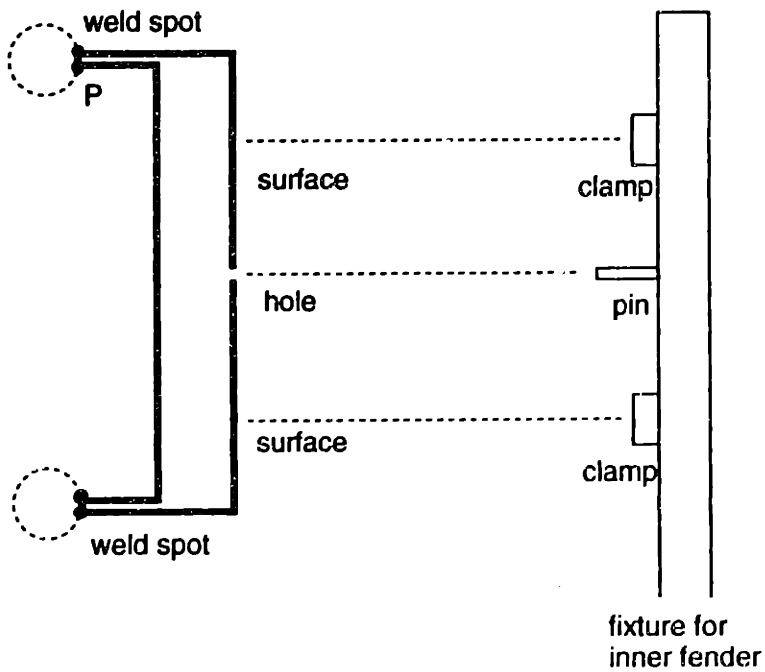

(b) Connectivity graph for the inspection station

Figure 5-5. Connectivity graphs for Option A

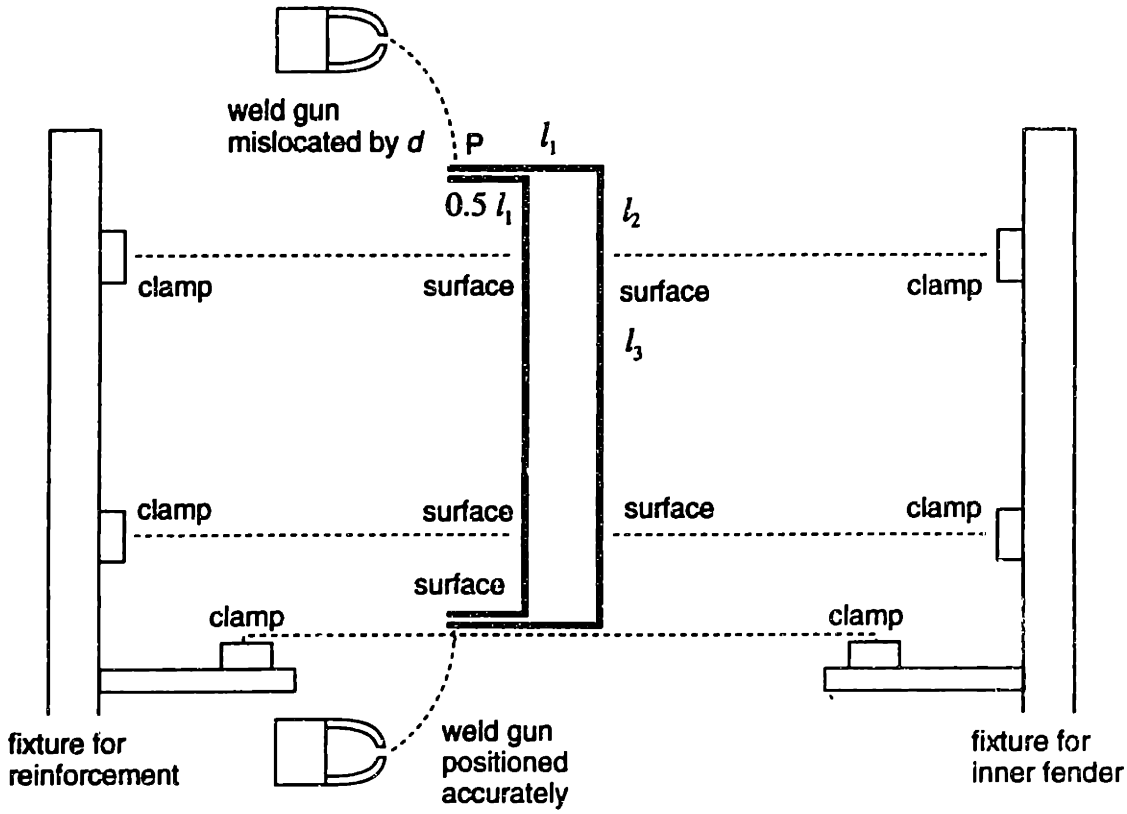

(a) Connectivity graph for the assembly station

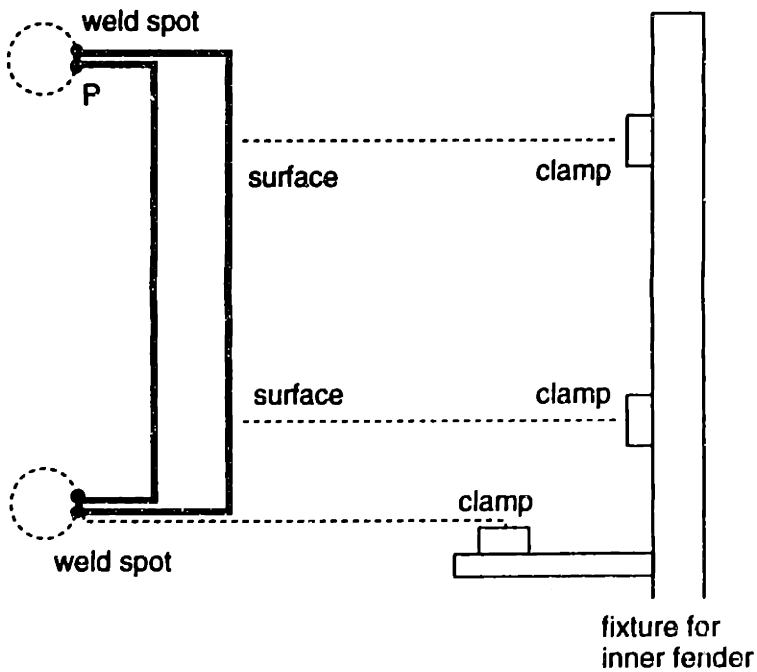

(b) Connectivity graph for the inspection station

Figure 5-6. Connectivity graphs for Option B

point P (see Figure 5-5) on the fender inner has to be positioned precisely. So, for this analysis we will look at the high/low position of point P in the inspection station after the reinforcement has been welded to the inner fender.

The reinforcement and the inner panel are placed and clamped in the assembly fixture using their respective locator schemes. Next the welding guns fasten the to parts together. The clamps are released and the sub-assembly is removed from the fixture. The sub-assembly is then placed and clamped on the inspection fixture and the high/low position of point P is measured.

We will perform the analysis of this process as described in Chapter 2. To better understand how different parameters affect the assembly dimension of interest, we will perform the finite element analysis in symbolic form, instead of a numerical form.

5.4.3 Symbolic finite element analysis

We model the parts as beam elements (see Figure 5-7). Every beam element has two nodes each with 3 degrees of freedom. The element is assumed to have uniform cross-sectional area A, and a uniform flexural stiffness EI (moment of inertial I, and Young's modulus E) over its length L. At nodes 1 and 2, there exist nodal force F and corresponding nodal displacement u.

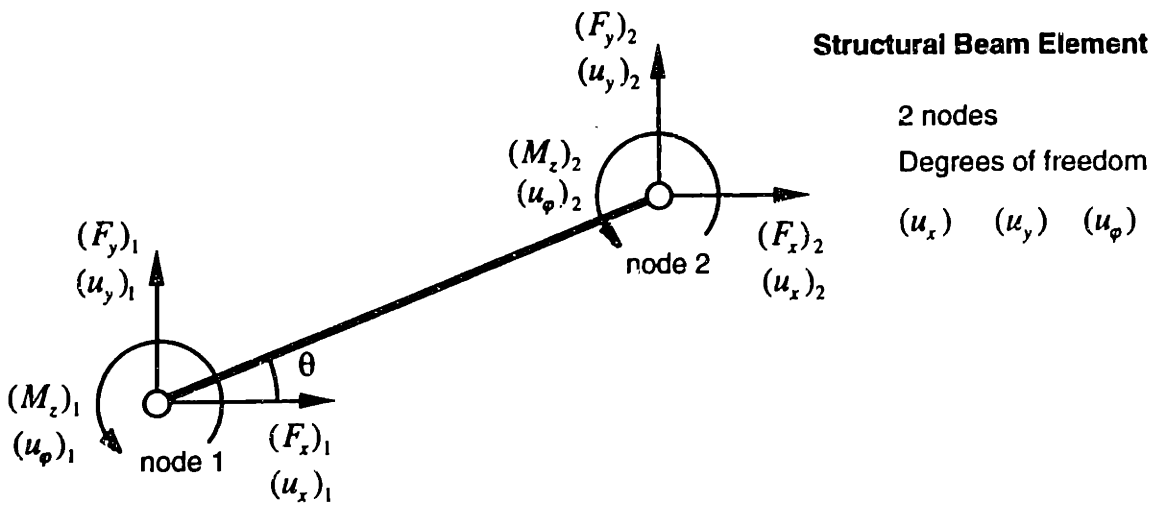

Figure 5-7. The beam element for symbolic FEM

The stiffness equation for the beam element can be represented in matrix form as (Martin66),

$$\mathbf{F = Ku} \qquad \text{Equation 5-1}$$

where,

$$\mathbf{F} = \begin{bmatrix} (F_x)_1 & (F_y)_1 & (M_z)_1 & (F_x)_2 & (F_y)_2 & (M_z)_2 \end{bmatrix}^T$$

$$\mathbf{u} = \begin{bmatrix} (u_x)_1 & (u_y)_1 & (u_\varphi)_1 & (u_x)_2 & (u_y)_2 & (u_\varphi)_2 \end{bmatrix}^T$$

Equation 5-2

and,

$$\mathbf{K} = EI \left[\begin{array}{ccc:ccc} A\lambda^2 + \frac{12I}{L^2}\mu^2 & & & & & \\ \left(A - \frac{12I}{L^2}\mu^2\right)\lambda\mu & A\mu^2 + \frac{12I}{L^2}\lambda^2 & & & \textit{Symmetric} & \\ \frac{6I}{L}\mu & -\frac{6I}{L}\lambda & 4I & & & \\ \hdashline -\left(A\lambda^2 + \frac{12I}{L^2}\mu^2\right) & -\left(A - \frac{12I}{L^2}\mu^2\right)\lambda\mu & -\frac{6I}{L}\mu & A\lambda^2 + \frac{12I}{L^2}\mu^2 & & \\ -\left(A - \frac{12I}{L^2}\mu^2\right)\lambda\mu & -\left(A\mu^2 + \frac{12I}{L^2}\lambda^2\right) & \frac{6I}{L}\lambda & \left(A - \frac{12I}{L^2}\mu^2\right)\lambda\mu & A\mu^2 + \frac{12I}{L^2}\lambda^2 & \\ \frac{6I}{L}\mu & -\frac{6I}{L}\lambda & 2I & -\frac{6I}{L}\mu & \frac{6I}{L}\lambda & 4I \end{array}\right]$$

Equation 5-3

Here, $\lambda = \cos\theta$, $\mu = \sin\theta$.

Equation 5-1 represents both, the deflection due to bending and due to uniaxial loading. For sheet metal parts, the deflection due to bending is the dominant mode of deformation. Deflection due to uniaxial loading is small and can be neglected. i.e. we can consider the beam element to be rigid for uniaxial loading. The displacements under these conditions can be found by,

$$\lim_{A \to \infty} \mathbf{u}$$

Equation 5-4

We can calculate the stiffness matrix *K* for every beam element using Equation 5-3. We obtain the stiffness matrix for the entire part, by assembling element stiffness matrices (Bathe82).

$$\mathbf{K} = \sum_i \mathbf{K}^{(i)}$$

Equation 5-5

where the matrix $\mathbf{K}^{(i)}$ is the stiffness matrix of the *i* th element and the summation goes over all elements in the assemblage.

Figure 5-8 shows finite elements and node numbering for options A and B. For both options we represent boundary conditions as discussed in Chapter 3. For example, boundary conditions for nodes 1 (weld gun/weld spot), 3 (clamp/surface) and 4 (pin/hole) for option A in the assembly station can be written as,

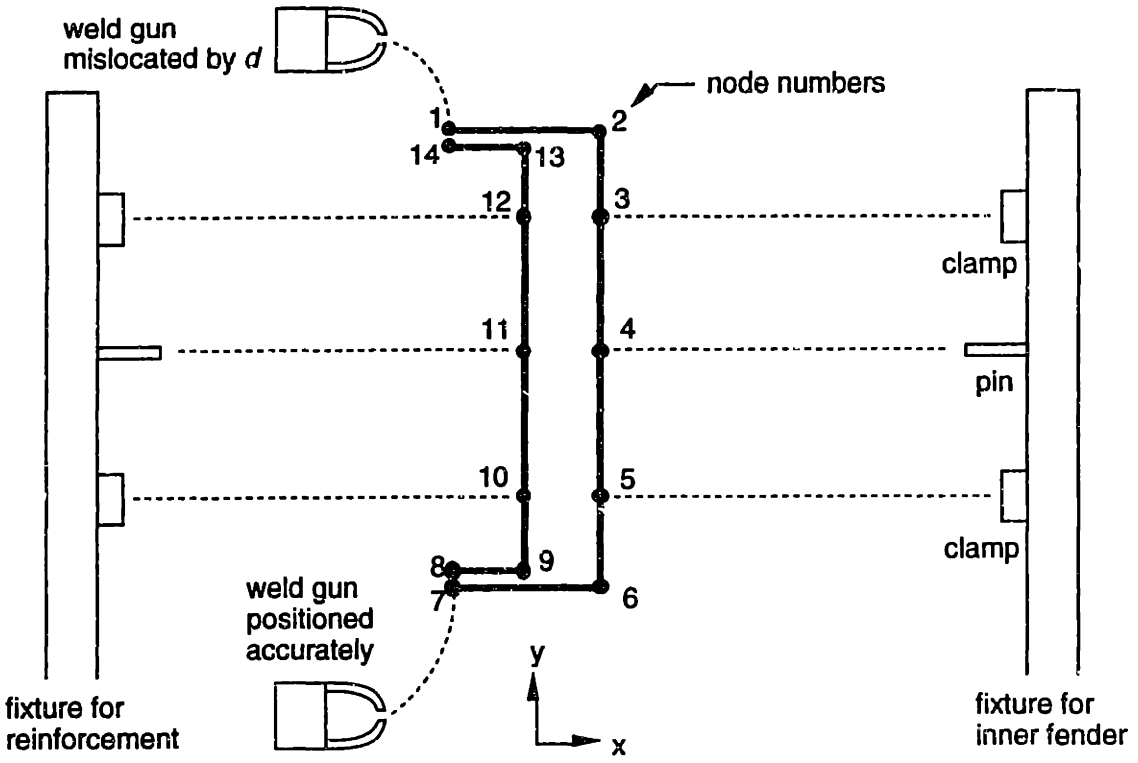

(a) Node numbers for Option A

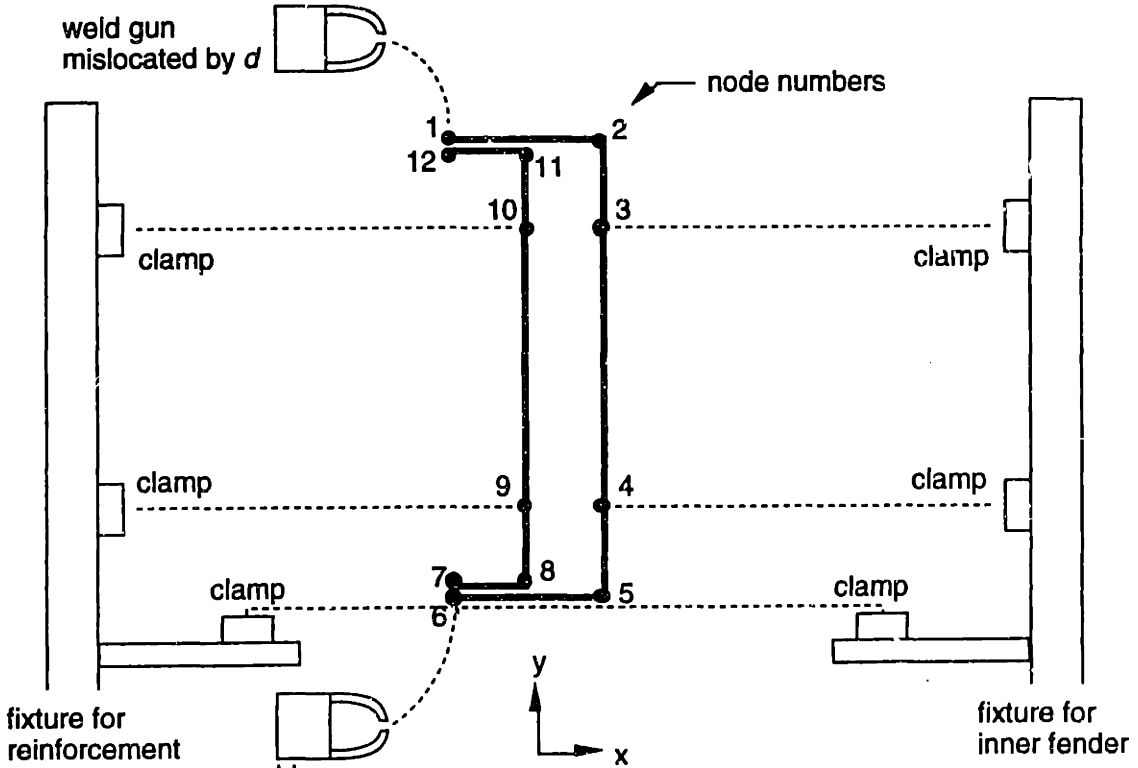

(b) Node numbers for Option B

Figure 5-8. Finite elements for option A and option B

$$(u_y)_1 = d,\ (u_\varphi)_1 = 0$$
$$(u_x)_3 = 0,\ (u_\varphi)_3 = 0$$
$$(u_y)_4 = 0$$

Equation 5-6

We then perform the finite element analysis to find the high/low position of point P in the inspection station $(u_y)_1$.

5.4.4 Results

5.4.4.1 Option A

After simulation of the connectivity graph for the fasten operation in the assembly station, we get,

$$(u_x)_1 = (u_x)_2 = \frac{3\,l_2^2 d}{l_1\,(4l_2 + l_1)}$$
$$(u_x)_{13} = (u_x)_{14} = \frac{12\,l_2^2 d}{l_1\,(8l_2 + l_1)}$$
$$(u_y)_1 = d$$
$$(u_\varphi)_2 = \frac{6\,l_2 d}{l_1\,(4l_2 + l_1)}$$
$$(u_\varphi)_{13} = \frac{24\,l_2 d}{l_1\,(8l_2 + l_1)}$$

Equation 5-7

all other displacements are zero and,

$$(F_y)_1 = -(F_y)_4 = \frac{12\,EI_f d\,(l_2 + l_1)}{l_1^3\,(4l_2 + l_1)}$$
$$(M_z)_1 = \frac{-6\,EI_f d\,(2l_2 + l_1)}{l_1^2\,(4l_2 + l_1)}$$
$$(M_z)_3 = \frac{-6\,EI_f d}{l_1\,(4l_2 + l_1)}$$
$$(F_y)_{14} = -(F_y)_{11} = \frac{96\,EI_r d\,(2l_2 + l_1)}{l_1^3 (8l_2 + l_1)}$$
$$(M_z)_{14} = \frac{-24\,EI_r d\,(4l_2 + l_1)}{l_1^2\,(8l_2 + l_1)}$$
$$(M_z)_{12} = \frac{-24\,EI_r d}{l_1\,(8l_2 + l_1)}$$

Equation 5-8

All other forces are zero and I_f, I_r are moment of inertia of the inner fender and the reinforcement respectively. We use forces from Equation 5-8 as force boundary conditions for simulating the inspection operation and obtain the displacements here. After adding the displacements calculated from the assembly operation and the inspection operation, we get the net displacement field. If $I_f = I_r$, we get the high/low position of point P as,

$$(u_y)_P = \frac{9\ d\ l_2^2\ A}{2\ B} \qquad \text{Equation 5-9}$$

where,

$$A = 3\,l_1^2 l_3 + 14\,l_1 l_2 l_3 + 16\,l_2^2 l_3 + 3\,l_1^2 l_2 + 11\,l_1 l_2^2 + 8\,l_2^3$$

$$B = 2\,l_1^2 l_3^3 + 24\,l_1 l_2 l_3^3 + 64\,l_2^2 l_3^3 + 9\,l_1^3 l_3^2 + 120\,l_1^2 l_2^1 l_3^2 + 432\,l_1 l_2^2 l_3^2 + 384\,l_2^3 l_3^2 + 18\,l_1^3 l_2 l_3$$
$$+ 228\,l_1^2 l_2^2 l_3 + 720\,l_1 l_2^3 l_3 + 384\,l_2^4 l_3 + 9\,l_1^3 l_2^2 + 112\,l_1^2 l_2^3 + 336\,l_1^1 l_2^4 + 128\,l_2^5$$

Equation 5-10

5.4.4.2 Option B

After simulation of the connectivity graph for the fasten operation in the assembly station, we get,

$$(u_x)_1 = (u_x)_2 = (u_x)_5 = (u_x)_6 = \frac{3\,l_2^2 d}{2\,l_1\,(4l_2 + l_1)}$$

$$(u_x)_7 = (u_x)_8 = (u_x)_{11} = (u_x)_{12} = \frac{6\,l_2^2 d}{l_1\,(8l_2 + l_1)}$$

$$(u_y)_1 = (u_y)_{12} = d$$

$$(u_y)_2 = (u_y)_3 = (u_y)_4 = (u_y)_5 = \frac{d}{2} \qquad \text{Equation 5-11}$$

$$(u_y)_8 = (u_y)_9 = (u_y)_{10} = (u_y)_{11} = \frac{d}{2}$$

$$(u_\varphi)_2 = -(u_\varphi)_5 = \frac{3\,l_2 d}{l_1\,(4l_2 + l_1)}$$

$$(u_\varphi)_{11} = -(u_\varphi)_8 = \frac{12\,l_2 d}{l_1\,(8l_2 + l_1)}$$

all other displacements are zero and,

$$(F_y)_1 = -(F_y)_6 = \frac{6\,EI_f d\,(l_2 + l_1)}{l_1^3\,(4l_2 + l_1)}$$

$$(M_z)_1 = -(M_z)_6 = \frac{-3\,EI_f d\,(2l_2 + l_1)}{l_1^2\,(4l_2 + l_1)}$$

$$(M_z)_3 = -(M_z)_4 = \frac{-3\,EI_f d}{l_1\,(4l_2 + l_1)}$$

$$(F_y)_7 = -(F_y)_{12} = \frac{-48\,EI_r d\,(2l_2 + l_1)}{l_1^3\,(8l_2 + l_1)}$$

$$(M_z)_7 = -(M_z)_{12} = \frac{12\,EI_r d\,(4l_2 + l_1)}{l_1^2\,(8l_2 + l_1)}$$

$$(M_z)_9 = -(M_z)_{10} = \frac{12\,EI_r d}{l_1\,(8l_2 + l_1)}$$

Equation 5-12

All other forces are zero and I_f, I_r are moment of inertia of the inner fender and the reinforcement respectively. We use forces from Equation 5-12 as force boundary conditions for simulating the inspection operation and obtain the displacements here. After adding the displacements calculated from the assembly operation and the inspection operation, we get the net displacement field. If $I_f = I_r$, we get the high/low position of point P as,

$$(u_y)_P = \frac{-12\;d\;l_1\;l_2^2\;C}{D}$$

Equation 5-13

where,

$$C = 768\,l_2^5 + 1411\,l_1^2 l_2^3 + 1784\,l_1^2 l_2^2 l_3 + 3144\,l_1 l_2^3 l_3 + 1584\,l_2^4 l_3 + 2266\,l_2^4 l_1 + 600\,l_2^3 l_3^2 + 932\,l_1 l_2^2 l_3^2 + 434\,l_1^2 l_2 l_3^2 + 328\,l_1^3 l_2 l_3 + 16\,l_1^4 l_2 + 8\,l_1^4 l_3 + 295\,l_1^3 l_2^2 + 80\,l_1^3 l_3^2$$

$$D = 2916\,l_1^6 l_3^2 + 23040\,l_2^8 + 69504\,l_1 l_2^4 l_3^3 + 271680\,l_1 l_2^7 + 39168\,l_2^7 l_3 + 27648\,l_2^6 l_3^2 + 9216\,l_2^5 l_3^3 + 1152\,l_2^4 l_3^4 + 312\,l_1^4 l_3^4 + 2576\,l_1^3 l_2 l_3^4 + 1318472\,l_1^3 l_2^4 l_3 + 1113887\,l_1^3 l_2^5 + 1159064\,l_1^2 l_2^5 l_3 + 256320\,l_1 l_2^5 l_3^2 + 112304\,l_1^2 l_2^3 l_3^3 + 6440\,l_1^2 l_2^2 l_3^4 + 572304\,l_1^3 l_2^3 l_3^2 + 11664\,l_1^6 l_2^2 + 899448\,l_1^2 l_2^6 + 11664\,l_1^6 l_2 l_3 + 5712\,l_1 l_2^3 l_3^4 + 148032\,l_1^5 l_2^2 l_3 + 603192\,l_1^2 l_2^4 l_3^2 + 406752\,l_1 l_2^6 l_3 + 140280\,l_1^5 l_2^3 + 2652\,l_1^5 l_3^3 + 670080\,l_1^4 l_2^3 l_3 + 45360\,l_1^5 l_2 l_3^2 + 245412\,l_1^4 l_2^2 l_3^2 + 25784\,l_1^4 l_2 l_3^3 + 600887\,l_1^4 l_2^4 + 85916\,l_1^3 l_2^2 l_3^3$$

Equation 5-14

A parametric study can be conducted based on the discussion in this section.

5.5 3D case study

In this section we will consider one case study and compare it with the example in chapter 4. We are interested in predicting the fender-to-hood margin in both these cases to evaluate which option makes the assembly robust to intentional gaps. Denote the example in chapter 4 as option C and the example in this section as option D. Both, options C and D, have identical geometry of incoming parts, identical assembly sequence, and locations of weld spots. The only difference is the locator scheme used in assembly station #2. For option D, the same locator scheme is used to position the inner fender in assembly station #2 as the one used in station #1 (unlike option C, which uses different locator schemes in the two assembly stations). The connectivity graphs for option D are the same as that of option C, except for the graph corresponding to assembly station #2 which is shown in Figure 5-9.

The deformations of option D during the assembly process are shown in Figure 5-10. Finally, a comparison is made of the resulting geometry of the outer fender for both options (see Figure 5-11). It is evident that option C is superior to option D. For option D, an intentional gap of 2 mm between the reinforcement, inner fender and the body get magnified into a displacement of almost 6 mm of the outer fender. This shows that locator schemes have a very strong influence on the final geometry of the assembled product.

5.6 Summary

This chapter discusses the application of our assembly model for the design of locator schemes for compliant parts. When designed artfully, locator schemes can be used to reduce the sensitivity of the assembled product to variation in geometry of parts, weld guns and fixtures. Manufacturing variation will always be there. Locator schemes can be designed smartly to minimize the effect of this variation on the assembly dimensions of interest.

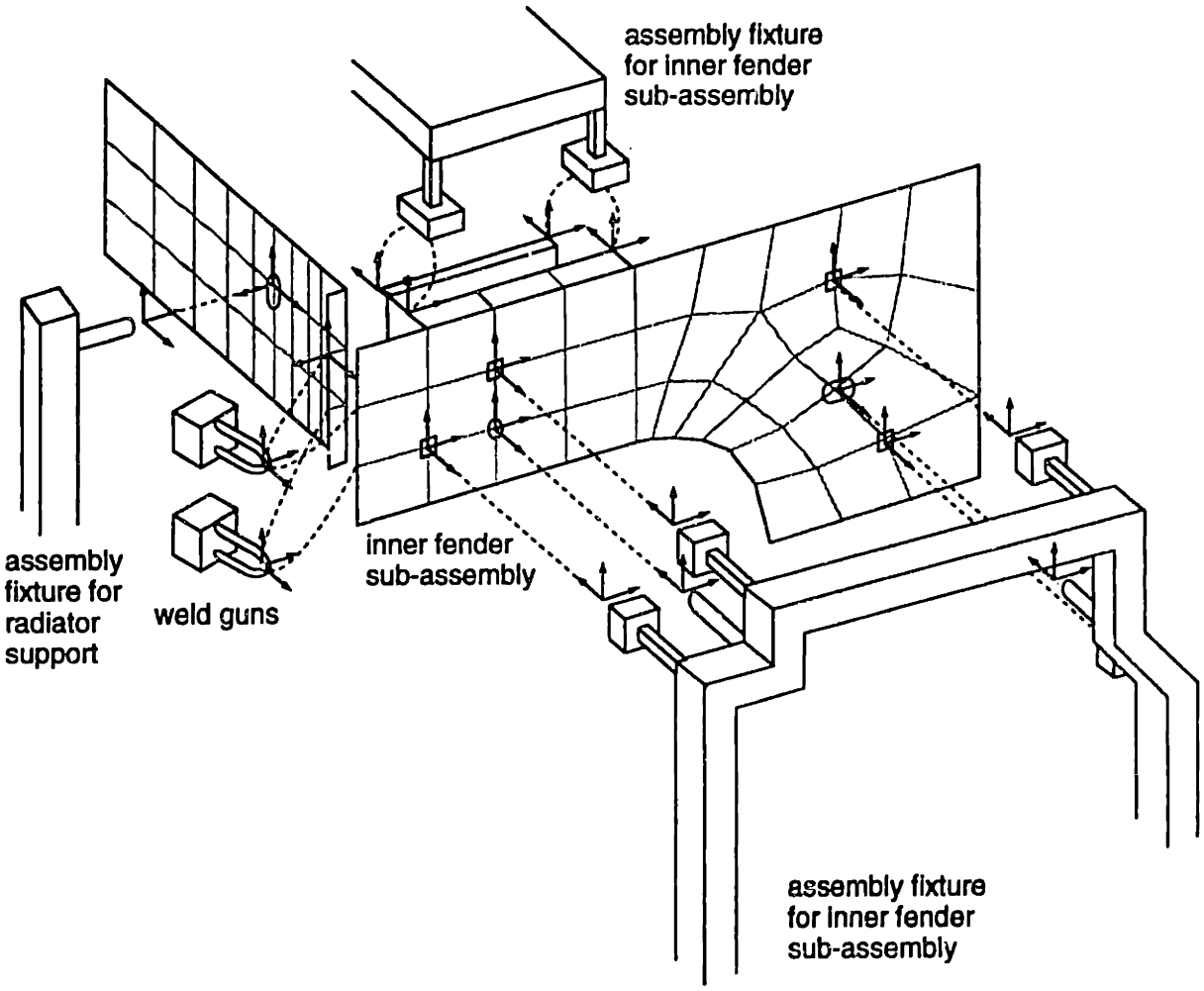

Figure 5-9. Connectivity graph for assembly station #2

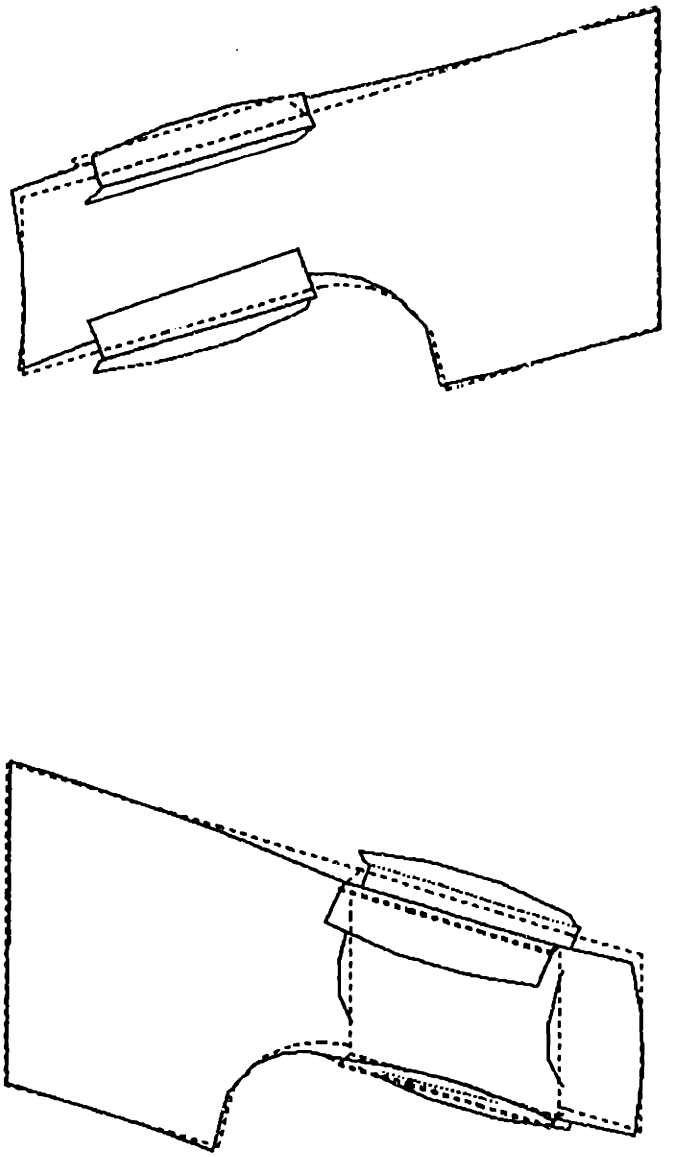

Figure 5-10 (a). Deformed geometry u_1 for assembly station #1 (Isometric and oblique view with deformed geometry shown in solid lines and reference geometry shown in dashed lines. Displacements are magnified 10 times)

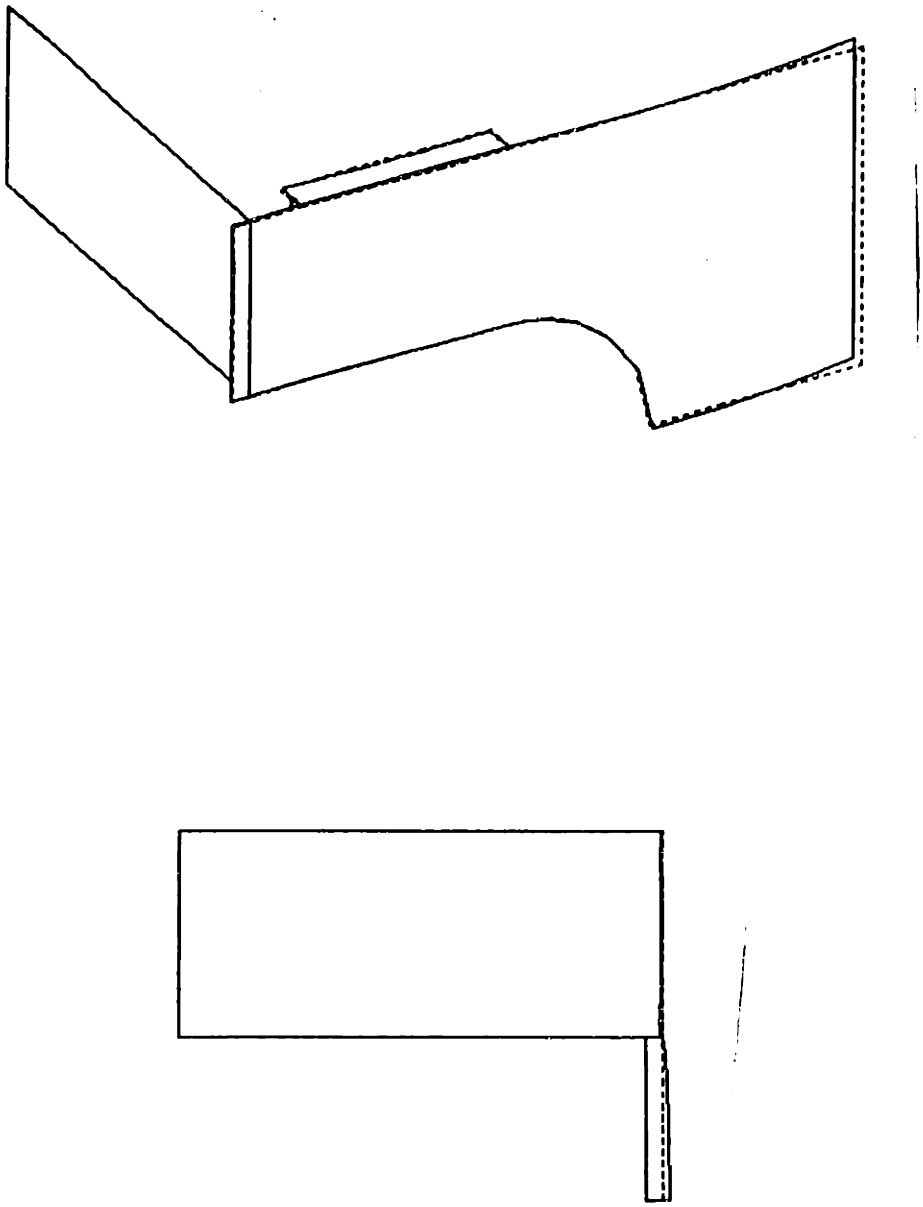

Figure 5-10 (b). Deformed geometry u_2 for assembly station #2 (Isometric and side view with deformed geometry shown in solid lines and reference geometry shown in dashed lines. Displacements are magnified 10 times)

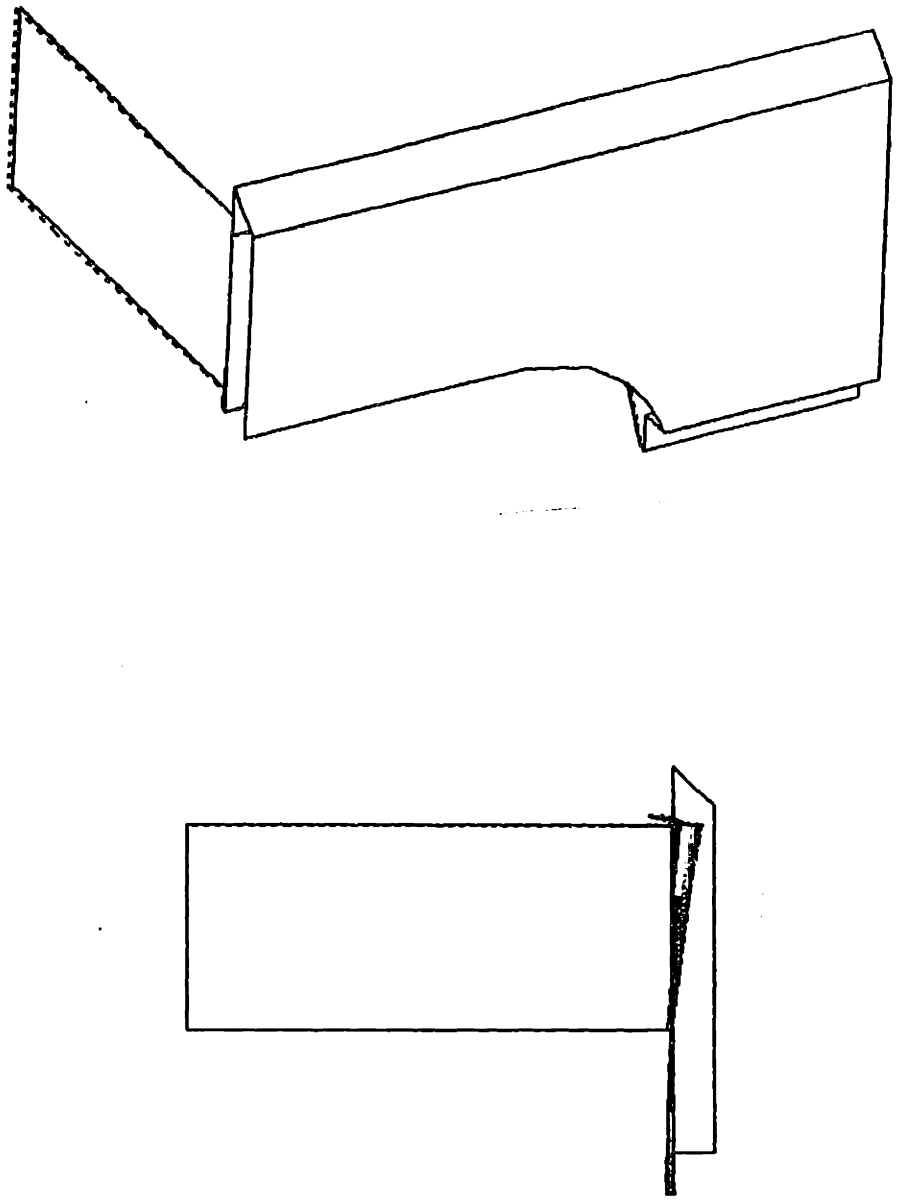

Figure 5-10 (c). Deformed geometry u_3 for assembly station #3 (Isometric and side view with deformed geometry shown in solid lines and reference geometry shown in dashed lines. Displacements are magnified 10 times)

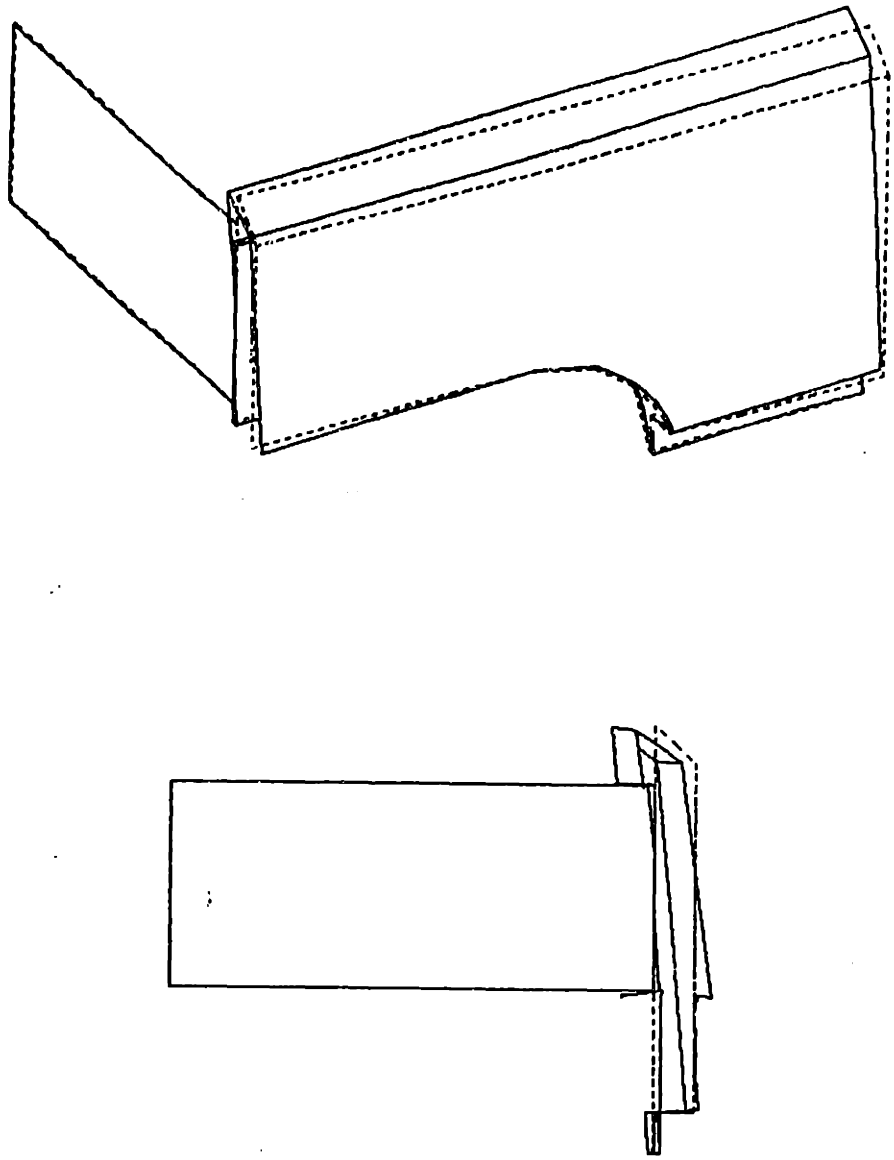

Figure 5-10 (d). Deformed geometry u_4 for inspection station (Isometric and side view with deformed geometry shown in solid lines and reference geometry shown in dashed lines. Displacements are magnified 10 times)

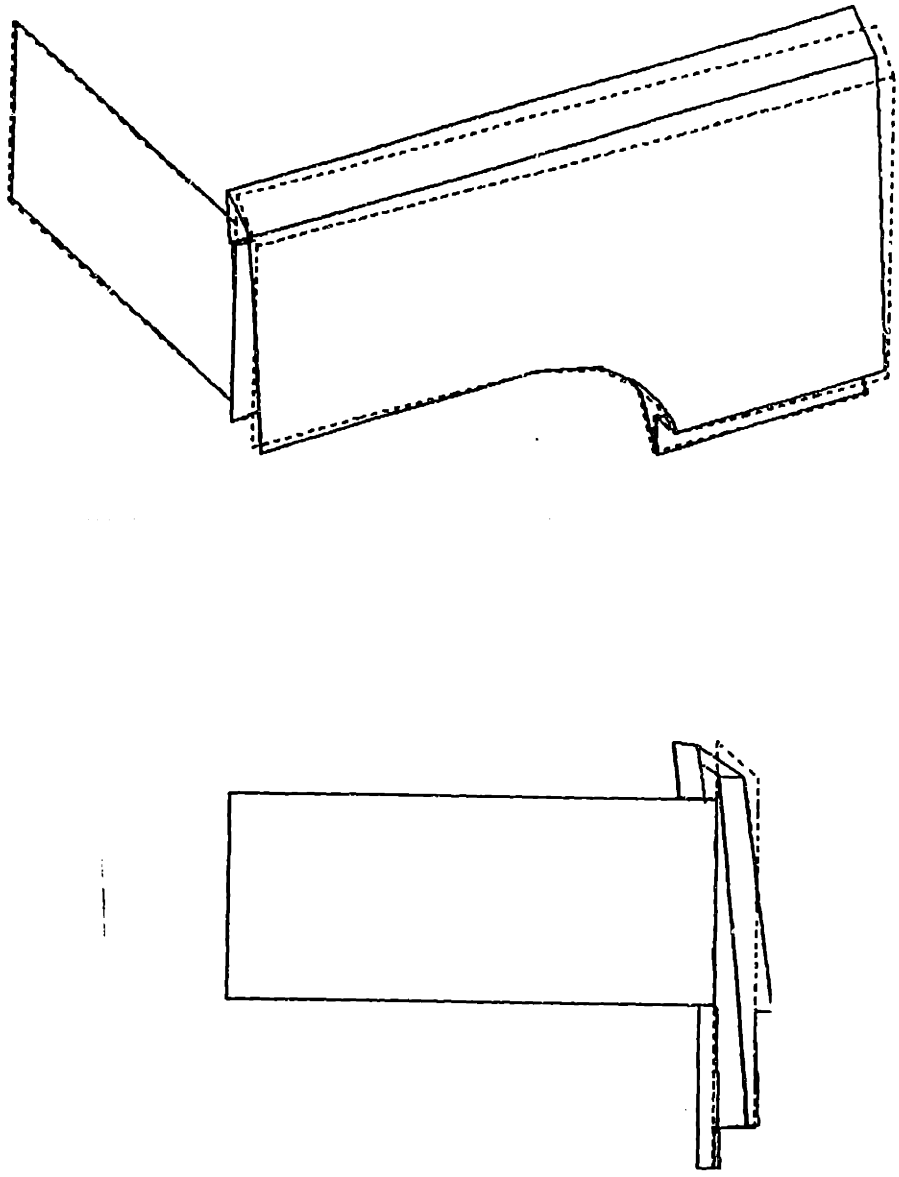

Figure 5-11. Geometry of final product in the inspection station $U_4 = \sum_{i=1}^{4} u_i$ (Isometric and side view with deformed geometry shown in solid lines and reference geometry shown in dashed lines. Displacements are magnified 10 times)

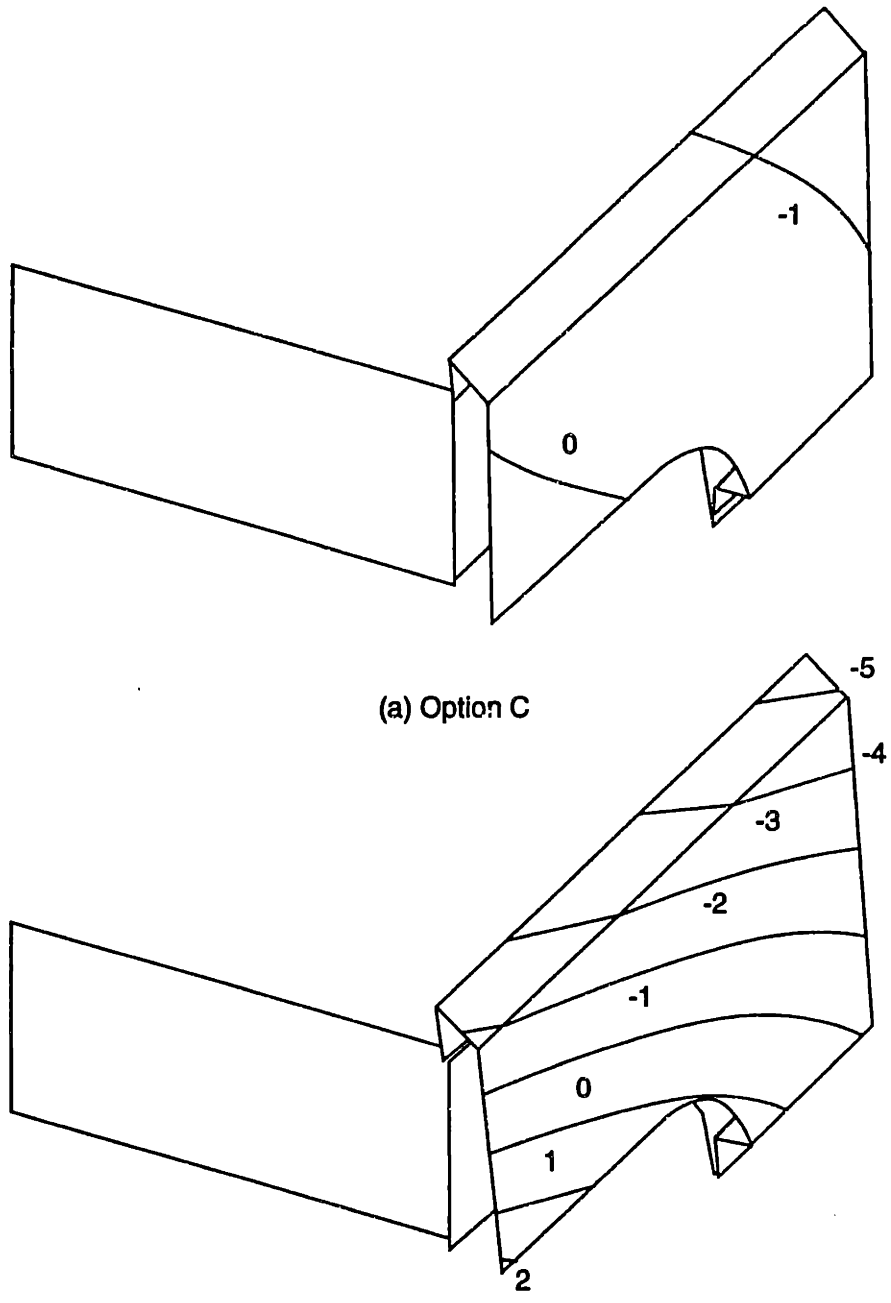

Figure 5-11. Comparison of geometry of outer fender for options C and D. The contours show deformation (in mm) of the outer fender away from nominal and along the fender-to-hood margin

6.

Conclusions

This chapter summarizes the thesis and presents its contributions to current research literature. It then provides suggestions to refine and extend the thesis for future work.

6.1 Summary of the Thesis

This work presented a model of the assembly of compliant parts. The model is used to quantify and predict the influence of intentional gaps and non-nominal geometry on assembly dimensions of interest.

The geometry of parts and tools were represented as a set of finite elements and nodes. The relationships between parts, tools and assembly configuration were depicted as a connectivity graph. Every operation in the assembly process was examined in detail to study the propagation of non-nominal geometry from one operation to the next.

This model was implemented to predict the geometry of the a simple assembly of two parts (inner fender and reinforcement) in two stations (one assembly station and one inspection station). It then presented a realistic assembly comprised of five parts (inner fender, reinforcement, radiator support, body and outer fender) in four stations (three assembly stations and one inspection station).

The method was then used to design locator schemes. Metrics were suggested to quantify the "goodness" of a locator scheme. Two examples were presented to demonstrate the use of these metrics in selecting a good locator scheme from candidates.

6.2 Major Findings

Some of the major findings of this research work are as follows:

- *Nominal parts with intentional gaps can create non-nominal assembly*

In the presence of intentional gaps, nominal geometry of incoming parts, fixtures and weld guns can result in a non-nominal sub-assembly. Weld gun close the intentional gap during the fastening process. This causes stresses to be locked into the resulting sub-assembly. These stresses manifest as a deformed sub-assembly.

- *Locator schemes have a significant impact on final assembly dimensions*

The three-dimensional case study in Chapter 5 demonstrated that locator schemes have a significant impact on final assembly dimensions. The two options considered in the chapter had identical part geometry, assembly sequence, and weld sequences. They differed only in the way the inner fender was located in assembly station #2. The resulting geometry of the outer fender is very different for the two cases.

- *Structural parts influence the position and geometry of the outer panels*

Structural parts support the outer panels. Outer panels are parts that are visible to the customer. In the example in this thesis, we considered the position and geometry of the outer fender. Although the outer panel was nominal before it was assembled to the front end, after assembly, there was a large change in position.

- *Errors magnify as parts propagate through the assembly line*

The out-going geometry of one assembly station becomes the incoming geometry of the subsequent assembly station. If there exist intentional gaps or non-nominal geometry, the outgoing assembly becomes distorted. i.e. there exists an error in its position and/or geometry. When this deformed sub-assembly goes into the next assembly station, there is further deformation. As parts propagate through the assembly line, these errors magnify. An example in this thesis demonstrated that an intentional gap of 2 mm between structural parts resulted in a 6 mm error in the position of the outer fender.

6.3 Contributions

This thesis has several contributions. This thesis presents a novel attempt to model and predict dimensions of the product after the assembly process is complete.

- *Model of multiple compliant parts in multiple stations*

Assemblies are comprised of multiple parts. These parts propagate through multiple assembly stations. Current research literature in assembly of rigid parts considers multiple bodies in multiple assembly stations. Most techniques used for rigid parts can not be applied to assemblies of compliant parts. Current research literature in assembly of compliant parts is in the area of fixture design which considers one part in one assembly station. Although some work has been done in representing two compliant parts, it is limited to one assembly station only. This thesis presented a model of multiple compliant parts in multiple assembly stations. It presented two examples with five parts and three stations.

- *Representation of intentional gaps and non-nominal geometry*

Most current CAD software represent the assembly of ideal or nominal geometry. Due to inherent limitations of manufacturing processes, parts are produced that have non-nominal geometry. This thesis provides a representation for it and also presents a method to quantify its effect on the product after its assembly is complete.

- *Framework for automation of assembly simulation*

An assembly line consists of a series of assembly stations. Outgoing parts for one assembly station become incoming parts for the subsequent assembly station. This thesis provides a framework to predict the outgoing geometry of one assembly station. This method can be used over and over for every assembly station to electronically simulate the assembly process. This iterative method provides an opportunity to automate the electronic simulation.

- *Three dimensional modeling*

The model presented in this thesis is applicable to three-dimensional assemblies and is not restricted to simple two-dimensional geometry. Every node of the finite element model can have six degrees of freedom.

- *Framework for a design tool*

The methodology proposed in this work can be implemented as a design tool for the design of the product and its assembly process. In the design phase, this tool can be used to anticipate expensive fit-up problems and pro-actively solve them. Different assembly strategies can be evaluated to quantify their influence on the dimensional integrity of the assembled product.

6.4 Recommendations for Future Work

- *Representation of geometric errors*

This model can be further extended by developing a representation for various geometric errors such as, parallelism, perpendicularity and so on. A detailed analysis can be conducted after identification, quantification and representation of anticipated geometric errors in parts, fixtures and weld guns.

- *Optimization of the design of locator schemes*

Design of locator schemes is a challenge that is very critical for the function of the assembly. It is experience-based rather than science-based. An optimization algorithm can be developed to automate this process. A locator scheme is characterized by the number, type and position of locators. A given configuration can be optimized to make the assembly robust to variations in parts, fixtures and weld guns.

- *Unmodeled dynamics*

The model can be refined by incorporating unmodeled dynamics. A good candidate is the representation of position uncertainties. When parts are placed and clamped on fixtures, there exists a range of possible positions that the part can take. This uncertainty in position is due to an imperfect mating of adjacent parts. e.g. if the pin on the fixture has a smaller diameter than that of the corresponding hole on the part, the part can move even after it is placed and clamped to the fixture.

Other phenomenon that have not been addressed by this thesis include heat affected zones, fastening methods other than spot welding (such as riveting, adhesives etc.).

7.

References

American National Standards Institute, 1983, "Dimensioning and Tolerancing ANSI Y 14.5M-1982," American Society of Mechanical Engineers, New York.

Asada, H, and By, A. B., 1985, "Kinematic Analysis of Workpart Fixturing for Flexible Assembly with Automatically Reconfigurable Fixtures," IEEE J. of Robotics and Auto., RA-1(2), pp. 86-94.

Bathe, K-J., "Finite Element Procedures in Engineering Analysis," Prentice-Hall Inc., 1982.

Bausch, J. J., Youcef-Toumi, K., 1990, "Kinematic Methods for Automated Fixture Reconfiguration Planning," Proc. 1990 IEEE Intl. Conf. Robotics and Auto., Vol. 2, Cincinnati, Ohio, May 13-18.

Bjorke, O., 1989, "Computer Aided Tolerancing," Second edition, New York, ASME Press.

Boyes, W. E., "Handbook of Jig and Fixture Design," SME, 1989.

Cai, W., Hu, S. J., Yuan, J., "Deformable Sheet Metal Fixturing: Principles, Algorithms, and Simulations," Mfg. Science and Engineering, PED-Vol. 68-1, Vol. 1, ASME, 1994, pp. 13-20.

Ceglarek, D., Shi, J. , and Wu, S. M., 1994, "A Knowledge-Based Diagnostic Approach for the Launch of the Auto-Body Assembly Process," J. Engineering for Industry, Vol. 116, Nov., pp. 491-499.

Chang, M., 1996, "Modeling the Assembly of Compliant, Non-ideal Parts," Ph. D. Thesis, Massachusetts Institute of Technology.

Chase, K. W., and Greenwood, W. H., 1987, "Design Issues in Mechanical Tolerance Analysis," ASME Mfg. Review, Vol. 1, No. 4, pp. 50-59.

Chon, C. T., Du, H. A., "An Alternative Approach to Design Sensitivity Analyses for Large-scale Structures," 1983 Intl. Computers in Eng. Conf. and Exhibit, Computers in Engineering, Vol. 3, 1983, pp. 233-237.

Chon, C. T., Mohammadtorab, H., and El-Essawi, M., "Generic Stick-Model of Vehicular Structures," Proc. of 6th Intl. Conf. on Vehicle Structural Mechanics, SAE, Detroit, Michigan, Apr. 1986, pp. 235-241.

Chou, Y-C, Chandru, V., Barash, M. M., 1989, "A Mathematical Approach to Automatic Configuration of Machining Fixtures: Analysis and Synthesis," J. of Eng. for Ind. Vol. 111, Nov., pp. 299-306.

Du, H. A., Chon, C. T., "Modeling of a Large-scale Vehicle Structure," Proc. 8th Conf. on Electronic Computation, ASCE, Houston, Texas, Feb. 21-23, 1983, pp. 326-335.

Early, R., and Thompson, J., "Variation Simulation Modeling: Variation Analysis Using Monte Carlo Simulation," pp. 139-144.

Fenyes, P. A., 1981, "Structural Optimization with Alternate Materials: Minimum Mass Design of Primary Structures," SAE preprints for Meeting Feb. 23-27, 1981.

Fleming, E. T., 1988, "Geometric Relationships between Toleranced Features," Artificial Intelligence 37.

Guilford, J., and Turner, J., 1993, "Representational Primitives for Geometric Tolerancing," CAD, Sept.

Hillyard, R. C., Braid, I. C., 1978, "Analysis of Dimensions and Tolerances in Computer-Aided Design," CAD, Vol. 10, No. 3, pp. 209-214.

Hu, S. J., and Wu, S. M., 1992, "Identifying Sources of Variation in Automobile Body Assembly Using Principal Component Analysis," Transactions of NAMRI/SME, Vol. XX, pp. 311-316.

Inui, M., and Kimura, F., 1991, "Algebraic Reasoning of Position Uncertainties of Parts in an Assembly," ACM.

Kang, S. J., Choi, J. H., "Design Sensitivity Analysis of Body Structure Using Skeleton Model," Proc. of the 6th Intl. Pacific Conf. on Automotive Engineering, Korean Society of Automotive Engineers, pp. 525-531, 1991.

Kardestuncer, H., and Norrie, D. H., 1987, "Finite Element Handbook," McGraw-Hill Inc., pp. 4.168-4.169.

Koltuniak, M., 1996, "PICO Basic Weld Gun Manual," Progressive Tools and Ind. Co. Basic Weld Gun Manual, June, pp. 9-13.

Lee, J. D., and Haynes, L. S. , 1986, "Finite Element Analysis of Flexible Fixturing System," Japan-USA Symposium on Flexible Automation, pp. 579-584,.

Lee, K., and Gossard, D. C., 1985, "A Hierarchical Data Structure for Representing Assemblies: Part 1," CAD, Jan., Vol. 17, No. 1, pp. 15-19.

Light, R., and Gossard, D. C., 1982, "Modification of Geometric Models Through Variational Geometry," CAD, July, Vol. 14, No. 4, pp. 209-213.

Liu, S. C., Hu, S. J., and Woo, T. C., 1996, "Tolerance Analysis for Sheet Metal Assemblies," Trans. of ASME, Mar., Vol. 118, pp. 62-67.

Martin, H. C., "Introduction to Matrix Methods of Structural Analysis," McGraw-Hill Book Co., 1966.

Martino, P. M., Gabriele, G. A., 1989, "Application of Variational Geometry to the Analysis of Mechanical Tolerances," Proc. of ASME, Advances in Design Automation Conf., Sept., Vol. 1, Montreal.

Menassa, R.J. and DeVries, W.R., 1988, "Optimization Methods Applied to Selecting Support Positions in Fixture Design" Proc. of the USA-Japan Sym. Flex. Auto., July 18-20, Vol. 1.

Naitoh, T., Yamamoto, K., Komada, Y., Honda, S., "The Development of Intelligent Body Assembly System."

Pham, D. T., and Lazaro, A., 1990, "AUTOFIX: An Expert CAD System for Jigs and Fixtures," Int. J. Machine. Tools Mfg., Vol. 30, No. 3, pp. 403-411.

Plonka, F. E., 1974, "A Methodology for Tolerancing, Process Evaluation and Control of the Automobile Body Subassembly Designs," Ph. D. Thesis, University of Michigan.

Requicha, A. A. G., 1993, "Mathematical Definition of Tolerance Specifications," ASME Mfg. Review, Vol. 6, No. 4, pp. 269-274.

Requicha, A. G., 1983, "Toward a Theory of Geometric Tolerancing," Intl. J. of Robotics Res., Winter, Vol. 2, No. 4, pp. 45-60,.

Sakurai, H., "Automatic Setup Planning and Fixture Design for Machining," Ph. D. Thesis, Massachusetts Institute of Technology, 1990.

Spotts, M. F., "Dimensioning Stacked Assemblies," Machine Design, April 1978, pp. 60-63.

Sweder, T. A., Pollock, J., "Full Vehicle Variability Modeling," SAE Intl., Intl. Truck and Bus Meeting and Exposition, Seattle, Washington, Nov. 7-9, 1994.

Takezawa, N., "An Improved Method for Establishing the Process-Wise Quality Standard," Rep. Stat. Application Research, JUSE, Vol. 27, No. 3, Sept. 1980, pp. 63-76.

Turner, J. U., "Relative Positioning of Parts in Assemblies Using Mathematical Programming," CAD, Vol. 22, No. 7, Sept. 1990, pp. 394-400.

Turner, J. U., and Wozny, M. J., "The M-Space Theory of Tolerances," Proc. of Adv. in Design Automation, Vol. 1, pp. 217-225, Chicago, Illinois, Sept. 1990.

Wang, N., Ozsoy, T. M., "Automatic Generation of Tolerance Chains from Mating Relations Represented in Assembly Models," Proc. Adv. Design Automation Conf., Vol. 1, pp. 227-233, Chicago, Illinois, Sept. 1990.

Whitney, D. E., Gilbert, O. L., Jastrzebski, M., "Representation of Geometric Variations Using Matrix Transforms for Statistical Tolerance Analysis in Assemblies," IEEE Robotics and Automation Conf., Atlanta, Georgia, 1993.

Youcef-Toumi, K., Liu, W. S., Asada, H., "Computer-Aided Analysis of Reconfigurable Fixtures and Sheet Metal Parts for Robotic Drilling," Robotics and CIM, Vol. 4, No. 3/4, 1988, pp. 387-393.